

# **Stability of a Structural Column under Stochastic Axial Loading**

by

Richard Wiebe

A thesis  
presented to the University of Waterloo  
in fulfilment of the  
thesis requirement for the degree of  
Master of Applied Science  
in  
Civil Engineering

Waterloo, Ontario, Canada, 2009

©Richard Wiebe 2009

## **Author's Declaration**

I hereby declare that I am the sole author of this thesis. This is a true copy of the thesis, including any required final revisions, as accepted by my examiners.

I understand that my thesis may be made electronically available to the public.

## Abstract

Columns subjected to time varying axial load may exhibit dynamic instability due to parametric resonance. This type of instability is inherent in structures; it is not due to material or geometrical imperfections, and can occur even in perfectly constructed structures. This characteristic makes parametric resonance a very difficult to predict and therefore dangerous phenomenon.

In this thesis the stability of a structural column under bounded noise axial load is studied by use of Lyapunov exponents. Bounded noise is especially useful as a loading because it may be used to represent both wide and narrow band processes, making the stability equations developed general enough to handle a wide variety of real world probabilistic loadings. The equation of motion of the first mode of vibration for this system is a second-order nonlinear stochastic ordinary differential equation. The nonlinearity makes the system exhibit bifurcating behaviour where stability shifts from the trivial solution to a non-zero mean stationary solution.

The stability of the trivial and non-trivial solutions is important in obtaining a complete picture of the dynamical behaviour of the system. The effect that damping, the amplitude of noise, and the level of nonlinearity have on the stability of a structural column is studied using both analytical and numerical approaches. The largest Lyapunov exponent of the trivial solution is determined analytically by using time averaged versions of the original equation of motion. The validity of the analytical time averaged equation of motion is also verified with Monte Carlo simulations. Due to the mathematical complexity the largest Lyapunov exponent of the non-trivial stationary solutions is obtained using Monte Carlo simulation only.

## Acknowledgments

I want to thank Professor Wei-Chau Xie for all of his advice and support through my years at the University of Waterloo. Professor Xie's passion for teaching and research has been an inspiration for me to pursue my own education further.

I also want to thank Dr. Lei Xu and Dr. Shawn Matott for taking the time to review this thesis.

Thanks also to Jing Zhou, Jinyu Zhu, Dongliang Lu, Tianjin Cheng, Dritan Topuzi, Shunhao Ni, Tianjin Cheng, Qinghua Huang, Agostino Monteleone, and Dr. Wang Min. Your friendship and support has made my experience at the University of Waterloo an experience I will never forget.

I am also grateful to the Natural Sciences and Engineering Research Council of Canada for their support through the Canada Graduate Scholarship.

This thesis was made possible by the facilities of the Shared Hierarchical Academic Research Computing Network (SHARCNET:[www.sharcnet.ca](http://www.sharcnet.ca)).

And to my mom, dad, sisters, brothers, nieces, and nephews I extend my most sincere gratitude. I cannot express how thankful I am to be surrounded by such a great environment of kindness and support.

TO

*My Family*

# Contents

<b>List of Figures</b>	<b>ix</b>
<b>1 Introduction</b> . . . . .	<b>1</b>
1.1 Instability of Structures under Periodic Loading	1
1.1.1 Dynamic Instability	1
1.1.2 Main Resonance	2
1.1.3 Parametric Resonance	6
1.2 Noise Models and Stochastic Differential Equations	12
1.2.1 Stochastic Processes – General	12
1.2.2 The Wiener Process	18
1.2.3 Bounded Noise Process	20
1.2.4 Stochastic Ordinary Differential Equations	20
1.3 Monte Carlo Simulation	21
1.4 Stochastic Stability and the Lyapunov Exponent	23
1.4.1 Stochastic Stability	23
1.4.2 The Lyapunov Exponent	24
1.5 Organization and Scope	26
<b>2 Mathematical Model of a Structural Column under Dynamic Loading</b> . . . . .	<b>28</b>
2.1 Equation of Motion	28
2.2 The Method of Averaging	32
2.2.1 First Order Averaging	32

2.2.2	Second Order Averaging	37
2.2.3	Third Order Averaging	41
2.3	Equations of Variation about Non-Trivial Stationary Solutions	43
2.3.1	Procedure for Setting up Equations of Variation	43
2.3.2	Equations of Variation from First Order Averaged System	45
2.3.3	Equations of Variation from Exact System	47
2.4	Remarks and Conclusions	48
<b>3</b>	<b>Stability of The Trivial Solution</b> . . . . .	<b>49</b>
3.1	Analytical Results – Lyapunov Exponents	49
3.2	Monte Carlo Simulation of Lyapunov Exponents	52
3.2.1	Numerical Algorithm	52
3.2.2	Comparison of Analytical and Numerical Solutions	57
3.3	Affect of System Parameters on the Lyapunov Exponent of the Trivial Solution	57
3.4	Remarks and Conclusions	63
<b>4</b>	<b>The Non-Trivial Stationary Solution</b> . . . . .	<b>64</b>
4.1	Analytical Results – Non-Trivial Stationary Solution	64
4.1.1	General	64
4.1.2	Special Case – Deterministic System	65
4.1.3	Special Case – High Noise Intensity	66
4.2	Monte Carlo Simulation of Non-Trivial Stationary Solution	72
4.2.1	General	72
4.2.2	Special Case – Deterministic System	72
4.2.3	Special Case – High Noise Intensity	73
4.3	Affect of System Parameters on Non-Trivial Stationary Solution	73
4.4	Remarks and Conclusions	77

<b>5</b>	<b>Stability of The Non-Trivial Stationary Solution . . . . .</b>	<b>78</b>
5.1	Monte Carlo Simulation of Lyapunov Exponents	78
5.2	Affect of System Parameters on the Lyapunov Exponent of the Non-Trivial Solution	80
5.3	Remarks and Conclusions	85
<b>6</b>	<b>Conclusions . . . . .</b>	<b>86</b>
6.1	Summary	86
6.2	Extension of Research	87
6.3	Future Work	87
	<b>Bibliography . . . . .</b>	<b>89</b>

# List of Figures

1.1	Structure Subjected to Dynamic Lateral Loading	2
1.2	Beam Subjected to Dynamic Loading	3
1.3	Dynamic Magnification Factor	4
1.4	Main Resonance - Linear Growth	5
1.5	Parametric Resonance — Exponential Growth	6
1.6	Exponential Stability of Parametric System Loaded at Non-Resonant Frequency	7
1.7	Stability Boundaries of Undamped Linear System	9
1.8	Stability Boundaries of Damped Linear System	10
1.9	Amplitude-Frequency Relationship of Nonlinear Systems	10
1.10	Potential Energy Surface	11
1.11	Effect of Damping in Linear and Nonlinear Systems	12
1.12	Illustration of a Stochastic Process and its Probability Densities	14
1.13	Ensemble and Time Averages of a Stochastic Process	16
1.14	Autocorrelation, $R(\tau)$ , and Power Spectral Density, $S(\tau)$	18
1.15	Realization of the Wiener Process	19
1.16	Power Spectral Density of a Bounded Noise Process	21
1.17	Illustration of Stochastic Stability	24
2.1	Column Under Axial Load	29

2.2	Deformed and Un-Deformed Differential Element of Column Under Axial Load	31
2.3	Time Varying Amplitude of a Function	34
2.4	Comparison of Averaged and Exact Amplitude	36
2.5	Comparison of Averaged and Exact Phase Angle	36
3.1	Typical Lyapunov Exponent vs. $\nu/2\omega$ Curves	52
3.2	Convergence of Lyapunov Exponent with Increasing T	56
3.3	Convergence of Lyapunov Exponent with Decreasing Time Step	56
3.4	Comparison of Analytical and Averaging Results with Exact - Lyapunov Exponents	58
3.5	Stability Surface vs. Damping	60
3.6	Cross-Sections of Stability Surface vs. Damping	60
3.7	Stability Surface vs. Load Intensity	61
3.8	Cross-Sections of Stability Surface vs. Load Intensity	61
3.9	Stability Surface vs. Noise Intensity	62
3.10	Cross-Sections of Stability Surface vs. Noise Intensity	62
4.1	Comparison of Amplitude-Frequency Relationships Obtained With and Without the Approximation $\nu \approx 2\omega$	67
4.2	Stationary Solution - Time Averaging	68
4.3	$E[\cos(2\bar{\phi}_s - \bar{\Psi})]$ vs. $\sigma$	69
4.4	$E[\sin(2\bar{\phi}_s - \bar{\Psi})]$ with Averaged Equations	70
4.5	Relationship Between $E[\cos(2\bar{\phi}_s - \bar{\Psi})]$ and $\zeta$	70
4.6	The Amplitude-Frequency Relationship for Limiting Cases of Noise	71
4.7	Comparison of Approximate Analytical and Simulated Exact Amplitude-Frequency Curves	73

4.8	The Effect of Noise on the Amplitude-Frequency Relationship	74
4.9	Amplitude-Frequency Relationship vs. Damping	74
4.10	Amplitude-Frequency Relationship vs. Load Intensity	76
4.11	Amplitude-Frequency Relationship vs. Nonlinearity	76
5.1	Lyapunov Exponent of Non-Trivial Stationary Solution	81
5.2	Non-Trivial Stationary Solution Stability Curve vs. Noise Intensity	82
5.3	Non-Trivial Stationary Solution Stability Curve vs. Load Intensity	84
5.4	Non-Trivial Stationary Solution Stability Curve vs. Nonlinearity	84

# C H A **1** P T E R

## Introduction

### 1.1 Instability of Structures under Periodic Loading

#### 1.1.1 Dynamic Instability

Instability is perhaps best defined as the lack of stability. Stability itself has been defined in many ways. In most general terms it can be thought of as durability, constancy, steadiness, immobility, ... ([3], p. 125). This definition is broad, but too subjective to be used in practice, therefore a more quantifiable definition is needed. In mathematical modelling of mechanical systems, a working definition is that a system is stable with respect to some input if its response to that input is bounded. Dynamic instability occurs when a system is made unstable by dynamic input. If the dynamic input is periodic, the instability is called resonance instability, or simply resonance.

Resonance of a structure occurs when the applied dynamic loading adds more energy to the system than the amount of energy lost through dissipative forces, causing the response to grow without bound. Intuitively, because energy is the product of force and distance traveled, this requires that there be some correlation between the frequency of the loading and the frequency of the structural vibration. The natural frequencies of a structure play a very important role in this. Natural frequencies are the frequencies at which structure will oscillate at when subjected to an impulse load and are an intrinsic property of every elastic system.

Depending on the nature of the loading, resonance may be further divided into main resonance and parametric resonance.

### 1.1.2 Main Resonance

The classical study of structural dynamics usually focuses on main resonance. This case presents itself most commonly in transverse, or out of plane, dynamic loading of columns, beams, or entire structures.

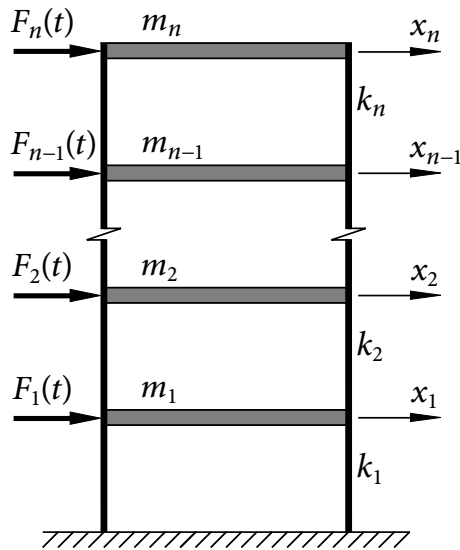


**Figure 1.1** Structure Subjected to Dynamic Lateral Loading

The multistorey structure in Figure 1.1 may be mathematically modelled by ordinary differential equations (ODE's), which are in general given by

$$\mathbf{M}\ddot{\mathbf{x}}(t) + \mathbf{C}\dot{\mathbf{x}}(t) + \mathbf{K}\mathbf{x}(t) = \mathbf{F}(t), \quad (1.1.1)$$

where  $\mathbf{x}$  is the floor displacement vector,  $\mathbf{M}$  is the floor mass matrix,  $\mathbf{C}$  is a damping matrix representing energy dissipation,  $\mathbf{K}$  is a stiffness matrix determined by the lateral stiffnesses of each storey with respect to lateral displacement, and  $\mathbf{F}(t)$  is the applied forces vector.

In the case of an individual beam, as shown in Figure 1.2, the equation of motion is a partial differential equation (PDE):

$$\rho A \frac{\partial^2 v(x, t)}{\partial t^2} + EI \frac{\partial^4 v(x, t)}{\partial x^4} = w(x, t), \quad (1.1.2)$$

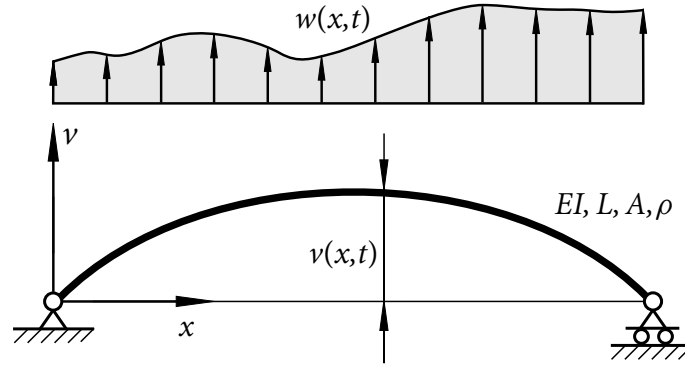


**Figure 1.2** Beam Subjected to Dynamic Loading

where  $\rho$  is the mass density per unit volume,  $A$  is the cross-sectional area,  $EI$  is the cross-sectional bending stiffness,  $L$  is the span length,  $v$  is the transverse displacement,  $x$  is the position,  $t$  is time, and  $w(x, t)$  is the applied distributed load.

Important in these systems is that the loading terms appear on their own on the right side of the equations of motion. The system parameters are therefore independent of the loading. Systems of this type are all susceptible to main resonance.

The properties of main resonance may be understood by studying a discrete single degree-of-freedom example. Consider equation (1.1.1) in the case of a single story structure under sinusoidal loading,

$$m\ddot{x}(t) + c\dot{x}(t) + kx(t) = F_0 \sin \nu t, \quad (1.1.3)$$

or in standard form,

$$\ddot{x}(t) + 2\zeta\omega\dot{x}(t) + \omega^2x(t) = \frac{F_0}{m} \sin \nu t, \quad (1.1.4)$$

with

$$\omega^2 = \frac{k}{m}, \quad \zeta = \frac{c}{2m\omega},$$

where  $F_0$  is the applied force magnitude,  $\nu$  is forcing frequency,  $\omega$  is undamped natural frequency, and  $\zeta$  is the damping coefficient.

The damping coefficient,  $\zeta$ , is very important and dictates the nature of the response. There exists a threshold level of damping ( $\zeta = 1$ ), called critical damping, where the response changes from oscillatory exponential decay to non-oscillatory exponential decay. In

structures the level of damping is usually much lower than this threshold, in which case it may easily be shown that solution of equation (1.1.4) is given by

$$x(t) = \frac{F_0}{m} \frac{1}{\sqrt{(\omega^2 - \nu^2)^2 + (2\zeta\omega\nu)^2}} \sin(\nu t + \phi), \quad (1.1.5)$$

where

$$\phi = \arctan\left(\frac{2\zeta\omega\nu}{\omega^2 - \nu^2}\right).$$

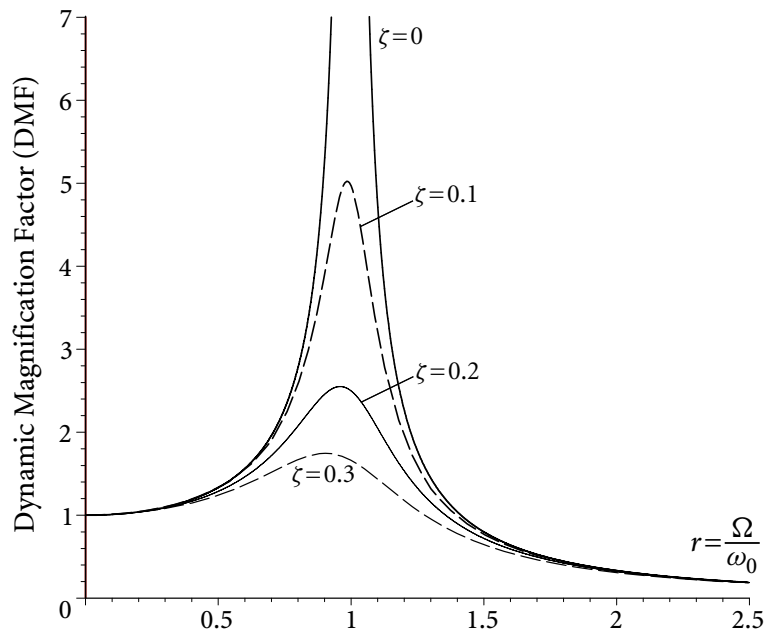


**Figure 1.3** Dynamic Magnification Factor

The stability of this system may be determined by studying the amplitude of vibration, which is the coefficient of the sine term in equation (1.1.5). In practice this coefficient is usually normalized by dividing by  $F_0/m$ . The normalized coefficient is often called the dynamic magnification factor (DMF). Figure 1.3 shows a graph of the DMF vs.  $\nu/\omega$  for different values of  $\zeta$ . The DMF shows that the system will always be stable, i.e. have a finite amplitude of vibration, unless there is no damping ( $\zeta = 0$ ) and the forcing frequency,  $\nu$ , is exactly equal to the undamped natural frequency,  $\omega$ . The system may vibrate with large amplitude, but it will always be bounded unless both of the above conditions are satisfied. In all real structures there is always some form of damping present, be it slipping

in connections, friction caused by movement of non-structural components, or even atomic scale inelasticities ([12], p. 15). Therefore main resonance cannot occur in a real structure.

It can also be shown that in the case of resonance of an undamped system, i.e.  $\omega = \nu$ , the response is given by

$$x(t) = -\frac{F_0}{2m\omega}t \cos \omega t. \quad (1.1.6)$$

This result is graphed in Figure 1.4, which shows that, while the response grows without bound, it does so in a linear fashion.

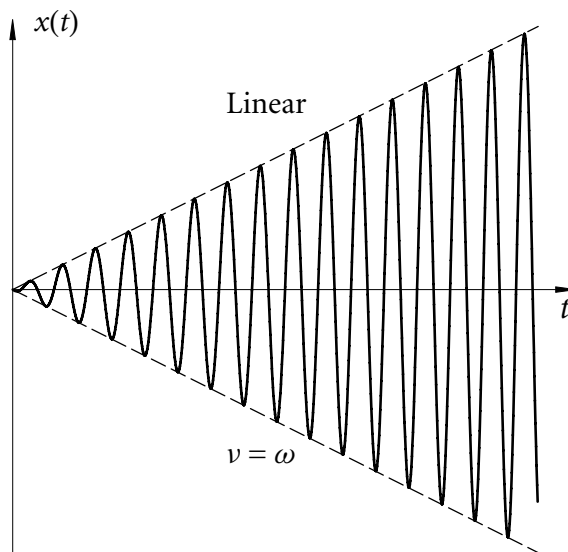


**Figure 1.4** Main Resonance - Linear Growth

These conclusions may be extended to multiple degrees-of-freedom and continuous structures as well. An  $n$  degrees-of-freedom system has  $n$  natural frequencies  $\omega_1, \omega_2, \dots, \omega_n$ , and  $n$  corresponding modes, while a continuous system has infinitely many discrete natural frequencies  $\omega_1, \omega_2, \dots$ , and corresponding modes. When the excitation frequency  $\nu$  is equal to  $\omega_i, i = 1, 2, \dots$  the system is in resonance in the  $i^{\text{th}}$  mode. Zero damping and perfect matching of forcing and natural frequencies is however still required for resonance to occur.

### 1.1.3 Parametric Resonance

Parametric resonance differs fundamentally from main resonance. It may occur when the input to a system appears in differential equation of motion as coefficients, e.g.

$$m\ddot{x}(t) + c\dot{x}(t) + [k - F(t)]x(t) = 0, \quad (1.1.7)$$

where  $F(t)$  is periodic with frequency  $\nu$ . The forcing function is therefore a parameter of the system; hence the name parametric resonance. This leads to drastically different behaviour than main resonant systems. The largest detrimental difference that this change causes is that parametric resonance can occur even in the presence of damping, unlike main resonance.

It is not possible to derive an explicit or implicit general solution of equation (1.1.7), but it can be shown that in the case of resonance, the response grows exponentially as opposed to linearly for main resonance ([14], p. 73). Figure 1.5 shows the behaviour of a typical unstable system under parametric loading.

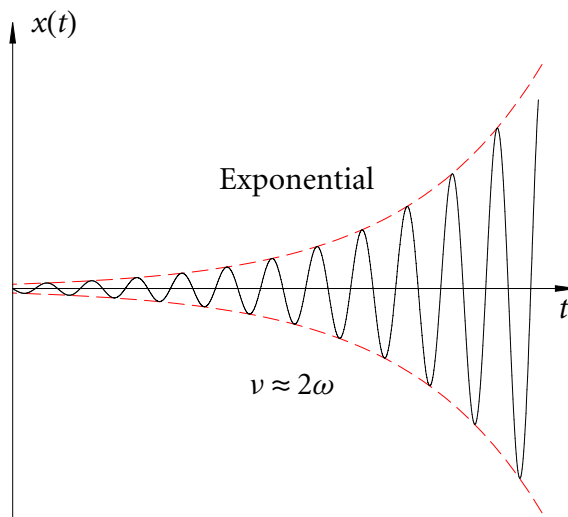


**Figure 1.5** Parametric Resonance — Exponential Growth

One characteristic of parametrically loaded systems that is actually beneficial is that in the case of non-resonant loading (forcing frequency far from resonant frequencies) the system is exponentially stable if damping is present, that is the response will decay to zero even if the loading persists. Figure 1.6 shows the response of such a stable system.

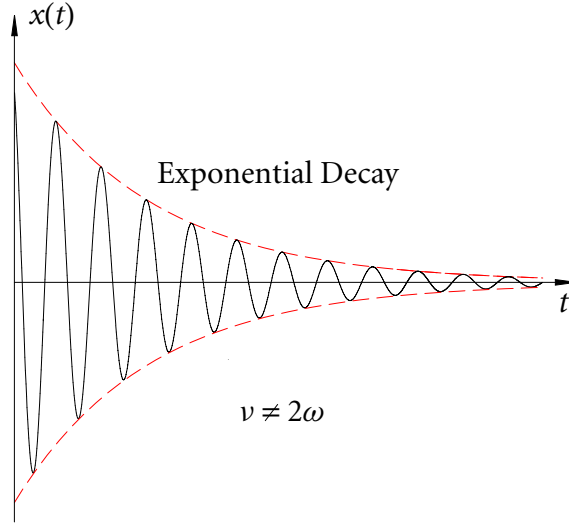


**Figure 1.6** Exponential Stability of Parametric System Loaded at Non-Resonant Frequency

Systems under non-resonant, non-parametric loading on the other hand will always reach a stable, but non-zero steady state solution whether they are damped or undamped (see equation (1.1.5)).

Therefore, parametrically loaded systems are, in a sense, exponential in nature. They are either exponentially unstable (at resonant frequencies) or exponentially stable (at non-resonant frequencies). For this thesis, however, the focus will be on resonant and near resonant frequency loading as this is most crucial to structural stability.

The resonance behaviour of parametrically loaded systems is also affected by the presence of nonlinearities. Consider a nonlinear system under sinusoidal loading

$$\ddot{q}(t) + 2\varepsilon\zeta\omega\dot{q}(t) + \omega^2 [1 - 2\varepsilon\mu \cos vt + \varepsilon\gamma q(t)^2] q(t) = 0, \quad (1.1.8)$$

where  $\mu$  is the applied load magnitude, and  $\gamma$  is a nonlinearity coefficient. The parameter  $\varepsilon$  is introduced to control the order of magnitude of damping, load, and nonlinearity.

The system response to  $F(t)$  depends greatly on the value of  $\gamma$ .

**Linear System, i.e.  $\gamma = 0$**

In this case equation(1.1.8) becomes

$$\ddot{q}(t) + 2\varepsilon\zeta\omega\dot{q}(t) + \omega^2 [1 - 2\varepsilon\mu \cos vt] q(t) = 0. \quad (1.1.9)$$

It is clear that the trivial solution,  $q(t) = 0$ , is an equilibrium solution to equation (1.1.9). If the equation represents a structural system, this trivial solution is also the desirable solution, as it represents the neutral state. Therefore the stability of this trivial solution is important.

This system is known as the damped Mathieu equation. The stability of the trivial solution of the Mathieu equation is well understood, and is discussed in detail in [14]. Figure 1.7 shows the first four stability boundaries of the trivial solution in  $(\nu/2\omega, \mu)$  space for the undamped system.

Theoretically there exist an infinite number of instability regions, however, they become increasingly small. The first instability region is of primary concern as the other regions are small in the case of small load magnitude and therefore difficult to realize in practice ([14], p. 64).

Figure 1.8 shows the first stability boundary for both a damped ( $\zeta \neq 0$ ) and undamped ( $\zeta = 0$ ) system. The first instability region is centred above  $\nu/2\omega = 1$ . This is a typical characteristic of parametrically loaded systems, and differs from main resonance where instability occurs when  $\nu = \omega$ .

It is clear from Figure 1.8 that, if the loading parameter,  $\mu$ , is sufficiently large, instability can even occur in the presence of damping. Also of note is that for a given value of  $\mu$ , the instability region is a continuous frequency band as opposed to the single frequency,  $\nu = \omega$ , in the case of main resonance.

### **Nonlinear System, i.e. $\gamma \neq 0$**

In general nonlinear differential equations may exhibit behaviour where the stability of equilibrium solutions changes, or where several equilibrium solutions are present at the same time ([2], p. 489). Both of these phenomena occur with equation (1.1.8).

If the dependant variable,  $q(t)$ , is written in terms of amplitude,  $a(t)$ , and phase,  $\phi(t)$ , i.e.

$$q(t) = a(t) \cos [\nu t + \phi(t)], \quad (1.1.10)$$

it can be shown that, together with the trivial equilibrium solution, there exist non-trivial equilibrium amplitudes of vibration,  $a_0$ , if  $\nu/2\omega \approx 1$  ([14], p. 113-118).

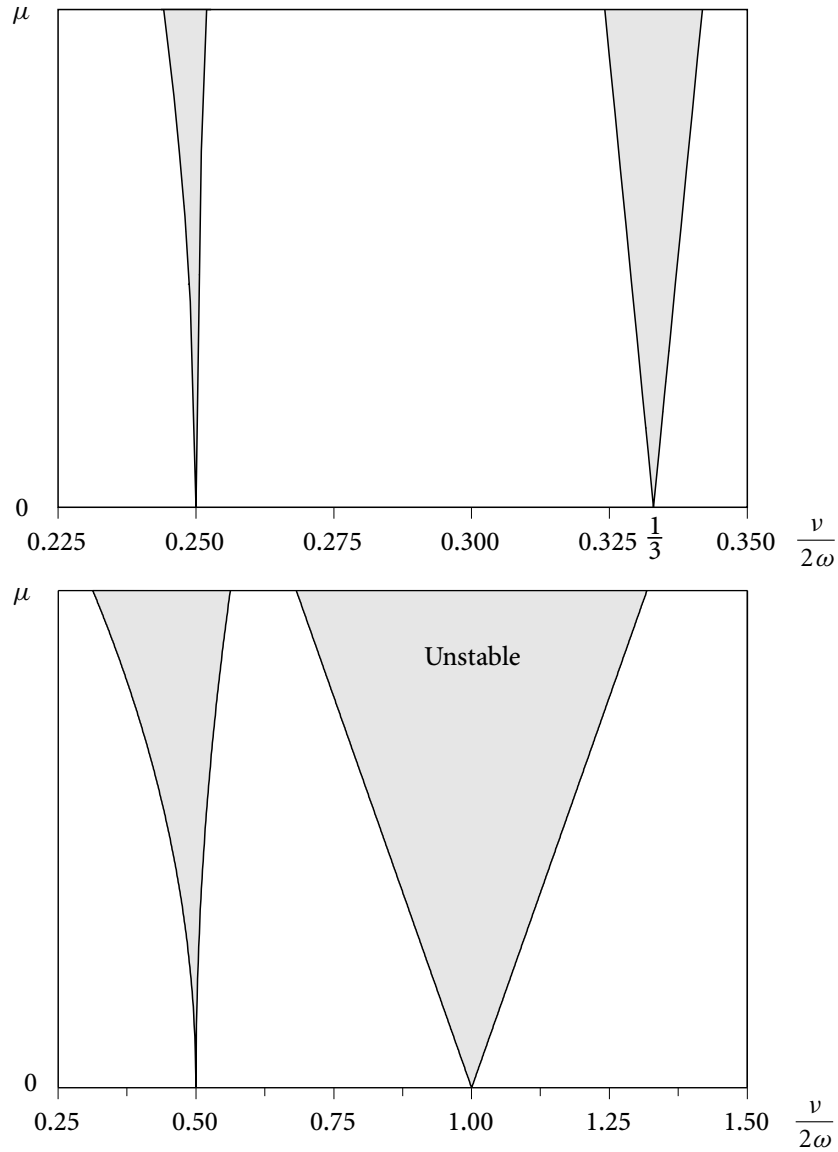


**Figure 1.7** Stability Boundaries of Undamped Linear System

Not all of the equilibrium solutions of this system are stable, however. Figure 1.9 is a typical graph of  $\bar{a}_0$  vs.  $\nu/2\omega$  for both damped ( $\zeta \neq 0$ ) and undamped ( $\zeta = 0$ ) systems. The stability of the equilibrium solutions,  $a_0$ , is also indicated by line type.

From the amplitude-frequency relationship in Figure 1.9 it is clear that the nonlinear system given by equation (1.1.8) has both stable and unstable non-trivial equilibrium amplitudes of vibration. It also shows the effect that damping has on the behaviour. In

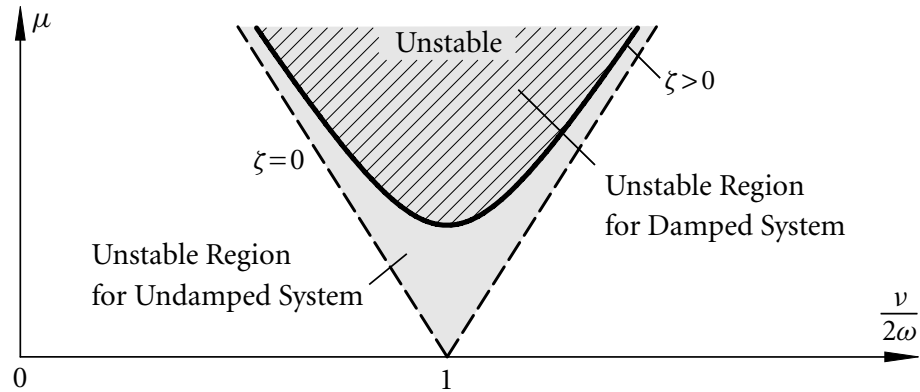


**Figure 1.8** Stability Boundaries of Damped Linear System

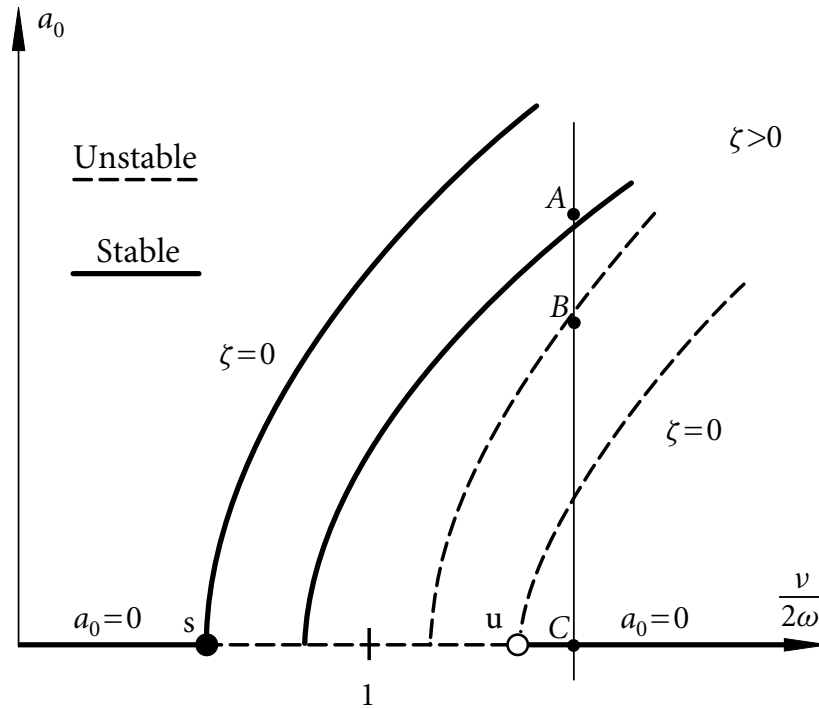


**Figure 1.9** Amplitude-Frequency Relationship of Nonlinear Systems

the presence of damping the stable and unstable equilibrium curves converge while in the undamped case they are parallel. The stems of the stable amplitude-frequency curves (curves in solid line type in Figure 1.9), which are called a pitchfork bifurcations due to their shape, are where stability shifts from the trivial solution to a non-trivial solution. The trivial

solution regains stability at the stem of the unstable amplitude-frequency curve, which results in two simultaneously locally stable solutions (the stability can only be considered to be local if two or more stable solutions co-exist).

The presence of simultaneous locally stable solutions is potentially cause for concern. Two locally stable solutions may result in jump phenomena where the response jumps back and forth between the two stable states when perturbed. This situation is analogous to the potential energy surface in Figure 1.10, where the ball could move from point A to point C if perturbed enough to get over the hill at point B. Jumping from one equilibrium position to another would appear as the vertical line in Figure 1.9, with the points A, B, C matching the same points in Figure 1.10.

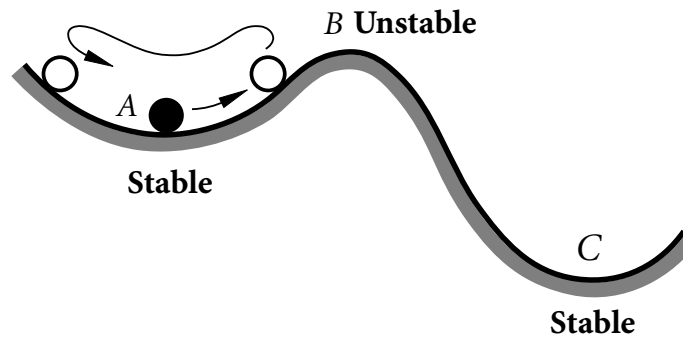


**Figure 1.10** Potential Energy Surface

Figure 1.11 shows the relationship between linear and nonlinear systems with and without damping. It is clear that the linear and nonlinear systems exhibit the same trivial solution stability behaviour. This is expected because the nonlinear term in equation (1.1.8) will always be of lower order of magnitude than linear terms near the trivial solution.

Nonlinearity actually improves the performance of the system in a certain sense. This is because in the region of trivial solution instability, a new stable non-trivial solution becomes stable. Therefore the response does not grow without bound, as it does in linear systems.

The amplitude-frequency relationships of this system will be discussed in further detail in Section 4.1.1.

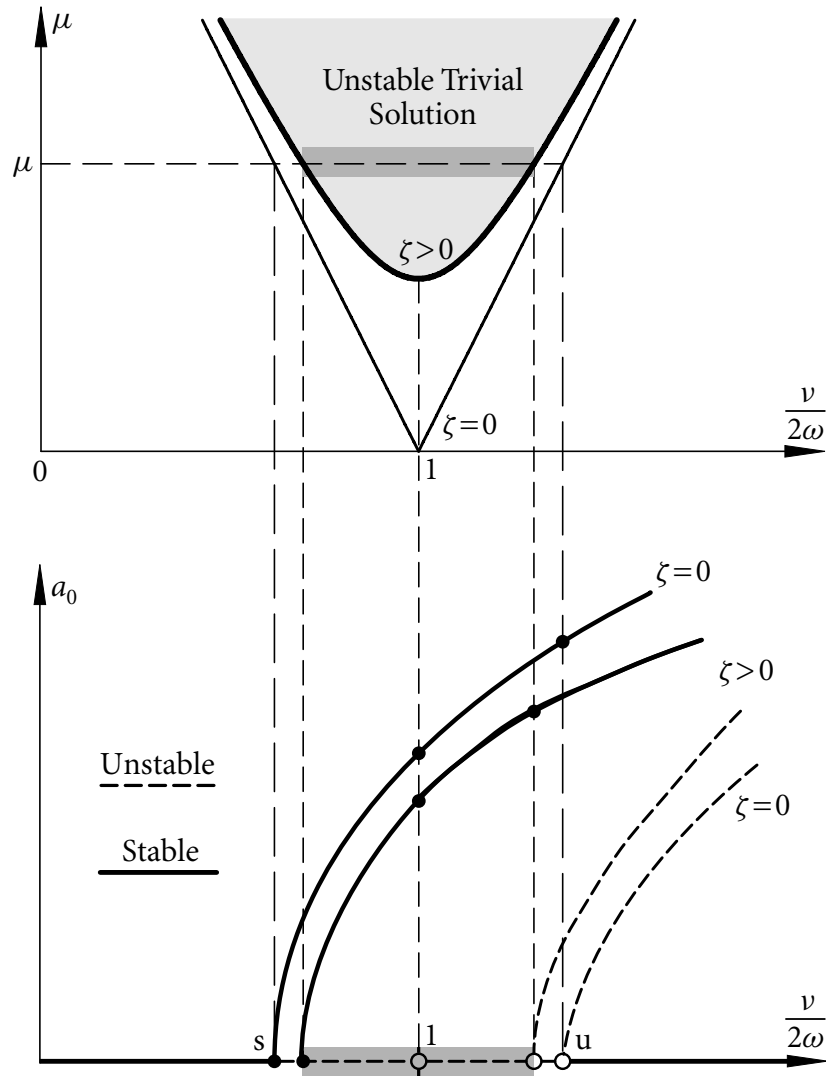


Figure 1.11 Effect of Damping in Linear and Nonlinear Systems

## 1.2 Noise Models and Stochastic Differential Equations

### 1.2.1 Stochastic Processes – General

Real world structural loadings, such as earthquake motion, wind load, and wave loading, are incredibly complex. They are the aggregate result of many correlated environmental factors working together ([9], p. 3). While it may be argued that these loads are actually deterministic at the fundamental level, when the final aggregate result is observed it appears

to behave with at least some level of randomness. Because of this, random, or stochastic processes represent real world loading of structural systems much more realistically than deterministic functions.

Consider a set of continuous random variables,  $\xi(t_i)$ , for  $i = 1, 2, \dots, N$ , where the probability distribution is given by

$$F_N(x_1, t_1; x_2, t_2; \dots; x_N, t_N) = P[\xi(t_1) < x_1, \xi(t_2) < x_2, \dots, \xi(t_N) < x_N], \quad (1.2.1)$$

and  $P[E]$  is the probability of event  $E$  occurring.

If  $t_i$  is taken to be time, then the set of all  $\xi(t_i)$  is called a discrete time stochastic process. Further, if

$$t_i = t_0 + \frac{t_{\max} - t_0}{N}i, \quad (1.2.2)$$

and the limit  $N \rightarrow \infty$  is taken, one obtains an uncountable set of random variables,  $\xi(t)$ , for all values of  $t$  between  $t_0$  and  $t_{\max}$ , which is called a continuous time stochastic process ([6], p. 269). The limits  $t_0$  and  $t_{\max}$  may be taken as small and large as desired; therefore this can also represent a process over  $0 \leq t < \infty$ .

This is a very general definition of a random process, and unfortunately the full probability density function in equation (1.2.1) is not generally attainable. In many cases, however, lower order probability distribution functions are sufficient ([14], p. 159). In the case of Gaussian distributed processes, the first and second order probability distribution functions completely describe the process.

General first and second order probability distribution functions of a stochastic process  $\xi(t)$  are given by

$$\begin{aligned} F_1(x_1, t_1) &= P[\xi(t_1) < x_1], \\ F_2(x_1, t_1; x_2, t_2) &= P[\xi(t_1) < x_1, \xi(t_2) < x_2], \end{aligned} \quad (1.2.3)$$

while the probability density functions are

$$\begin{aligned} f_1(x_1, t_1) &= P[x_1 < \xi(t_1) < x_1 + dx_1], \\ f_2(x_1, t_1; x_2, t_2) &= P[x_1 < \xi(t_1) < x_1 + dx_1, x_2 < \xi(t_2) < x_2 + dx_2]. \end{aligned} \quad (1.2.4)$$

Figure 1.12 shows a single typical realization of a stochastic process, along with the first order probability density function shown as a cross section at a few select locations. It is

important to understand that there is actually a probability density function for the random process at every point in time.

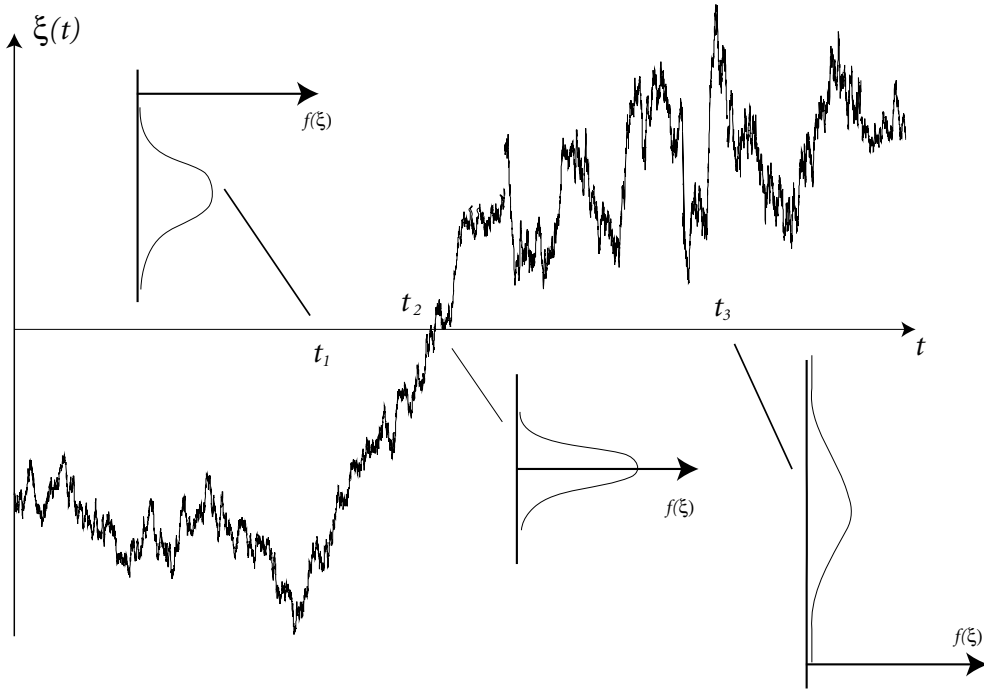


**Figure 1.12** Illustration of a Stochastic Process and its Probability Densities

### Descriptive Statistical Properties of Random Processes

If the first order probability density function of a stochastic process,  $f_1(x_1, t_1)$ , is known, it is possible to exactly determine the first moment, or mean, as well as higher moments of the process as follows:

$$m_k(t) = E[\xi^k(t)] = \int_{-\infty}^{\infty} x^k f_1(x, t) dx, \quad (1.2.5)$$

where  $m_k(t)$  is the  $k^{\text{th}}$  moment of  $\xi(t)$ .

For a stochastic process to be useful in the modelling of real systems, it should yield at least locally Lipschitz continuous realizations with probability one (w.p.1), because real events are always continuous. For example, the wind pressure at a given point on a structure cannot change instantaneously with respect to time or space.

In order for a stochastic process to be continuous there must be non-zero autocorrelation. If the second order probability density function is known, then the autocorrelation of a

random process is given by

$$R(t_1, t_2) = E[\xi(t_1)\xi(t_2)] = \int_{-\infty}^{\infty} x_1 x_2 f_2(x_1, t_1; x_2, t_2) dx_1 dx_2, \quad (1.2.6)$$

Unfortunately the probability density functions of real processes are seldom available, as the processes can often only be studied experimentally. Therefore the statistical properties cannot be obtained by direct integration as in equations (1.2.5) and (1.2.6). In general the  $k^{\text{th}}$  moment,  $m_k$  of  $\xi(t)$  is given by

$$m_k(t) = E[\xi^k(t)] = \frac{1}{N} \sum_{n=0}^N [\xi^{(n)}(t)]^k, \quad (1.2.7)$$

where  $\xi^{(n)}(t)$  is the  $n^{\text{th}}$  realization of the random process  $\xi(t)$ .

Notice that in order to evaluate equation (1.2.7) one requires the knowledge of every realization of  $\xi(t)$ . These properties are therefore called ensemble averages because the averaging is done over the entire ensemble of realizations of the process, as shown in Figure 1.13.

In practice it is impossible to obtain an ensemble average of a real process, because one can only ever observe a finite number of samples. It could even be argued that it is only possible to observe one occurrence of a real stochastic event in nature, such as wind pressures or earthquake ground accelerations. This is because every time the event occurs, it does so with different parameters as environmental factors change with time. Therefore a reoccurring event is actually an entirely new event with new parameters. In order to get an ensemble average of a real stochastic event one would need relive the event a multitude of times, which is of course ridiculous.

### Ergodic Random Processes

Ergodic processes have the property that the ensemble average is equal to the time average of individual realizations. This is a very useful property, as it allows moments to be calculated from only one sample realization of the random process ([10], p. 56 – 57). The time average of the  $k^{\text{th}}$  moment of  $\xi(t)$  is given by

$$m_k(t) = E[\xi^k(t)] = \lim_{T \rightarrow \infty} \frac{1}{T} \int_0^T [\xi^{(p)}(t)]^k dt, \quad (1.2.8)$$

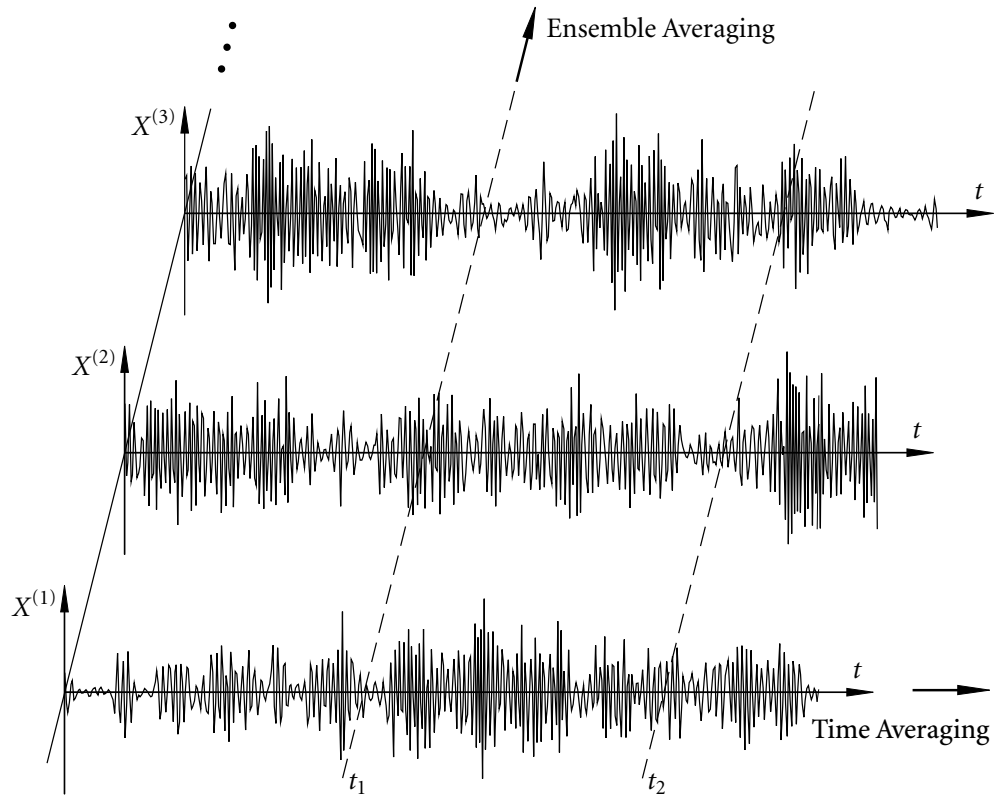


**Figure 1.13** Ensemble and Time Averages of a Stochastic Process

where the  $p^{\text{th}}$  realization from Figure 1.13 of the random process,  $\xi(t)$ , can be chosen arbitrarily.

### Stationary Random Processes

If the first order probability distribution function,  $F_1(x, t)$ , of a random process is independent of time and the second order probability distribution function depends only on the time difference  $\tau = t_2 - t_1$ , i.e. if

$$F_2(x_1, t_1; x_2, t_2) = F_2(x_1, t_1, x_2, t_1 + \tau), \quad (1.2.9)$$

is independent of  $t_1$ , the process is known as a stationary random process. Stationary processes occur when the factors driving a process do not change with time ([14], p. 158). For example, the pressure of a turbulently flowing fluid is a stationary process if the flow is

steady, earthquake ground acceleration however would not be a stationary process because all of the driving factors change rapidly.

In the case of stationary processes the autocorrelation function is also a function of the time difference only, i.e.

$$R(t_1, t_1 + \tau) = E[\xi(t_1)\xi(t_1 + \tau)], \quad (1.2.10)$$

is also independent of  $t_1$ . The proof of this is trivial and follows from the independence of  $F_2(x_1, t_1, x_2, t_1 + \tau)$  with respect to  $t_1$  in equation (1.2.9) and the definition of autocorrelation from equation (1.2.6). Autocorrelation may therefore be represented by  $R = R(\tau)$  in the case of stationary processes.

Stationarity is implied by ergodicity, and many processes are assumed to be ergodic ([14], p. 163). In this case autocorrelation can be calculated via time averaging of an individual sample, for example realization  $p$ , as follows

$$R(\tau) = \lim_{T \rightarrow \infty} \frac{1}{T} \int_0^T \xi^{(p)}(t)\xi^{(p)}(t + \tau) dt. \quad (1.2.11)$$

### Power Spectral Density

The autocorrelation function is also helpful as it may be used to obtain the power spectral density of a random process. If a random process is thought of as a signal, the power spectral density gives the distribution of the signal power at each frequency ([10], p. 68). It is therefore analogous to the frequency spectrum for deterministic processes. Power spectral density is given by the Fourier transform of the autocorrelation function, i.e.

$$S(\omega) = \int_{-\infty}^{\infty} R(\tau)e^{-i\omega\tau} d\tau. \quad (1.2.12)$$

Figure 1.14 shows several autocorrelation and corresponding power spectral density functions. This figure shows that, as one would expect, the power of a sinusoidal function is focused on only frequency (both positive and negative of same frequency), while a constant function (also a sinusoidal function with frequency zero) has power at frequency zero. Functions that are not periodic have power spread across a band of frequencies.

When modelling the dynamic stability of a structural system, the choice of stochastic process should of course be based on the properties of the loading. Because the stability of

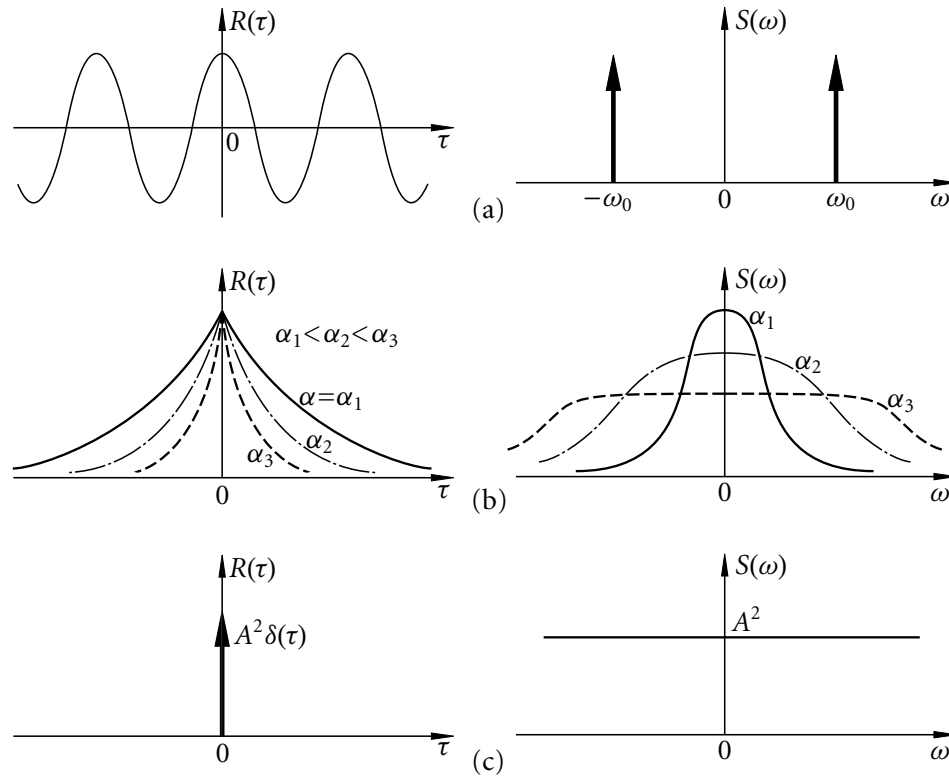


**Figure 1.14** Autocorrelation,  $R(\tau)$ , and Power Spectral Density,  $S(\tau)$

structures is primarily dependant on loading frequency, it is important that the stochastic process chosen for the model has a similar frequency spectrum. Power spectral density is therefore very useful in choosing a random process for a structural model to ensure the true resonant behaviour is properly captured.

Many stochastic processes have been developed over time for use in a wide range of applied sciences from finance to engineering. Two particular processes have proved useful in modelling of structural loads, these are the Wiener process and the bounded noise process.

### 1.2.2 The Wiener Process

The Wiener process,  $\tilde{W}(t)$ , is a zero mean Gaussian distributed continuous time random process with  $\tilde{W}(0) = 0$ . Figure 1.15 shows a typical realization of the standard Wiener process,  $W(t)$ , which is a Wiener process with variance one.

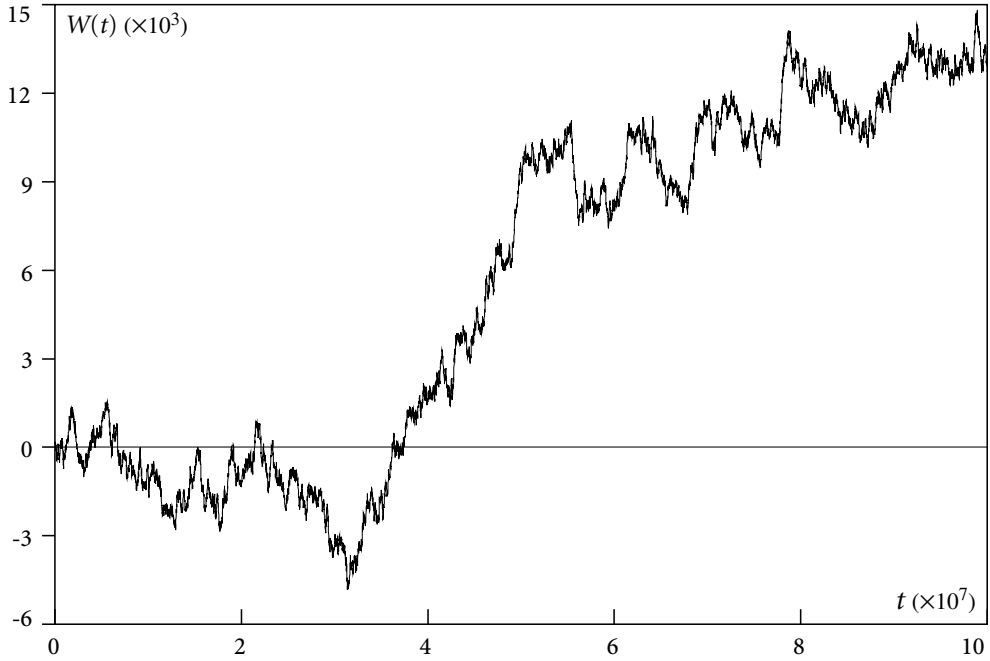


**Figure 1.15** Realization of the Wiener Process

It can be shown that  $\tilde{W}(t)$  is continuous, non-differentiable, and unbounded in its growth ([8], p./ 122-125). The autocorrelation function is

$$R(t_1, t_2) = \sigma^2 \min(t_1, t_2), \quad (1.2.13)$$

which may be used to obtain the variance of the Wiener process,

$$\text{Var}[\tilde{W}(t)] = E[\tilde{W}^2(t)] = R(t, t) = \sigma^2 t. \quad (1.2.14)$$

This result can be used to redefine the general Wiener process in terms of a unit variance Wiener process, i.e.  $\tilde{W}(t) = \sigma W(t)$ , where,  $\text{Var}[W(t)] = t$ .

When simulating the Wiener process it is useful to know the properties of its finite difference, i.e.  $\Delta \tilde{W}(t)$ . It may be shown that that it is normally distributed with mean zero and variance  $\sigma^2 \Delta t$ . The Wiener process is discussed in detail in the books by Lin & Cai [8] and Xie [14].

### 1.2.3 Bounded Noise Process

The unbounded nature of the Wiener process makes it unsuitable to modelling structural loading, as structural loads are always bounded by certain limits. However, the Wiener process is still helpful as it may be used to generate other stochastic processes.

Consider the following random process

$$\xi(t) = \cos(\nu t + \sigma W(t) + \theta). \quad (1.2.15)$$

where  $\theta$  is a uniformly distributed random variable in  $(0, 2\pi)$ , which can be shown to make the process stationary ([14], p. 199).

The process is of course bounded between  $-1$  and  $+1$ . Also notice that if  $\sigma \rightarrow 0$  the process becomes a periodic function with frequency  $\nu$ . Intuitively, one would expect that as  $\sigma$  is increased the signal should gradually lose its periodic behaviour. This is indeed true and can be seen by viewing the power spectral density of the bounded noise process in equation (1.2.15) for various  $\nu$  values and increasing  $\sigma$ , as shown in Figure 1.16.

Figure 1.16 shows that the frequency  $\nu$  begins to lose its relative dominance as  $\sigma$  increases. Therefore the process shift from a narrow band to a wide band process, as the signal's power spectral density is spread over a wider frequency band. Bounded noise therefore presents an ideal model for use as a structural loading because it may be used to represent varying types of loads.

### 1.2.4 Stochastic Ordinary Differential Equations

If the forcing function input into a differential equation of motion, such as equation (1.1.7), is a stochastic process, i.e.  $F(t) = \xi(t)$ , then the resulting equation,

$$\ddot{q}(t) + 2\varepsilon\zeta\omega\dot{q}(t) + \omega^2[1 - 2\varepsilon\mu\xi(t) + \varepsilon\gamma q(t)^2]q(t) = 0. \quad (1.2.16)$$

is a known as a stochastic ordinary differential equation (SODE).

The solution of an SODE, in this case  $q = q(t)$ , is also a stochastic process. This means that the solution can only be understood in a probabilistic sense, and no two sample outcomes will ever be exactly the same. Therefore all statements made about the behaviour of such systems must be accompanied by a probability.

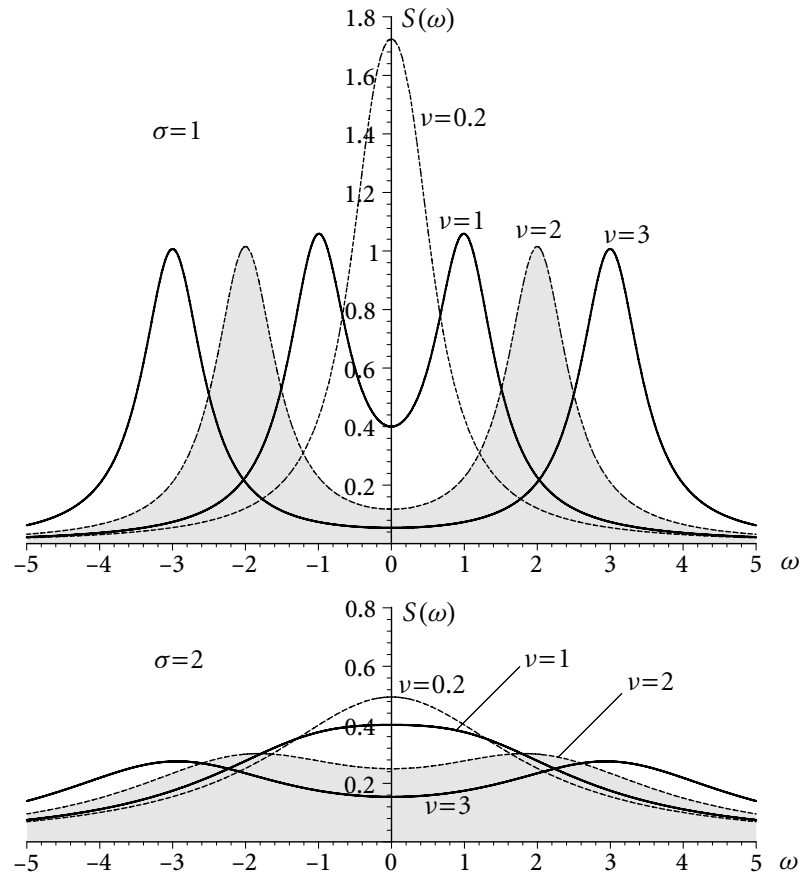


**Figure 1.16** Power Spectral Density of a Bounded Noise Process

Stochastic differential equations are usually very difficult to solve analytically if at all possible. The mathematics necessary to solve SODE's is often very complex and requires use of measure theory and functional analysis. Fortunately for systems such as equation (1.2.16), while the general solution is not attainable, the stability may be determined without directly applying these branches of mathematics. The stability may instead be determined by using Lyapunov exponents, which is introduced in Section 1.4.2.

### 1.3 Monte Carlo Simulation

In many cases where the stability of a SODE is too complex to solve analytically, it may be done numerically using Monte Carlo simulations. Monte Carlo simulation and the forward Euler numerical scheme can provide useful numerical results for nearly any SODE.

Consider the general state equation of a stochastically loaded system

$$\dot{\mathbf{x}}(t) = \mathbf{F}(\mathbf{x}(t), \xi(t), t). \quad (1.3.1)$$

Approximating the derivative with a finite difference yields

$$\Delta \mathbf{x}(t) = \mathbf{F}(\mathbf{x}(t), \xi(t), t) \Delta t. \quad (1.3.2)$$

The forward Euler time step equation is therefore

$$\mathbf{x}(t + \Delta t) = \mathbf{x}(t) + \Delta \mathbf{x}(t) = \mathbf{x}(t) + \mathbf{F}(\mathbf{x}(t), \xi(t), t) \Delta t. \quad (1.3.3)$$

Notice, however, that evaluation of this time step requires knowledge of the value of the random process,  $\xi(t)$ . Assuming for the moment that it is possible to generate samples of this random process, one may augment equation (1.3.3) with forward Euler time step equation for  $\xi(t)$ .

$$\begin{aligned} \mathbf{x}(t + \Delta t) &= \mathbf{x}(t) + \Delta \mathbf{x}(t) = \mathbf{x}(t) + \mathbf{F}(\mathbf{x}(t), \xi(t), t) \Delta t, \\ \xi(t + \Delta t) &= \xi(t) + \Delta \xi(t). \end{aligned} \quad (1.3.4)$$

If the statistical properties of  $\xi(t)$  are known, then the finite difference  $\Delta \xi(t)$  may be simulated by use of Monte Carlo simulation. Given the properties of the Wiener process discussed in Section 1.2.2, it is easy to show that

$$\Delta W(t) = \sigma \Delta W(t) = \sigma \sqrt{\Delta t} r, \quad r \sim N(0, 1). \quad (1.3.5)$$

Therefore a pseudo random number generator is necessary to simulate SODE's. The numbers are considered to be pseudo random because a deterministic algorithm can never create true random numbers. Pseudo randomness is usually sufficient however, because their statistical properties resemble true random numbers ([7], p. 11). Many random number generators have been developed over time. A procedure for generating random numbers is discussed in [14].

### Time Scaling of the Wiener Process

It is often necessary to use time scaling when solving SODE's. If time is scaled by  $\tau = \nu t$  it is clear that the Wiener process must also be scaled. This follows from

$$\Delta W(\tau) = \sqrt{\Delta \tau} r = \sqrt{\nu \Delta t} r = \sqrt{\nu} \sqrt{\Delta t} r = \sqrt{\nu} \Delta W(t), \quad (1.3.6)$$

which implies that

$$W(t) = \frac{1}{\sqrt{v}} W(\tau). \quad (1.3.7)$$

## 1.4 Stochastic Stability and the Lyapunov Exponent

### 1.4.1 Stochastic Stability

Consider once again the general SODE in equation (1.3.1). If the model represents displacements in structural system than the stability of the trivial solution is important, as zero displacement is desirable. It is however possible to define stability in a more general fashion for stationary solutions. A stationary solution  $\mathbf{x}_s(t)$  is stable in the sense of Lyapunov if ([13], p. 62, 63)

$$\|\mathbf{x}(t, \mathbf{x}(0)) - \mathbf{x}_s(t)\| < \varepsilon \text{ for all } t > 0, \text{ if } \|\mathbf{x}(0) - \mathbf{x}_s(0)\| < \delta(\varepsilon), \quad (1.4.1)$$

and asymptotically Lyapunov stable if

$$\|\mathbf{x}(t, \mathbf{x}(0)) - \mathbf{x}_s(t)\| \rightarrow 0 \text{ as } t \rightarrow \infty. \quad (1.4.2)$$

Intuitively, this means that solutions, which begin within the vicinity of a stable stationary solution, will remain within the vicinity of that solution, or even approach that solution in the asymptotically stable case. This concept may also be represented graphically. The three different paths of the two dimensional example in Figure 1.17 represent all three cases: asymptotic stability, stability, and instability.

Note that the origin in Figure 1.17 is the stationary solution whose stability is being studied. This means that the origin will move with time; however, the definitions of Lyapunov stability are still suitable and the shaded regions representing the distances  $\varepsilon$  and  $\delta(\varepsilon)$  will move together with the origin.

The stability of the trivial solution of an SODE is a special case where  $\mathbf{x}_s(t) = 0$ . The stability of steady state, or equilibrium, solutions of deterministic systems may also be encompassed by this definition. Steady state solutions are simply stationary processes with a variance of zero.

The definitions of stability and asymptotic stability in equations (1.4.1) and (1.4.2) are general enough to apply to both linear and nonlinear systems. In practice, however, it is

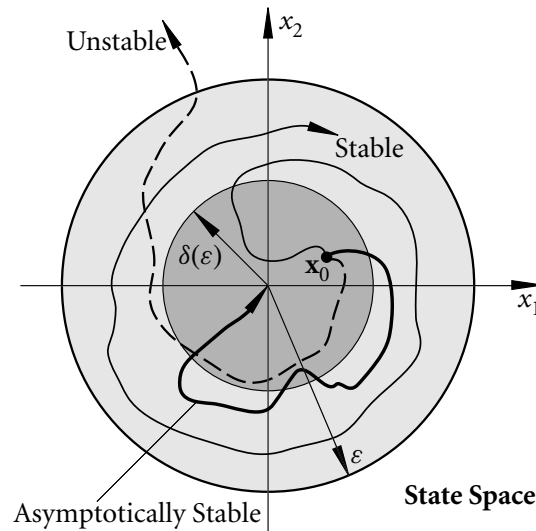


**Figure 1.17** Illustration of Stochastic Stability

usually very difficult to prove stability of solutions of nonlinear system directly. It can however be shown that if a linearized system is asymptotically stable then the full nonlinear system is also asymptotically stable ([4], p. 84-93). This is a very useful fact, and makes determining the stability of solutions of nonlinear systems much easier. Unfortunately if a linearized system is stable but not asymptotically stable, the stability of the original nonlinear system cannot be determined. In this situation the nonlinear terms in the system need to be included in the stability analysis.

## 1.4.2 The Lyapunov Exponent

The definitions of stability given in Section 1.4.1 cannot be applied directly to determine stability. Instead stochastic stability may be determined via the Lyapunov exponent.

Recall the stochastic system in equation (1.3.1). If the system is linear the largest Lyapunov exponent, often just termed the Lyapunov exponent, of the trivial solution is given by

$$\lambda = \lim_{t \rightarrow \infty} \frac{1}{t} \ln \|\mathbf{x}(t)\|. \quad (1.4.3)$$

It has been shown that, even for stochastic systems,  $\lambda$  is a deterministic number that represents the average rate of growth or decay of the system [11]. Furthermore, if  $\lambda < 0$  the

system is asymptotically stable with probability 1 (w.p.1), and if  $\lambda = 0$  it is stable w.p.1. It is an incredible result that such a concrete statement may be made about the stability of stochastic systems.

Considering that linear deterministic systems permit a solution of the form

$$y = \sum_{n=0}^N a_n e^{mx}, \quad (1.4.4)$$

it is easy to see that equation (1.4.3) returns a growth or decay rate for deterministic systems. Furthermore, because the largest eigenvalue of such systems dominates the behaviour as time grows large, the limit  $t \rightarrow \infty$  ensures that the Lyapunov exponent converges to the largest growth rate. Therefore from a heuristic standpoint it is logical that the Lyapunov exponent returns the largest average growth rate for stochastic systems.

The Lyapunov exponent is only suitable for linear systems. However, as mentioned in Section 1.4.1, the stability of nonlinear systems may be investigated via the linearized systems except for  $\lambda = 0$ . Therefore Lyapunov exponents can be used to determine the stability of nonlinear systems by simply linearizing about a solution of interest, even non-trivial solutions.

Lyapunov exponents can occasionally be determined via an analytical approach, or at least an approximate analytical approach. Unfortunately this is only possible in certain cases. The other option is to use Monte Carlo Simulation which can always give a result. The problem with using simulation alone is that the results are too specific, that is, they are only good for the parameters selected. There are so many possible combinations of parameters in most systems that using simulation to test every combination is infeasible. Simulation can also miss special or singular behaviour with specific parameters. This is especially true for nonlinear systems that exhibit bifurcating behaviour as shown in Figure 1.8. The bifurcation points are discrete, and can only be found approximately with simulation methods. Therefore the best approach is usually to get the general behaviour of the system using the analytical methods available, then use simulations in a verification role.

### Lyapunov exponent of time scaled systems

The Lyapunov exponent is a growth/decay rate. Therefore, if the time scaling  $\tau = \nu t$  is applied, the Lyapunov exponent will be changed. Given that regardless of the time variable used, a system,  $\mathbf{x}(t)$ , should have decayed or grown to the same value after some elapsed time  $t^*$  one gets

$$\begin{aligned}\|\mathbf{x}(t^*)\| &\sim e^{\lambda_t t^*}, \\ \|\mathbf{x}(\tau^*)\| &\sim e^{\lambda_\tau \tau^*} = e^{\lambda_t \nu t^*}, \\ \|\mathbf{x}(t^*)\| &= \|\mathbf{x}(\tau^*)\|,\end{aligned}\tag{1.4.5}$$

where the subscripts have been added to clarify which time scale is being used. This implies that  $\lambda_t = \nu \lambda_\tau$ . For this thesis, while many of the derivations are done in  $\tau$  space, the Lyapunov exponents will be given in  $t$  space.

## 1.5 Organization and Scope

This thesis focuses on the stability of a nonlinear stochastic differential equation representing a structural column subjected to bounded noise axial loading. Stability is determined both analytically and numerically by studying the Lyapunov exponent of the system.

In Chapter 2 the general equation of motion is derived for a structural column under bounded noise axial loading. The method of averaging is then introduced and applied to the equation of motion in order to simplify it into a more manageable form. This chapter also introduces the concept of stationary solutions of SODE's, and uses this to write the equations of variation about the stationary solutions.

Chapter 3 discusses the stability of the trivial solution. The Lyapunov exponent is derived analytically, then validated by comparison with the results of Monte Carlo simulations. Finally the effect that the system parameters, damping, load intensity, nonlinearity, and noise level have on stability is presented and discussed.

Chapter 4 covers the non-trivial stationary solutions of the system. A combined analytical-numerical approach is used to determine the mean amplitude vs. frequency relationship in the limiting cases of zero noise and large noise. This is compared with the results from Monte Carlo simulations in order to verify the results. There seems to be no analytical method capable of determining the stationary solutions for intermediate noise levels; therefore they

are determined via Monte Carlo simulations alone. The effect of system parameters have on the behaviour of the non-trivial stationary solutions is also examined.

In Chapter 5 the stability of the non-trivial stationary solution is determined by studying the Lyapunov exponent of the equation of variation. Due to the complexity of the system, this can also only be done with Monte Carlo simulations.

Finally, Chapter 6 summarizes the findings of the thesis.

# C H A **2** P T E R

## Mathematical Model of a Structural Column under Dynamic Loading

### 2.1 Equation of Motion

The stability of a column under axial loading is especially important in structural engineering. The importance is also magnified because column instability in a structure is often the worst possible scenario and can lead to progressive collapse.

What follows in this chapter is the derivation of the equation of motion of a column under bounded noise axial load for small displacements, light damping, low noise intensity, and low applied force magnitude. These restrictions are required to make the system solvable using approximate analytical methods, but do not hinder the usefulness of the model for determining stability. This seems counter intuitive, because instability generally leads to large magnitudes, i.e. large displacements or forces. However, a system must first lose stability in a small local region before it can produce these large magnitudes. Dynamic instability is also of the nature that, amplitude and damping merely have a scaling effect on the response; the decay/growth behaviour is primarily dictated by the relationship between natural frequency and loading frequency.

Consider a structural column under dynamic axial load as seen in Figure 2.1, where  $L$  is the column length,  $EI$  is the cross-sectional bending stiffness,  $A$  is the cross-sectional area,  $F(t)$  is the applied dynamic axial force,  $P$  is the internal compressive force,  $S$  is the shear

force,  $M$  is the bending moment,  $\rho$  is the mass density per unit volume,  $\beta$  is the damping,  $v$  is the transverse displacement,  $x$  is the position, and  $t$  is time.

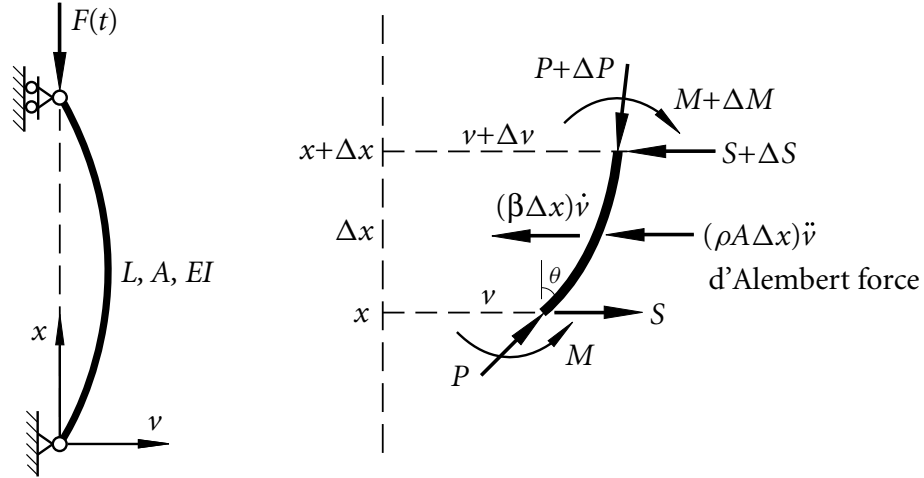


**Figure 2.1** Column Under Axial Load

Note that damping is the aggregate result of macro and microscopic energy dissipations that occur during vibration. It is not possible to model damping in its true detail but in the study of mechanical vibrations it is typically taken to be proportional to velocity.

Using dynamic force equilibrium on the differential element in the horizontal direction yields

$$\Delta S + \rho A \Delta x \ddot{v} + \beta \dot{v} \Delta x + (P + \Delta P) \sin(\theta + \Delta\theta) - P \sin \theta = 0. \quad (2.1.1)$$

For small angles one may use the relation,  $\sin \theta \approx \theta$  for  $\theta \ll 1$ , to further simplify this to

$$\Delta S + \rho A \Delta x \ddot{v} + \beta \dot{v} \Delta x + (P + \Delta P) \Delta\theta = 0. \quad (2.1.2)$$

Taking the limit as  $\Delta x$  goes to zero and ignoring all second order terms leads to

$$\frac{\partial S}{\partial x} + \rho A \ddot{v} + \beta \dot{v} + P \frac{\partial \theta}{\partial x} = 0. \quad (2.1.3)$$

Because the displacements are small one may also use the approximation  $\theta \approx v'$ , to simplify equation (2.1.3) to

$$\frac{\partial S}{\partial x} + \rho A \ddot{v} + \beta \dot{v} + P \frac{\partial^2 v}{\partial x^2} = 0. \quad (2.1.4)$$

To eliminate  $S$  one may use dynamic moment equilibrium about the centre of the differential element:

$$\Delta M - S\Delta x = 0. \quad (2.1.5)$$

Notice, however, that the moment about the centre caused by the axial forces is of higher order and may be neglected. Taking the limit as  $\Delta x \rightarrow 0$  gives

$$\frac{\partial M}{\partial x} = S \implies \frac{\partial^2 M}{\partial x^2} = \frac{\partial S}{\partial x}. \quad (2.1.6)$$

Using equation (2.1.4) to eliminate  $S$  gives

$$\frac{\partial^2 M}{\partial x^2} + \rho A \ddot{v} + \beta \dot{v} + P \frac{\partial^2 v}{\partial x^2} = 0. \quad (2.1.7)$$

The moment,  $M$ , can also be eliminated with the moment curvature relationship  $M = EIv''$  from elastic beam theory to yield

$$EI \frac{\partial^4 v}{\partial x^4} + \rho A \ddot{v} + \beta \dot{v} + P \frac{\partial^2 v}{\partial x^2} = 0. \quad (2.1.8)$$

Notice that  $EI$  is constant with respect to  $x$ , so it may be removed from the derivative.

The axial force,  $P = P(x, t)$ , is more difficult to eliminate. It is however known from elasticity theory that,  $P(x, t) = -EA\epsilon_0(x, t)$ , where  $\epsilon_0(x, t)$  is axial strain along the centre-line of the column.

It is expected that axial force will not vary greatly along the length of the column. Therefore one can approximate  $P(x, t)$  with the average axial load over the entire column,  $P_{\text{avg}}(t)$ , where

$$P = P(x, t) \approx P_{\text{avg}}(t) = -EA\epsilon_{0, \text{avg}}(t). \quad (2.1.9)$$

An expression for the average strain,  $\epsilon_{0, \text{avg}}$ , can be obtained from the deformation of a differential element of the column as shown in Figure 2.2, where  $u$  is axial deformation.

The following relationships may be easily obtained from the geometry of the differential element:

$$\Delta u = u_x \Delta x, \quad \Delta v = v_x \Delta x, \quad \Delta s = \sqrt{(\Delta u + \Delta x)^2 + \Delta v^2}. \quad (2.1.10)$$

Strain is defined as

$$\epsilon_0 = \lim_{\Delta x \rightarrow 0} \frac{\Delta s - \Delta x}{\Delta x}. \quad (2.1.11)$$

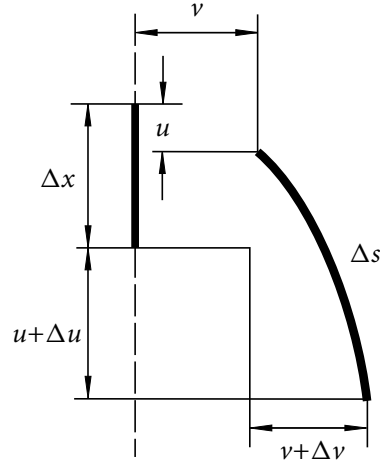


**Figure 2.2** Deformed and Un-Deformed Differential Element of Column Under Axial Load

Substituting  $\Delta s$  from equation (2.1.10) into equation (2.1.11) yields

$$\epsilon_0 = \sqrt{(1 + u_x)^2 + v_x^2} - 1. \quad (2.1.12)$$

For small displacements a second order Maclaurin series approximation:

$$f(x, y) \approx f(0, 0) + f_x(0, 0)x + f_y(0, 0)y + \frac{1}{2}[f_{xx}(0, 0) + 2f_{xy}(0, 0) + f_{yy}(0, 0)] \quad (2.1.13)$$

may be used to simplify the right side of equation (2.1.12) to

$$\epsilon_0 \approx u_x + \frac{1}{2}v_x^2. \quad (2.1.14)$$

Therefore

$$\epsilon_{0, \text{avg}} \approx \frac{1}{L} \int_0^L (u_x + \frac{1}{2}v_x^2) dx = \frac{1}{L} \left[ u(L, t) + \frac{1}{2} \int_0^L v_x^2 dx \right]. \quad (2.1.15)$$

Total axial displacement of the column  $u(L, t)$  is easily determined from strength of materials theory,

$$u(L, t) = -\frac{F(t)}{EA}L. \quad (2.1.16)$$

Finally, substituting equations (2.1.16), (2.1.15), and (2.1.9) into (2.1.8) yields the partial integro-differential equation of motion

$$EI \frac{\partial^4 v}{\partial x^4} + \rho A \ddot{v} + \beta \dot{v} + \left[ F(t) - \frac{EA}{2L} \int_0^L \left( \frac{\partial v}{\partial x} \right)^2 dx \right] \frac{\partial^2 v}{\partial x^2} = 0. \quad (2.1.17)$$

This equation is of course too complex to solve analytically. It is however not necessary to solve this system as is. The first mode of vibration is generally the most dominant; therefore it is usually enough to understand the behaviour of only the first mode. If a general expression of the first mode of vibration

$$v(x, t) = q(t) \sin \frac{\pi x}{L}, \quad (2.1.18)$$

is substituted into equation (2.1.17), one recovers a much more manageable nonlinear ordinary differential equation of the first mode displacement,  $q$ :

$$\ddot{q} + 2\varepsilon\zeta\omega\dot{q} + \omega^2[1 - \varepsilon\mu F(t) + \varepsilon\gamma q^2]q = 0, \quad (2.1.19)$$

where

$$2\varepsilon\zeta\omega = \frac{\beta}{\rho A}, \quad \omega^2 = \frac{1}{\rho A} P_1 \frac{\pi^2}{L^2}, \quad \varepsilon\mu = \frac{1}{P_1}, \quad \varepsilon\gamma = \frac{A}{4I}, \quad P_1 = EI \frac{\pi^2}{L^2}.$$

It is interesting, but not surprising, that the Euler buckling load of the first mode,  $P_1$  appears in the equation. This shows that there must be some correlation between the static and dynamic stability of columns.

The parameter  $\varepsilon$  is assumed to be small, and is introduced as a matter of convenience. As mentioned earlier, the damping and forcing are assumed to be small for this system. Furthermore, it can be seen, from the derivation of equation (2.1.19), that the nonlinear term describes the shearing effect caused by the out of place component of the axial force when the column is displaced from its neutral position. This effect can be assumed to be small because the out of plane component of the axial load is small. Therefore, the introduction of  $\varepsilon$  allows the order of magnitude of the three small terms to be controlled by just one parameter.

## 2.2 The Method of Averaging

### 2.2.1 First Order Averaging

As discussed in Section 1.2.3, the bounded noise process is well suited to modelling real world processes, due to its bounded nature and narrow band behaviour. If the function  $F(t)$  is taken to be the bounded noise process  $F(t) = 2 \cos(\nu t + \Psi)$ , where  $\Psi = \Psi(t) =$

$\varepsilon^{1/2}\sigma W(t) + \theta$ , equation (2.1.19) becomes

$$\ddot{q} + 2\varepsilon\zeta\omega\dot{q} + \omega^2[1 - 2\varepsilon\mu \cos(\nu t + \Psi) + \varepsilon\gamma q^2]q = 0. \quad (2.2.1)$$

Applying the time scaling  $\tau = \nu t$  and taking  $\tau$  as the new independent variable leads to

$$q'' + 2\varepsilon\zeta\frac{\omega}{\nu}q' + \frac{\omega^2}{\nu} [1 - 2\varepsilon\mu \cos(\tau + \bar{\Psi}) + \varepsilon\gamma q^2]q = 0. \quad (2.2.2)$$

where  $(\cdot)'$  represents differentiation with respect to  $\tau$ .

The time scaled random process  $\bar{\Psi} = \bar{\Psi}(\tau)$  may be determined from equation (1.3.7), and is given by

$$\bar{\Psi}(\tau) = \left(\frac{\varepsilon}{\nu}\right)^{1/2} \sigma W(\tau) + \theta. \quad (2.2.3)$$

Rearranging equation (2.2.2) and further introducing the parameters  $\Delta_0$  (detuning parameter) and  $\omega_0$  (reference frequency) which are defined by  $\nu = \omega_0(1 - \varepsilon\Delta_0)$  and  $\kappa = \omega/\omega_0$  in the stiffness gives

$$q'' + \left(\frac{\kappa}{1 - \varepsilon\Delta_0}\right)^2 q = \varepsilon \left[ -2\zeta\frac{\omega}{\nu}q' + 2\mu\frac{\omega^2}{\nu} \cos(\tau + \bar{\Psi})q - \gamma\frac{\omega}{\nu}q^3 \right]. \quad (2.2.4)$$

As mentioned earlier  $\varepsilon$  is small so one may use the first order Taylor series approximation  $(1 - \varepsilon\Delta_0)^{-1} \approx 1 + 2\varepsilon\Delta_0$ , which after collecting terms in  $\varepsilon$  on the right hand side yields

$$q'' + \kappa^2 q = \varepsilon \left[ -2\zeta\frac{\omega}{\nu}q' - 2\Delta_0\kappa^2 q + 2\mu\frac{\omega^2}{\nu} \cos(\tau + \bar{\Psi})q - \gamma\frac{\omega}{\nu}q^3 \right]. \quad (2.2.5)$$

The dependant variable,  $q = q(\tau)$ , appears on the right hand side of equation (2.2.5) as a forcing function, but because it is preceded by the small parameter  $\varepsilon$  its effect is small. Therefore one is tempted to use variation of parameters as if the right side was an independent forcing function. Given that the homogeneous solution to the system is given by

$$q(\tau) = a \cos(\kappa\tau + \phi) \quad (2.2.6)$$

$$q'(\tau) = -a\kappa \sin(\kappa\tau + \phi),$$

the particular solution can be taken to be

$$q(\tau) = a(\tau) \cos[\kappa\tau + \phi(\tau)] \quad (2.2.7)$$

$$q'(\tau) = -a(\tau)\kappa \sin[\kappa\tau + \phi(\tau)].$$

This relationship is illustrated in Figure 2.3. The figure clearly shows the greatest benefit of solving the system in amplitude-phase coordinates, which is that amplitude,  $a(\tau)$ , is slowly changing, whereas the original variable,  $q(\tau)$ , is fast changing. This makes the amplitude and phase equations much less sensitive to time and easier to solve.

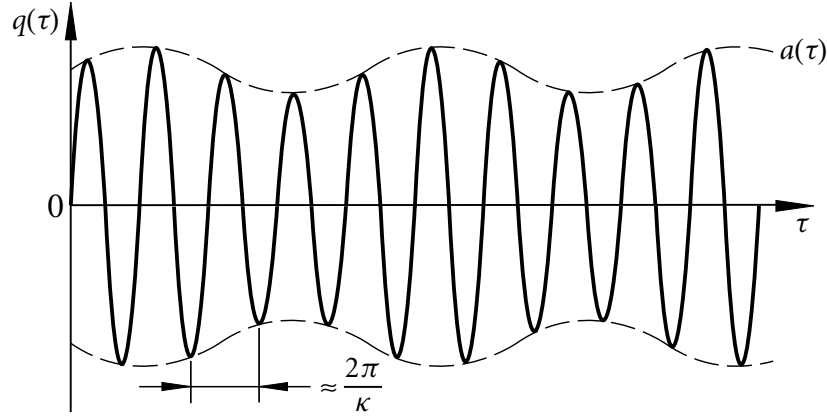


**Figure 2.3** Time Varying Amplitude of a Function

Using the method of variation of parameters and equation (2.3.5) leads to the equation of motion as a system of equations for amplitude,  $a(\tau)$ , and phase angle,  $\phi(\tau)$ ,

$$\begin{aligned}
 a' &= \varepsilon a \left\{ -\frac{\zeta \omega}{\nu} [1 - \cos(2\kappa\tau + 2\phi)] + \kappa \Delta_0 \sin(2\kappa\tau + 2\phi) \right. \\
 &\quad + \frac{\gamma \omega^2}{\kappa \nu^2} a^2 \left[ \frac{1}{8} \sin(4\kappa\tau + 4\phi) + \frac{1}{4} \sin(2\kappa\tau + 2\phi) \right] \\
 &\quad \left. - \frac{\mu \omega^2}{2\kappa \nu^2} [\sin(2\kappa\tau + 2\phi - \tau - \bar{\Psi}) + \sin(2\kappa\tau + 2\phi + \tau + \bar{\Psi})] \right\}, \\
 \phi' &= \varepsilon \left\{ -\frac{\zeta \omega}{\nu} \sin(2\kappa\tau + 2\phi) + \kappa \Delta_0 [1 + \cos(2\kappa\tau + 2\phi)] \right. \\
 &\quad + \frac{\gamma \omega^2}{\kappa \nu^2} a^2 \left[ \frac{1}{8} \cos(4\kappa\tau + 4\phi) + \frac{1}{4} \cos(2\kappa\tau + 2\phi) + \frac{3}{8} \right] \\
 &\quad - \frac{\mu \omega^2}{2\kappa \nu^2} \left[ \cos \tau + \frac{1}{2} \cos(2\kappa\tau + 2\phi - \tau - \bar{\Psi}) \right. \\
 &\quad \left. + \frac{1}{2} \cos(2\kappa\tau + 2\phi + \tau + \bar{\Psi}) \right] \left. \right\}. \tag{2.2.8}
 \end{aligned}$$

These equations are still too complex to solve analytically. Notice, however, that the right hand side is small for both equations because of the presence of the small parameter

$\varepsilon$ . This means that both  $a$  and  $\phi$  change slowly. Therefore one should obtain reasonably accurate results by averaging the response over one period. This may be done by applying the averaging operator given by [1]

$$\mathcal{M}(\cdot) = \lim_{T \rightarrow \infty} \int_{\tau}^{\tau+T} (\cdot) d\tau, \quad (2.2.9)$$

where  $(\cdot)$  represents the equations of motion. When applying the averaging operator the integration is performed over explicitly appearing  $\tau$  only.

The thin line in Figure 2.4,  $a(\tau)$ , is typical solution of equation (2.2.8). The solution demonstrates a low amplitude high frequency oscillation about a dominant low frequency large amplitude trend. The method of averaging smooths higher order fluctuation, leaving only the dominant trend. The thick line in Figure 2.4,  $\bar{a}(\tau)$ , is a typical solution of the equations of motion after application of the averaging operator. The averaging operator is also applied to the phase equation.

The effect of averaging on the phase angle is shown in Figure 2.5. This figure shows clearly that the averaged phase angle,  $\bar{\phi}$ , closely approximates the true phase angle,  $\phi$ .

It is easy to show that

$$\begin{aligned} \mathcal{M} \begin{Bmatrix} \cos \\ \sin \end{Bmatrix} (n\tau + \bar{\Psi}) &= \begin{Bmatrix} 0 \\ 0 \end{Bmatrix}, \quad n \neq 0, \\ \mathcal{M} \begin{Bmatrix} \cos \\ \sin \end{Bmatrix} (n\tau + \bar{\Psi}) &= \begin{Bmatrix} \cos \\ \sin \end{Bmatrix} (n\bar{\Psi}), \quad n = 0, \end{aligned} \quad (2.2.10)$$

which greatly simplifies equation (2.2.8), depending on the value of  $\kappa$ .

### Case 1: $\kappa \neq \frac{1}{2}$

If  $\nu$  is not near  $2\omega$ , all of the trigonometric terms vanish once the averaging operator is applied to equation (2.2.8), leaving only

$$\begin{aligned} \bar{a}' &= -\varepsilon \frac{\zeta \omega}{\nu} \bar{a}, \\ \bar{\phi}' &= \varepsilon \kappa \left( \Delta_0 + \frac{3\gamma \omega^2}{8\kappa^2 \nu^2} \bar{a}^2 \right), \end{aligned} \quad (2.2.11)$$

where  $\bar{a}$  and  $\bar{\phi}$  are the averaged amplitude and phase angle, respectively. It is clear that in the presence of damping the amplitude is exponentially stable, while in the undamped case it is stable.

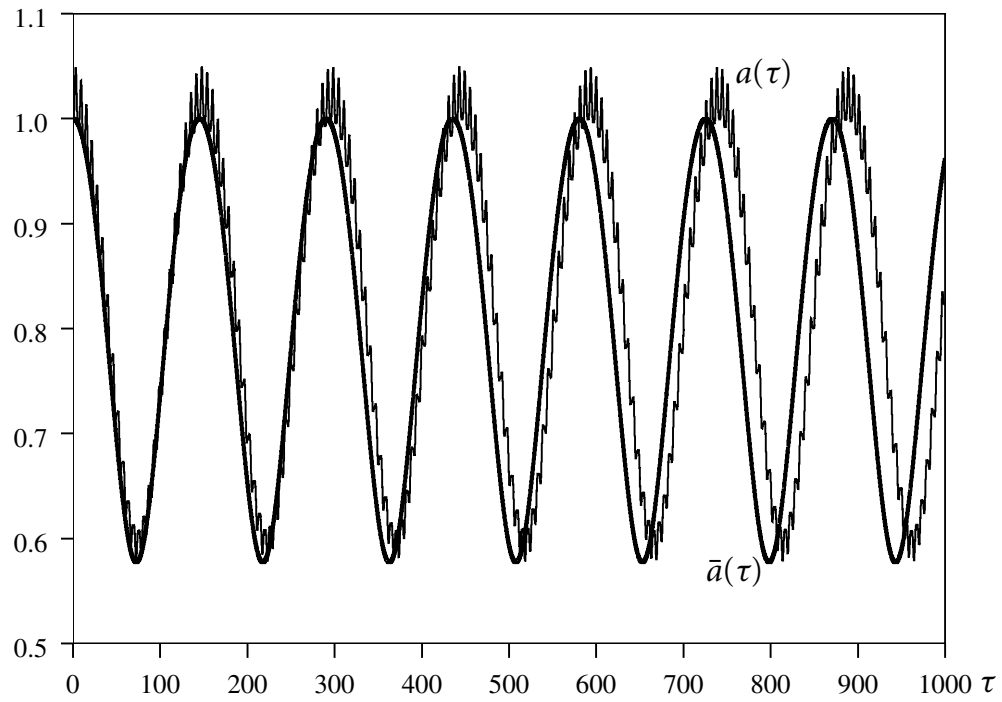


**Figure 2.4** Comparison of Averaged and Exact Amplitude

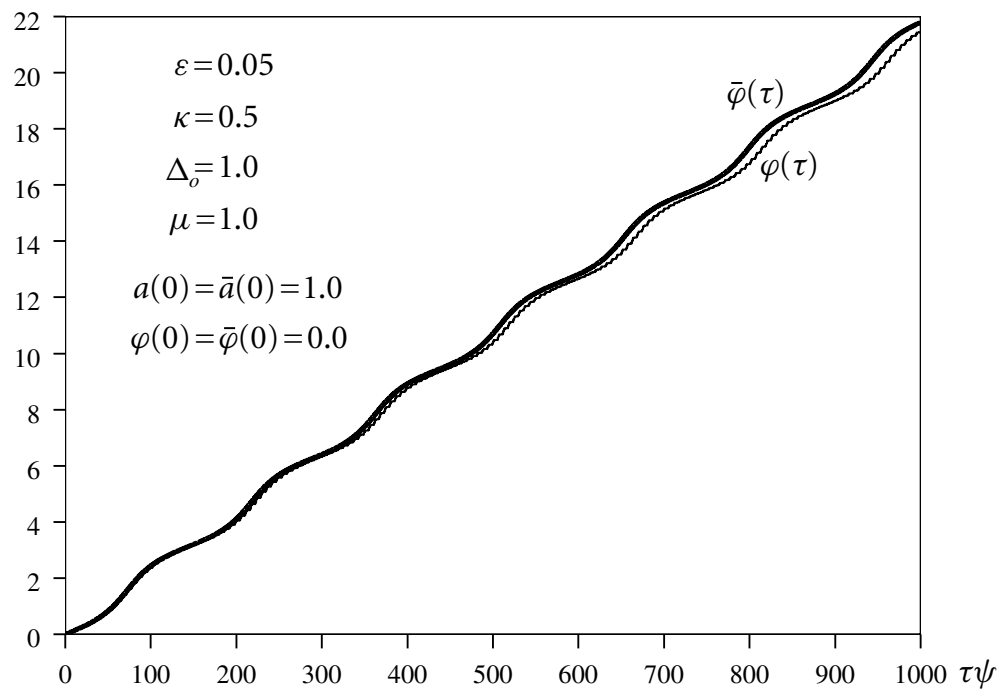


**Figure 2.5** Comparison of Averaged and Exact Phase Angle

**Case 2:**  $\kappa = \frac{1}{2}$

In this case some of the trigonometric terms do not vanish once averaged and the equations of motion become

$$\begin{aligned}\bar{a}' &= \varepsilon \bar{a}^{(1)} = -\varepsilon \left[ \frac{\zeta \omega}{\nu} + \frac{\mu \omega^2}{\nu^2} \sin(2\bar{\phi} - \bar{\Psi}) \right] \bar{a}, \\ \bar{\phi}' &= \varepsilon \bar{\phi}^{(1)} = \frac{1}{2} \varepsilon \left[ \Delta_0 + \frac{3\gamma \omega^2}{2\nu^2} \bar{a}^2 - \frac{2\mu \omega^2}{\nu^2} \cos(2\bar{\phi} - \bar{\Psi}) \right],\end{aligned}\tag{2.2.12}$$

These are the first order averaged equations of motion in the region  $\nu \approx 2\omega$ . This is the region in which instability may occur, and therefore the stability of these equations is more interesting than case 1. The equations derived in the following sections are also for this region.

## 2.2.2 Second Order Averaging

The first order averaged equations are very convenient, as they are simple enough to obtain some analytical results. They are, however, only approximations of the real system; therefore it is necessary to verify the first order results. It is difficult, if not impossible, to analytically prove convergence or divergence of the first order averaging technique. The higher order averaging techniques used in [5] can be used to heuristically check the convergence of the averaging schemes to the exact solution by inspection and comparison of results.

As seen in Figures 2.4 and 2.5, the difference between the exact and first order averaged equations, or the error, is a small higher order fluctuation. It is possible to iteratively improve on the first order averaging results by adding the averaged error. Without loss of generality, the error  $(\varepsilon a_1, \varepsilon \phi_1)$  about some, as yet unknown, averaged solutions  $\bar{a}$  and  $\bar{\phi}$  (they will be shown to be the first order averaged equations) may be given by

$$\varepsilon a_1(\bar{a}, \bar{\phi}, \tau) = a(\tau) - \bar{a}(\tau),\tag{2.2.13}$$

$$\varepsilon \phi_1(\bar{a}, \bar{\phi}, \tau) = \phi(\tau) - \bar{\phi}(\tau),\tag{2.2.14}$$

where  $(a, \phi)$  are the exact equations of motion (2.2.8). Solving for the exact equations and dropping the postscripts for clarity yields

$$a = \bar{a} + \varepsilon a_1, \quad (2.2.15)$$

$$\phi = \bar{\phi} + \varepsilon \phi_1, \quad (2.2.16)$$

Substituting equations (2.2.15) and (2.2.16) into the original equations of motion (2.2.8) and keeping only terms of orders  $\varepsilon$  and  $\varepsilon^2$ , gives

$$\begin{Bmatrix} a' \\ \phi' \end{Bmatrix} = \varepsilon \begin{Bmatrix} f_{11} \\ f_{21} \end{Bmatrix} + \varepsilon^2 \begin{Bmatrix} f_{12} \\ f_{22} \end{Bmatrix}. \quad (2.2.17)$$

where

$$\begin{aligned} f_{11} &= \bar{a} \left\{ -\frac{\zeta \omega}{\nu} [1 - C_\tau] + \frac{1}{2} \Delta_0 S_\tau + \frac{2\gamma \omega^2}{\nu^2} a^2 \left[ \frac{1}{8} S_{2\tau} + \frac{1}{4} S_\tau \right] \right. \\ &\quad \left. - \frac{\mu \omega^2}{\nu^2} [\sin(\tau + 2\bar{\phi} - \tau - \bar{\Psi}) + \sin(\tau + 2\bar{\phi} + \tau + \bar{\Psi})] \right\}, \\ f_{21} &= \left\{ -\frac{\zeta \omega}{\nu} S_\tau + \frac{1}{2} \Delta_0 [1 + C_\tau] + \frac{2\gamma \omega^2}{\nu^2} \bar{a}^2 \left[ \frac{1}{8} C_{2\tau} + \frac{1}{4} C_\tau + \frac{3}{8} \right] \right. \\ &\quad \left. - \frac{\mu \omega^2}{\nu^2} \left[ \cos \tau + \frac{1}{2} \cos(\tau + 2\bar{\phi} - \tau - \bar{\Psi}) + \frac{1}{2} \cos(\tau + 2\bar{\phi} + \tau + \bar{\Psi}) \right] \right\}, \\ f_{12} &= \frac{1}{4\nu^2} \left[ -8\bar{a}\omega\zeta\nu S_\tau \phi_1 - 8\bar{a}\mu\omega^2 \cos(2\tau + 2\bar{\phi} + \bar{\Psi}) \phi_1 + 4\bar{a}\Delta_0 C_\tau \phi_1 \nu^2 \right. \\ &\quad + 3\bar{a}^2\gamma\omega^2 a_1 S_{2\tau} - 8\bar{a}\mu\omega^2 \cos(-2\bar{\phi} + \bar{\Psi}) \phi_1 - 4a_1\omega\zeta\nu \\ &\quad + 4\gamma\omega^2 \bar{a}^3 C_\tau \phi_1 + 4\gamma\omega^2 \bar{a}^3 C_{2\tau} \phi_1 + 2a_1\Delta_0 S_\tau \nu^2 + 6\bar{a}^2\gamma\omega^2 a_1 S_\tau \\ &\quad \left. + 4a_1\omega\zeta\nu C_\tau + 4a_1\mu\omega^2 \sin(-2\bar{\phi} + \bar{\Psi}) - 4a_1\mu\omega^2 \sin(2\tau + 2\bar{\phi} + \bar{\Psi}) \right], \\ f_{22} &= \frac{1}{4\nu^2} \left[ -8\bar{a}^2\gamma\omega^2 S_\tau \phi_1 - 4\bar{a}^2\gamma\omega^2 S_{2\tau} \phi_1 + 8\mu\omega^2 \sin(2\tau + 2\bar{\phi} + \bar{\Psi}) \phi_1 \right. \\ &\quad - 8\mu\omega^2 \sin(-2\bar{\phi} + \bar{\Psi}) \phi_1 - 4\Delta_0 S_\tau \phi_1 \nu^2 - 8\omega\zeta C_\tau \phi_1 \nu + \\ &\quad \left. 8\bar{a}\gamma\omega^2 a_1 C_\tau + 6\bar{a}\gamma\omega^2 a_1 + 2\bar{a}\gamma\omega^2 a_1 C_{2\tau} \right], \\ C_\tau &= \cos(\tau + 2\bar{\phi}), \quad C_{2\tau} = \cos(2\tau + 4\bar{\phi}), \quad S_\tau = \sin(\tau + 2\bar{\phi}), \quad S_{2\tau} = \sin(2\tau + 4\bar{\phi}). \end{aligned} \quad (2.2.18)$$

Differentiating equations (2.2.15) and (2.2.16) with respect to  $\tau$  yields another expression for  $a'$  and  $\phi'$

$$\begin{Bmatrix} a' \\ \phi' \end{Bmatrix} = \begin{bmatrix} 1 + \varepsilon \frac{\partial a_1}{\partial \bar{a}} & \varepsilon \frac{\partial a_1}{\partial \bar{\phi}} \\ \varepsilon \frac{\partial \phi_1}{\partial \bar{a}} & 1 + \varepsilon \frac{\partial \phi_1}{\partial \bar{\phi}} \end{bmatrix} \begin{Bmatrix} \bar{a}' \\ \bar{\phi}' \end{Bmatrix} + \varepsilon \begin{Bmatrix} \frac{\partial a_1}{\partial \tau} \\ \frac{\partial \phi_1}{\partial \tau} \end{Bmatrix}, \quad (2.2.19)$$

or

$$\begin{Bmatrix} a' \\ \phi' \end{Bmatrix} = \mathbf{A} \begin{Bmatrix} \bar{a}' \\ \bar{\phi}' \end{Bmatrix} + \varepsilon \begin{Bmatrix} \frac{\partial a_1}{\partial \tau} \\ \frac{\partial \phi_1}{\partial \tau} \end{Bmatrix}. \quad (2.2.20)$$

By comparing equations (2.2.42) and (2.2.20) it is easy to see that

$$\begin{Bmatrix} \bar{a}' \\ \bar{\phi}' \end{Bmatrix} = \mathbf{A}^{-1} \left[ \varepsilon \begin{Bmatrix} f_{11} \\ f_{21} \end{Bmatrix} + \varepsilon^2 \begin{Bmatrix} f_{12} \\ f_{22} \end{Bmatrix} - \varepsilon \begin{Bmatrix} \frac{\partial a_1}{\partial \tau} \\ \frac{\partial \phi_1}{\partial \tau} \end{Bmatrix} \right]. \quad (2.2.21)$$

The inverse matrix,  $\mathbf{A}^{-1}$ , may be calculated as a Taylor polynomial in  $\varepsilon$  to any order desired. It is clear that for the right side of equation (2.2.21) to be of order  $\varepsilon^2$ ,  $\mathbf{A}^{-1}$  need only be determined to order  $\varepsilon$ , which can be shown to be

$$\mathbf{A}^{-1} = \begin{bmatrix} 1 - \varepsilon \frac{\partial a_1}{\partial \bar{a}} & -\varepsilon \frac{\partial a_1}{\partial \bar{\phi}} \\ -\varepsilon \frac{\partial \phi_1}{\partial \bar{a}} & 1 - \varepsilon \frac{\partial \phi_1}{\partial \bar{\phi}} \end{bmatrix}. \quad (2.2.22)$$

Applying this to equation (2.2.21) and ignoring terms of order  $\varepsilon^3$  and higher gives

$$\begin{Bmatrix} \bar{a}' \\ \bar{\phi}' \end{Bmatrix} = \begin{Bmatrix} \varepsilon \left( f_{11} - \frac{\partial a_1}{\partial \tau} \right) + \varepsilon^2 \left[ -\frac{\partial a_1}{\partial \bar{a}} \left( f_{11} - \frac{\partial a_1}{\partial \tau} \right) - \frac{\partial a_1}{\partial \bar{\phi}} \left( f_{21} - \frac{\partial \phi_1}{\partial \tau} \right) + f_{12} \right] \\ \varepsilon \left( f_{21} - \frac{\partial \phi_1}{\partial \tau} \right) + \varepsilon^2 \left[ -\frac{\partial \phi_1}{\partial \bar{a}} \left( f_{11} - \frac{\partial a_1}{\partial \tau} \right) - \frac{\partial \phi_1}{\partial \bar{\phi}} \left( f_{21} - \frac{\partial \phi_1}{\partial \tau} \right) + f_{22} \right] \end{Bmatrix}, \quad (2.2.23)$$

If the terms of order  $\varepsilon^2$  are ignored this system must return to the first order averaged equations of motion. Therefore the term of order  $\varepsilon$  in equation (2.2.23) must be equal to the first order averaging results in equation (2.2.12). This leads to

$$\begin{Bmatrix} \bar{a}^{(1)} \\ \bar{\phi}^{(1)} \end{Bmatrix} = \begin{Bmatrix} f_{11} - \frac{\partial a_1}{\partial \tau} \\ f_{21} - \frac{\partial \phi_1}{\partial \tau} \end{Bmatrix} \implies \begin{Bmatrix} a_1 \\ \phi_1 \end{Bmatrix} = \int \begin{Bmatrix} f_{11} - \bar{a}^{(1)} \\ f_{21} - \bar{\phi}^{(1)} \end{Bmatrix} d\tau, \quad (2.2.24)$$

where  $(\bar{a}^{(1)}, \bar{\phi}^{(1)})$  are indirectly defined in equation (2.2.12). Explicitly they are given by

$$\begin{Bmatrix} \bar{a}^{(1)} \\ \bar{\phi}^{(1)} \end{Bmatrix} = \begin{Bmatrix} -\left[\frac{\zeta\omega}{\nu} + \frac{\mu\omega^2}{\nu^2} \sin(2\bar{\phi} - \bar{\Psi})\right]\bar{a} \\ \frac{1}{2}\left[\Delta_0 + \frac{3\gamma\omega^2}{2\nu^2}\bar{a}^2 - \frac{2\mu\omega^2}{\nu^2} \cos(2\bar{\phi} - \bar{\Psi})\right] \end{Bmatrix}, \quad (2.2.25)$$

while  $f_{11}$  and  $f_{21}$  are defined in equation (2.2.18). Therefore  $(a_1, \phi_1)$  may be determined by substituting equations (2.2.25) and (2.2.18) into equation (2.2.24) and integrating over explicitly appearing  $\tau$ .

With  $(a_1, \phi_1)$  now known, the terms of order  $\varepsilon^2$  in equation (2.2.23) are completely defined as well. Denoting these terms as  $(a^{(2)}, \phi^{(2)})$  one has

$$\begin{Bmatrix} a^{(2)} \\ \phi^{(2)} \end{Bmatrix} = \begin{Bmatrix} -\frac{\partial a_1}{\partial \bar{a}}(f_{11} - \frac{\partial a_1}{\partial \tau}) - \frac{\partial a_1}{\partial \bar{\phi}}(f_{21} - \frac{\partial \phi_1}{\partial \tau}) + f_{12} \\ -\frac{\partial \phi_1}{\partial \bar{a}}(f_{11} - \frac{\partial a_1}{\partial \tau}) - \frac{\partial \phi_1}{\partial \bar{\phi}}(f_{21} - \frac{\partial \phi_1}{\partial \tau}) + f_{22} \end{Bmatrix}, \quad (2.2.26)$$

where  $f_{12}$  and  $f_{22}$  are also defined in equation (2.2.18).

These second order terms are very complex in their original form, however, applying the averaging operator yields

$$\begin{Bmatrix} \bar{a}^{(2)} \\ \bar{\phi}^{(2)} \end{Bmatrix} = \mathcal{N} \begin{Bmatrix} a^{(2)} \\ \phi^{(2)} \end{Bmatrix}, \quad (2.2.27)$$

which, can be shown to be:

$$\begin{aligned} \bar{a}^{(2)} &= \varepsilon \frac{\omega^2}{\nu^2} \left( 2\bar{a}\zeta\mu C_c \frac{\omega}{\nu} + \bar{a}\Delta_0\mu C_s + \frac{5}{4}\bar{a}^3\gamma C_s \frac{\omega^2}{\nu^2} \right), \\ \bar{\phi}^{(2)} &= \varepsilon \frac{\omega^2}{\nu^2} \frac{1}{32} \left( -32\zeta - 52\bar{a}^4\gamma^2 \frac{\omega^2}{\nu^2} - 48\bar{a}^2\gamma\Delta_0 + 32\Delta_0\mu C_c \right. \\ &\quad \left. + 80\gamma\bar{a}^2\mu C_c \frac{\omega^2}{\nu^2} - 64\zeta\mu C_s \frac{\omega}{\nu} - 16\mu^2 \frac{\omega^2}{\nu^2} - 8\Delta_0^2 \frac{\nu^2}{\omega^2} \right), \end{aligned} \quad (2.2.28)$$

where

$$C_c = \cos(2\bar{\phi} - \bar{\Psi}), \quad C_s = \sin(2\bar{\phi} - \bar{\Psi}). \quad (2.2.29)$$

Finally, with knowledge of both the first and second order averaged terms of equation (2.2.23), one may get the second order averaged equations of motion

$$\begin{Bmatrix} \bar{a}' \\ \bar{\phi}' \end{Bmatrix} = \varepsilon \begin{Bmatrix} \bar{a}^{(1)} \\ \bar{\phi}^{(1)} \end{Bmatrix} + \varepsilon^2 \begin{Bmatrix} \bar{a}^{(2)} \\ \bar{\phi}^{(2)} \end{Bmatrix}. \quad (2.2.30)$$

### 2.2.3 Third Order Averaging

The same procedure may be iterated to obtain the third order averaged equations of motion. For this section, however, the intermediate results  $f_{13}$  and  $f_{23}$  are not shown as they are very long winded and only disrupt the discussion. Let

$$a = \bar{a} + \varepsilon a_1 + \varepsilon^2 a_2, \quad (2.2.31)$$

$$\phi = \bar{\phi} + \varepsilon \phi_1 + \varepsilon^2 \phi_2. \quad (2.2.32)$$

Substituting these equations into the original equations of motion (2.2.8), and keeping terms of orders  $\varepsilon$ ,  $\varepsilon^2$ , and  $\varepsilon^3$ , gives

$$\begin{Bmatrix} a' \\ \phi' \end{Bmatrix} = \varepsilon \begin{Bmatrix} f_{11} \\ f_{21} \end{Bmatrix} + \varepsilon^2 \begin{Bmatrix} f_{12} \\ f_{22} \end{Bmatrix} + \varepsilon^3 \begin{Bmatrix} f_{13} \\ f_{23} \end{Bmatrix}, \quad (2.2.33)$$

Differentiating equations (2.2.31) and (2.2.32) with respect to  $\tau$  gives another expression for  $a'$  and  $\phi'$

$$\begin{Bmatrix} a' \\ \phi' \end{Bmatrix} = \begin{bmatrix} 1 + \varepsilon \frac{\partial a_1}{\partial \bar{a}} + \varepsilon^2 \frac{\partial a_2}{\partial \bar{a}} & \varepsilon \frac{\partial a_1}{\partial \bar{\phi}} + \varepsilon^2 \frac{\partial a_2}{\partial \bar{\phi}} \\ \varepsilon \frac{\partial \phi_1}{\partial \bar{a}} + \varepsilon^2 \frac{\partial \phi_2}{\partial \bar{a}} & 1 + \varepsilon \frac{\partial \phi_1}{\partial \bar{\phi}} + \varepsilon^2 \frac{\partial \phi_2}{\partial \bar{\phi}} \end{bmatrix} \begin{Bmatrix} \bar{a}' \\ \bar{\phi}' \end{Bmatrix} + \varepsilon \begin{Bmatrix} \frac{\partial a_1}{\partial \tau} \\ \frac{\partial \phi_1}{\partial \tau} \end{Bmatrix} + \varepsilon^2 \begin{Bmatrix} \frac{\partial a_2}{\partial \tau} \\ \frac{\partial \phi_2}{\partial \tau} \end{Bmatrix}, \quad (2.2.34)$$

or

$$\begin{Bmatrix} a' \\ \phi' \end{Bmatrix} = \mathbf{A} \begin{Bmatrix} \bar{a}' \\ \bar{\phi}' \end{Bmatrix} + \varepsilon \begin{Bmatrix} \frac{\partial a_1}{\partial \tau} \\ \frac{\partial \phi_1}{\partial \tau} \end{Bmatrix} + \varepsilon^2 \begin{Bmatrix} \frac{\partial a_2}{\partial \tau} \\ \frac{\partial \phi_2}{\partial \tau} \end{Bmatrix}. \quad (2.2.35)$$

By comparing equations (2.2.33) and (2.2.35) it is easy to see that

$$\begin{Bmatrix} \bar{a}' \\ \bar{\phi}' \end{Bmatrix} = \mathbf{A}^{-1} \left[ \varepsilon \begin{Bmatrix} f_{11} \\ f_{21} \end{Bmatrix} + \varepsilon^2 \begin{Bmatrix} f_{12} \\ f_{22} \end{Bmatrix} + \varepsilon^3 \begin{Bmatrix} f_{13} \\ f_{23} \end{Bmatrix} - \varepsilon \begin{Bmatrix} \frac{\partial a_1}{\partial \tau} \\ \frac{\partial \phi_1}{\partial \tau} \end{Bmatrix} - \varepsilon^2 \begin{Bmatrix} \frac{\partial a_2}{\partial \tau} \\ \frac{\partial \phi_2}{\partial \tau} \end{Bmatrix} \right]. \quad (2.2.36)$$

It is clear that, for the right side of equation (2.2.36) to be of order  $\varepsilon^3$ ,  $\mathbf{A}^{-1}$  need only be determined to order  $\varepsilon^2$ , which can be shown to be

$$\mathbf{A}^{-1} = \begin{bmatrix} 1 - \varepsilon \frac{\partial a_1}{\partial \bar{a}} + \varepsilon^2 \alpha_{11} & -\varepsilon \frac{\partial a_1}{\partial \bar{\phi}} + \varepsilon^2 \alpha_{12}, \\ -\varepsilon \frac{\partial \phi_1}{\partial \bar{a}} + \varepsilon^2 \alpha_{21} & 1 - \varepsilon \frac{\partial \phi_1}{\partial \bar{\phi}} + \varepsilon^2 \alpha_{22} \end{bmatrix}, \quad (2.2.37)$$

where

$$\begin{aligned}\alpha_{11} &= \frac{\partial a_1}{\partial \bar{a}} \frac{\partial \phi_1}{\partial \bar{a}} - \frac{\partial a_2}{\partial \bar{a}} + \left( \frac{\partial a_1}{\partial \bar{a}} \right)^2, & \alpha_{12} &= \frac{\partial a_1}{\partial \bar{\phi}} \frac{\partial \phi_1}{\partial \bar{\phi}} - \frac{\partial a_2}{\partial \bar{\phi}} + \frac{\partial a_1}{\partial \bar{\phi}} \frac{\partial a_1}{\partial \bar{a}}, \\ \alpha_{21} &= \frac{\partial \phi_1}{\partial \bar{\phi}} \frac{\partial \phi_1}{\partial \bar{a}} - \frac{\partial \phi_2}{\partial \bar{a}} + \frac{\partial \phi_1}{\partial \bar{a}} \frac{\partial a_1}{\partial \bar{a}}, & \alpha_{22} &= \frac{\partial a_1}{\partial \bar{\phi}} \frac{\partial \phi_1}{\partial \bar{a}} - \frac{\partial \phi_2}{\partial \bar{\phi}} + \left( \frac{\partial \phi_1}{\partial \bar{\phi}} \right)^2.\end{aligned}$$

Applying this to equation (2.2.36) and ignoring terms of order  $\varepsilon^4$  and higher gives

$$\begin{aligned}\begin{Bmatrix} \bar{a}' \\ \bar{\phi}' \end{Bmatrix} &= \begin{Bmatrix} \varepsilon(f_{11} - \frac{\partial a_1}{\partial \tau}) + \varepsilon^2 \left[ -\frac{\partial a_1}{\partial \bar{a}} (f_{11} - \frac{\partial a_1}{\partial \tau}) - \frac{\partial a_1}{\partial \bar{\phi}} (f_{21} - \frac{\partial \phi_1}{\partial \tau}) + f_{12} - \frac{\partial a_2}{\partial \tau} \right] \\ \varepsilon(f_{21} - \frac{\partial \phi_1}{\partial \tau}) + \varepsilon^2 \left[ -\frac{\partial \phi_1}{\partial \bar{a}} (f_{11} - \frac{\partial a_1}{\partial \tau}) - \frac{\partial \phi_1}{\partial \bar{\phi}} (f_{21} - \frac{\partial \phi_1}{\partial \tau}) + f_{22} - \frac{\partial \phi_2}{\partial \tau} \right] \end{Bmatrix} \\ + \varepsilon^3 &\begin{Bmatrix} \alpha_{11}(f_{11} - \frac{\partial a_1}{\partial \tau}) + f_{13} + \frac{\partial a_1}{\partial \bar{a}} (\frac{\partial a_2}{\partial \tau} - f_{12}) + \frac{\partial a_1}{\partial \bar{\phi}} (\frac{\partial \phi_2}{\partial \tau} - f_{22}) + \alpha_{12}(f_{21} - \frac{\partial \phi_1}{\partial \tau}) \\ \alpha_{22}(f_{21} - \frac{\partial \phi_1}{\partial \tau}) + f_{23} + \frac{\partial \phi_1}{\partial \bar{a}} (\frac{\partial a_2}{\partial \tau} - f_{12}) + \frac{\partial \phi_1}{\partial \bar{\phi}} (\frac{\partial \phi_2}{\partial \tau} - f_{22}) + \alpha_{21}(f_{11} - \frac{\partial a_1}{\partial \tau}) \end{Bmatrix}.\end{aligned}\tag{2.2.38}$$

If terms of order  $\varepsilon^3$  are ignored this should return to the second order equations of motion. Therefore the second order terms in equation (2.2.38) are equal to the averaged second order terms in equation (2.2.28). This relationship yields

$$\begin{Bmatrix} \bar{a}^{(2)} \\ \bar{\phi}^{(2)} \end{Bmatrix} = \begin{Bmatrix} -\frac{\partial a_1}{\partial \bar{a}} (f_{11} - \frac{\partial a_1}{\partial \tau}) - \frac{\partial a_1}{\partial \bar{\phi}} (f_{21} - \frac{\partial \phi_1}{\partial \tau}) + f_{12} - \frac{\partial a_2}{\partial \tau} \\ -\frac{\partial \phi_1}{\partial \bar{a}} (f_{11} - \frac{\partial a_1}{\partial \tau}) - \frac{\partial \phi_1}{\partial \bar{\phi}} (f_{21} - \frac{\partial \phi_1}{\partial \tau}) + f_{22} - \frac{\partial \phi_2}{\partial \tau} \end{Bmatrix}.\tag{2.2.39}$$

It is clear from equation (2.2.26) that this is also

$$\begin{Bmatrix} \bar{a}^{(2)} \\ \bar{\phi}^{(2)} \end{Bmatrix} = \begin{Bmatrix} a^{(2)} - \frac{\partial a_2}{\partial \tau} \\ \phi^{(2)} - \frac{\partial \phi_2}{\partial \tau} \end{Bmatrix} \implies \begin{Bmatrix} a_2 \\ \phi_2 \end{Bmatrix} = \int \begin{Bmatrix} a^{(2)} - \bar{a}^{(2)} \\ \phi^{(2)} - \bar{\phi}^{(2)} \end{Bmatrix} d\tau,\tag{2.2.40}$$

where the integration is again performed over explicit  $\tau$  only.

The terms of order  $\varepsilon^3$  in equation (2.2.38) can be determined with the new knowledge of  $(a_2, \phi_2)$ . Once again these terms are very long and complex, however, it can be shown that

once averaged these terms, denoted by  $(\bar{a}^{(3)}, \bar{\phi}^{(3)})$ , become

$$\begin{aligned}
\bar{a}^{(3)} &= \varepsilon \frac{\bar{a}}{64} \left[ 119 \frac{\omega^5}{\nu^5} \zeta \gamma^2 \bar{a}^4 - 12 \bar{a}^2 \frac{\omega^6}{\nu^6} \gamma \mu^2 \sin(4\bar{\phi} - 2\bar{\Psi}) + 32 \Delta_0 \frac{\omega^2}{\nu^2} \mu C_s \right. \\
&\quad + 64 \mu \frac{\omega^3}{\nu^3} \zeta C_c + 251 \gamma \frac{\omega^6}{\nu^6} \bar{a}^4 \mu C_s + 84 \bar{a}^2 \frac{\omega^5}{\nu^5} \gamma \mu \zeta + 80 \bar{a}^2 \frac{\omega^3}{\nu^3} \gamma \Delta_0 \zeta \\
&\quad \left. - 112 \frac{\omega^6}{\nu^6} \mu C_s + 226 \gamma \frac{\omega^4}{\nu^4} \bar{a}^2 \mu C_s \right], \\
\bar{\phi}^{(3)} &= \varepsilon \frac{1}{512} \left[ 512 \Delta_0 \frac{\omega^3}{\nu^3} \zeta \mu C_s + 96 \frac{\omega^6}{\nu^6} \bar{a}^2 \mu \gamma \cos(4\bar{\phi} - 2\bar{\Psi}) + 896 \frac{\omega^6}{\nu^6} \mu^3 C_c \right. \\
&\quad + 1392 \gamma \frac{\omega^2}{\nu^2} \bar{a}^2 \Delta_0^2 + 2643 \gamma^3 \frac{\omega^6}{\nu^6} \bar{a}^6 + 512 \Delta_0 \frac{\omega^3}{\nu^3} \zeta^2 - 384 \frac{\omega^4}{\nu^4} \mu^2 \Delta_0 \\
&\quad + 1600 \frac{\omega^5}{\nu^5} \bar{a}^2 \zeta \mu C_c - 256 \Delta_0^2 \mu \frac{\omega^2}{\nu^2} C_c - 1008 \gamma \frac{\omega^6}{\nu^6} \bar{a}^2 \mu + 128 \Delta_0^3 \\
&\quad - 2464 \frac{\omega^4}{\nu^4} \bar{a}^2 \Delta_0 \mu C_c + 1984 \bar{a}^2 \frac{\omega^4}{\nu^4} \gamma \zeta^2 + 3600 \gamma^2 \frac{\omega^4}{\nu^4} \bar{a}^4 \Delta_0 \\
&\quad \left. - 3360 \gamma^2 \frac{\omega^6}{\nu^6} \bar{a}^4 \mu C_c \right], \tag{2.2.41}
\end{aligned}$$

where  $C_c$  and  $C_s$  are as defined in equation (2.2.29).

Finally the third order averaged equations of motion are

$$\begin{Bmatrix} \bar{a}' \\ \bar{\phi}' \end{Bmatrix} = \varepsilon \begin{Bmatrix} \bar{a}^{(1)} \\ \bar{\phi}^{(1)} \end{Bmatrix} + \varepsilon^2 \begin{Bmatrix} \bar{a}^{(2)} \\ \bar{\phi}^{(2)} \end{Bmatrix} + \varepsilon^3 \begin{Bmatrix} \bar{a}^{(3)} \\ \bar{\phi}^{(3)} \end{Bmatrix}. \tag{2.2.42}$$

The second and third order averaged equations are too complex to obtain any analytical expressions for the Lyapunov exponent. They can, however, be used in the numerical scheme introduced in Section 1.3 to check the convergence of the averaged solutions to the exact solution, and thereby supply validation to the analytical expressions derived from the much simpler first order averaged equations of motion (2.2.12).

## 2.3 Equations of Variation about Non-Trivial Stationary Solutions

### 2.3.1 Procedure for Setting up Equations of Variation

The trivial solution,  $a(\tau)=0$ , of equation (2.2.8) is obviously an equilibrium solution of the equation of motion; the same is true for all of the averaged equations of motion. The

stability of this solution may be determined from Lyapunov exponent of the linearized equations of motion as discussed in Section 1.4.2. Linearization about the trivial solution may be done by simply ignoring all nonlinear terms.

In Chapter 5 it will also be shown that there exist nontrivial stationary solutions  $a(\tau) = a_s(\tau)$  of this system as well. The presence of non-trivial stationary solutions is interesting. However, to have the complete picture one must also know the stability of these solutions. The stability of a non-trivial stationary solution may be explored by studying the Lyapunov exponent of the linearized equations of variation about the stationary solutions. Equations of variation are equations of motion that describe how a system behaves in relation to some a chosen reference function or process. If the equations of variation are linearized then they can be used to study the stability of the reference function.

Consider a general first order system

$$\begin{aligned} a' &= f(a, \phi), \\ \phi' &= g(a, \phi). \end{aligned} \tag{2.3.1}$$

This may be the exact or any averaged equation of motion.

Let  $a_s$  and  $\phi_s$  be stationary solutions of the system in equation (2.3.1). These stationary solutions must also, by definition, solve the equations of motion, i.e.

$$\begin{aligned} a'_s &= f(a_s, \phi_s), \\ \phi'_s &= g(a_s, \phi_s). \end{aligned} \tag{2.3.2}$$

The general solution of any system may be written as the sum of a reference function and a variation about that reference function. Using the stationary solutions as the reference gives

$$\begin{aligned} a &= a_s + u, \\ \phi &= \phi_s + v, \end{aligned} \tag{2.3.3}$$

where  $u$  and  $v$  are the variations about the stationary solutions. Substituting this into equation (2.3.1) gives

$$\begin{aligned} a'_s + u' &= f(a_s + u, \phi_s + v), \\ \phi'_s + v' &= g(a_s + v, \phi_s + v). \end{aligned} \tag{2.3.4}$$

By subtracting equation (2.3.2) from (2.3.4), one obtains the equations of variation about the nontrivial stationary solution

$$\begin{aligned} u' &= f(a_s + u, \phi_s + \nu) - f(a_s, \phi_s), \\ \nu' &= g(a_s + \nu, \phi_s + \nu) - g(a_s, \phi_s). \end{aligned} \quad (2.3.5)$$

The final step is to linearize equation (2.3.5), which is necessary to determine Lyapunov exponents. This procedure is general enough to use on the exact equation of motion (2.2.8) or on the averaged equations of any order. While the procedure is straight forward, it can be very difficult to implement because the equations involved are long and trigonometric identities are often necessary to get the system into a form which can be linearized.

### 2.3.2 Equations of Variation from First Order Averaged System

It is quite easy to derive the equations of variation from the first order averaged system (2.2.12). Assuming a stationary solution exists, it must satisfy the equation of motion, i.e.

$$\begin{aligned} a'_s &= -\varepsilon \left[ \frac{\zeta \omega}{\nu} + \frac{\mu \omega^2}{\nu^2} \sin(2\phi_s - \bar{\Psi}) \right] a_s, \\ \phi'_s &= \frac{1}{2} \varepsilon \left[ \Delta_0 + \frac{3\gamma \omega^2}{2\nu^2} a_s^2 - \frac{2\mu \omega^2}{\nu^2} \cos(2\phi_s - \bar{\Psi}) \right]. \end{aligned} \quad (2.3.6)$$

Rewriting the general solution about the stationary solution

$$\begin{aligned} a &= a_s + u, \\ \phi &= \phi_s + \nu, \end{aligned} \quad (2.3.7)$$

and substituting this into equation (2.2.12) gives

$$\begin{aligned} a'_s + u' &= -\varepsilon \left[ \frac{\zeta \omega}{\nu} + \frac{\mu \omega^2}{\nu^2} \sin(2\phi_s + 2\nu - \bar{\Psi}) \right] (a_s + u), \\ \phi'_s + \nu' &= \frac{1}{2} \varepsilon \left[ \Delta_0 + \frac{3\gamma \omega^2}{2\nu^2} (a_s + u)^2 - \frac{2\mu \omega^2}{\nu^2} \cos(2\phi_s + 2\nu - \bar{\Psi}) \right]. \end{aligned} \quad (2.3.8)$$

To simplify the system further, the following trigonometric identities are useful

$$\begin{aligned} \sin(2\phi_s - \bar{\Psi} + 2\nu) &= \sin(2\phi_s - \bar{\Psi}) \cos 2\nu + \cos(2\phi_s - \bar{\Psi}) \sin 2\nu, \\ \cos(2\phi_s - \bar{\Psi} + 2\nu) &= \cos(2\phi_s - \bar{\Psi}) \cos 2\nu - \sin(2\phi_s - \bar{\Psi}) \sin 2\nu. \end{aligned} \quad (2.3.9)$$

Expanding  $\cos 2\nu$  and  $\sin 2\nu$  in Taylor series' and linearizing leads to  $\cos 2\nu \approx 1$  and  $\sin 2\nu \approx 2\nu$ . Therefore

$$\begin{aligned}\sin(2\phi_s - \bar{\Psi} + 2\nu) &= \sin(2\phi_s - \bar{\Psi}) + \cos(2\phi_s - \bar{\Psi})2\nu, \\ \cos(2\phi_s - \bar{\Psi} + 2\nu) &= \cos(2\phi_s - \bar{\Psi}) - \sin(2\phi_s - \bar{\Psi})2\nu.\end{aligned}\tag{2.3.10}$$

Substituting this result into equation(2.3.8) leads to

$$\begin{aligned}a'_s + u' &= -\varepsilon \left[ \frac{\zeta\omega}{\nu} + \frac{\mu\omega^2}{\nu^2} \sin(2\phi_s - \bar{\Psi}) + \frac{\mu\omega^2}{\nu^2} \cos(2\phi_s - \bar{\Psi})2\nu \right] (a_s + u), \\ \phi'_s + v' &= \frac{1}{2}\varepsilon \left[ \Delta_0 + \frac{3\gamma\omega^2}{2\nu^2} (a_s + u)^2 - \frac{2\mu\omega^2}{\nu^2} \cos(2\phi_s - \bar{\Psi}) \right. \\ &\quad \left. + \frac{2\mu\omega^2}{\nu^2} \sin(2\phi_s - \bar{\Psi})2\nu \right].\end{aligned}\tag{2.3.11}$$

Linearizing  $u$  and  $v$  and rearranging yields

$$\begin{aligned}a'_s + u' &= -\varepsilon \left[ \frac{\zeta\omega}{\nu} + \frac{\mu\omega^2}{\nu^2} \sin(2\phi_s - \bar{\Psi}) \right] a_s - \varepsilon \left[ \frac{\mu\omega^2}{\nu^2} \cos(2\phi_s - \bar{\Psi})2\nu \right] a_s \\ &\quad - \varepsilon \left[ \frac{\zeta\omega}{\nu} + \frac{\mu\omega^2}{\nu^2} \sin(2\phi_s - \bar{\Psi}) \right] u, \\ \phi'_s + v' &= \frac{1}{2}\varepsilon \left[ \Delta_0 + \frac{3\gamma\omega^2}{2\nu^2} a_s^2 - \frac{2\mu\omega^2}{\nu^2} \cos(2\phi_s - \bar{\Psi}) \right] \\ &\quad + \frac{1}{2}\varepsilon \left[ \frac{3\gamma\omega^2}{\nu^2} u a_s + \frac{2\mu\omega^2}{\nu^2} \sin(2\phi_s - \bar{\Psi})2\nu \right].\end{aligned}\tag{2.3.12}$$

Finally, subtracting equation (2.3.6) gives

$$\begin{aligned}u' &= -\varepsilon \left[ \frac{\zeta\omega}{\nu} + \frac{\mu\omega^2}{\nu^2} \sin(2\phi_s - \bar{\Psi}) \right] u - 2\varepsilon \frac{\mu\omega^2}{\nu^2} \cos(2\phi_s - \bar{\Psi}) a_s v, \\ v' &= \varepsilon \frac{3\gamma\omega^2}{2\nu^2} a_s u + 2\varepsilon \frac{\mu\omega^2}{\nu^2} \sin(2\phi_s - \bar{\Psi}) v.\end{aligned}\tag{2.3.13}$$

The stationary solutions may be considered as forcing functions because they occur as input to the system. Notice also that this is a coupled system. Unfortunately, it is very difficult, if not impossible, to determine Lyapunov exponents of coupled systems analytically. Monte Carlo simulation is therefore applied to solve the Lyapunov exponents of the non-trivial stationary solutions.

### 2.3.3 Equations of Variation from Exact System

In the case of the trivial solution the exact system need only be used in a verification role, because analytical results are available. For the non-trivial solution the stability must however be determined by simulation alone. There is no motivation to use the averaged equations of motion in this case as the exact system will always provide best answer. The averaged systems also do not provide any validation of the results, because they originate from the exact system, so agreement of results is not a validation of the model, but rather a validation of the averaging technique. Hence, the equations of variation from the exact system is all that is used to study the stability of the non-trivial stationary solutions.

Using the procedure from Section 2.3.1, it can be shown that the equations of variation about stationary solutions of equation (2.2.8) are given by

$$\begin{aligned} u' &= \varepsilon B_{11}u + \varepsilon B_{12}v, \\ v' &= \varepsilon B_{21}u + \varepsilon B_{22}v, \end{aligned} \tag{2.3.14}$$

where,

$$\begin{aligned} B_{11} &= 2\gamma \frac{\omega^2}{\nu^2} a_s C_s C_c^3 (2 + a_s) + C_s C_c \left[ \Delta_0 - 4\mu \frac{\omega^2}{\nu^2} \cos(\tau + \bar{\Psi}) \right] - 2\zeta \frac{\omega}{\nu} C_s^2, \\ B_{12} &= a_s \left[ 2\gamma \frac{\omega^2}{\nu^2} a_s^2 C_c^2 (C_c^2 - 3C_s^2) + \Delta_0 (C_c^2 - C_s^2) - 4\zeta \frac{\omega}{\nu} C_s C_c \right. \\ &\quad \left. + 4\mu \frac{\omega^2}{\nu^2} (C_s^2 - C_c^2) \cos(\tau + \bar{\Psi}) \right], \\ B_{21} &= 4\gamma \frac{\omega^2}{\nu^2} a_s C_c, \\ B_{22} &= -8\gamma \frac{\omega^2}{\nu^2} a_s C_s C_c^3 + 8\mu \frac{\omega^2}{\nu^2} C_s C_c \cos(\tau + \bar{\Psi}) + 2\zeta \frac{\omega}{\nu} (C_s^2 - C_c^2) - 2\Delta_0 C_s C_c, \end{aligned}$$

with  $C_c$  and  $C_s$  as defined in equation (2.2.29).

Notice that unlike the averaged systems, time  $\tau$  appears explicitly in this system. In principle this does not pose any problems when using numerical methods; however, numerical stability could be of concern.

## 2.4 Remarks and Conclusions

In Chapter 2 the equation of motion for the first mode of vibration of a structural column subjected to bounded noise axial load was derived. The equation is a second order nonlinear stochastic ordinary differential equation.

The method of averaging was also introduced and applied to the equation of motion. Both first order and higher order averaged versions of the equation of motion were derived. The first order averaged equations are very useful, and are used in Chapter 3 to analytically determine the Lyapunov exponents of the system. In Chapter 4 the first order averaged system is also used to determine non-trivial stationary solutions of the system. The higher order averaged systems are actually more complex than the original exact equations of motion, and therefore cannot be used to provide any analytical result. These equations are used in Chapters 4 and 5 to check the convergence of the averaging method to the exact solution, and thereby provide a verification of the analytical results obtained via first order averaging.

The equations of variation about the non-trivial solutions were also derived in this chapter. These equations are used in Chapter 5 to determine the stability of the non-trivial stationary solutions.

# C H A 3 T E R

## Stability of The Trivial Solution

### 3.1 Analytical Results – Lyapunov Exponents

From a structural engineering perspective, an asymptotically stable trivial solution is usually desirable. If an asymptotically stable system is perturbed by some loading, it will always return to the neutral state eventually.

The stability of a column under bounded noise axial load may be determined analytically from the linearized first order averaged equations of motion (2.2.12), which are

$$\begin{aligned}\bar{a}' &= -\varepsilon \left[ \frac{\zeta \omega}{\nu} + \frac{\mu \omega^2}{\nu^2} \sin(2\bar{\phi} - \bar{\Psi}) \right] \bar{a}, \\ \bar{\phi}' &= \frac{1}{2} \varepsilon \left[ \Delta_0 - \frac{2\mu \omega^2}{\nu^2} \cos(2\bar{\phi} - \bar{\Psi}) \right],\end{aligned}\tag{3.1.1}$$

or

$$\begin{aligned}\frac{d\bar{a}}{\bar{a}} &= -\varepsilon \left[ \frac{\zeta \omega}{\nu} + \frac{\mu \omega^2}{\nu^2} \sin(2\bar{\phi} - \bar{\Psi}) \right] d\tau, \\ d\bar{\phi} &= \frac{1}{2} \varepsilon \left[ \Delta_0 - \frac{2\mu \omega^2}{\nu^2} \cos(2\bar{\phi} - \bar{\Psi}) \right] d\tau,\end{aligned}\tag{3.1.2}$$

where

$$\bar{\Psi} = \left( \frac{\varepsilon}{\nu} \right)^{1/2} \sigma W(\tau) + \theta.$$

Using the change of variables

$$\rho = \ln \bar{a}, \quad \Theta = \bar{\phi} - \frac{1}{2} \bar{\Psi},\tag{3.1.3}$$

and noting that

$$d\Theta = d\bar{\phi} - \frac{1}{2}d\bar{\Psi} = d\bar{\phi} - \frac{1}{2}\left(\frac{\varepsilon}{\nu}\right)^{1/2}\sigma dW, \quad (3.1.4)$$

one may get

$$\begin{aligned} d\rho &= -\varepsilon\left[\frac{\zeta\omega}{\nu} + \frac{\mu\omega^2}{\nu^2}\sin(2\Theta)\right]d\tau, \\ d\Theta &= \frac{1}{2}\varepsilon\left[\Delta_0 - \frac{2\mu\omega^2}{\nu^2}\cos(2\Theta)\right]d\tau - \frac{1}{2}\left(\frac{\varepsilon}{\nu}\right)^{1/2}\sigma dW. \end{aligned} \quad (3.1.5)$$

Using the definition of the Lyapunov exponent from Section 1.4.2, gives

$$\begin{aligned} \lambda_\tau &= \lim_{\tau \rightarrow \infty} \frac{1}{\tau} \ln \bar{a}(\tau) = \lim_{\tau \rightarrow \infty} \frac{1}{\tau} \rho(\tau) = \lim_{\tau \rightarrow \infty} \frac{1}{\tau} \int_0^\tau -\varepsilon\left[\frac{\zeta\omega}{\nu} + \frac{\mu\omega^2}{\nu^2}\sin(2\Theta)\right]d\tau \\ &= -\frac{\varepsilon\mu\omega^2}{\nu^2}E[\sin 2\Theta] - \frac{\varepsilon\zeta\omega}{\nu}. \end{aligned} \quad (3.1.6)$$

Note that while the equation of motion (3.1.1) is second order, the stability is determined by amplitude,  $\bar{a}$ , alone. Therefore,  $\bar{\phi}$  appears in equation (3.1.6) only indirectly due to the coupling of amplitude and phase in the equation of motion (3.1.1).

Unfortunately evaluation of the expectation  $E[\sin 2\Theta]$  is quite difficult and requires the use of a Fokker-Planck equation to determine the probability distribution of  $\Theta$  ([14], p. 312). The Fokker-Planck equation for  $\Theta$  in this system is given by

$$\frac{1}{2}\left(\sqrt{\frac{\varepsilon}{\nu}}\frac{1}{2}\sigma\right)^2 \frac{d^2p(\Theta)}{d\Theta^2} - \frac{d}{d\Theta}\left[\frac{1}{2}\varepsilon\left(\Delta_0 - \frac{2\mu\omega^2}{\nu^2}\cos 2\Theta\right)p(\Theta)\right] = 0. \quad (3.1.7)$$

Integrating this yields,

$$\frac{dp(\Theta)}{d\Theta} - 2(\alpha + \beta \cos 2\Theta)p(\Theta) = C_1, \quad (3.1.8)$$

where

$$\alpha = \frac{2\Delta_0\nu}{\sigma^2}, \quad \beta = -\frac{4\mu\omega^2}{\nu\sigma^2},$$

and  $C_1$  is an integration constant. The solution of this equation is quite complex; fortunately a general solution for this equation is given in ([14], p. 315). The solution is given by

$$E[\sin 2\Theta] = F_I(\alpha, \beta) = \frac{1}{2}\left[\frac{I_{i\alpha+1}(\beta)}{I_{i\alpha}(\beta)} + \frac{I_{-i\alpha+1}(\beta)}{I_{-i\alpha}(\beta)}\right], \quad (3.1.9)$$

where  $I_\eta(x)$  is the Bessel function of imaginary argument  $\eta$ . This may also be written as

$$I_\eta(x) = e^{-i\eta\pi/2} J_\eta(ix), \quad (3.1.10)$$

where  $J_\eta(x)$  is the Bessel function of the first kind.

Therefore, the Lyapunov exponent of the trivial solution is given by

$$\lambda_\tau = -\frac{\varepsilon\mu\omega^2}{\nu^2} F_I(\alpha, \beta) - \frac{\varepsilon\zeta\omega}{\nu}, \quad (3.1.11)$$

or in  $t$  space

$$\lambda_t = \nu\lambda_\tau = -\frac{\varepsilon\mu\omega^2}{\nu} F_I(\alpha, \beta) - \varepsilon\zeta\omega. \quad (3.1.12)$$

Note: For the remaining discussion, Lyapunov exponents are always in  $t$  space.

A symbolic mathematical software, such as Maple, may be used to evaluate the Bessel functions and calculate the Lyapunov Exponent. Figure 3.1 shows typical results of Lyapunov exponent vs.  $\nu/2\omega$  for typical values of damping  $\zeta$ , load intensity  $\mu$ , and noise intensity  $\sigma$ .

The Lyapunov exponent is positive in the region  $\nu \approx 2\omega$ . This means that the trivial solution is unstable and the response will diverge exponentially from the trivial solution as shown in Figure 1.5 in Chapter 1. The exponential divergence from the trivial solution will however only occur in a small region near the trivial solution. As the response grows, the nonlinear term in equation (2.2.12) begins to have a larger effect and the linearized model will no longer properly represent the system. Note that the effects of the system parameters in Figure 3.1 is discussed in Section 3.3.

This expression for the Lyapunov exponent is analytically obtainable because of several approximations that are made in the averaging process. Therefore it is necessary to validate using Monte Carlo simulation. The validation is done in two ways. First by comparing analytical results to those obtained numerically from the exact system (2.2.8). Second, the convergence of the averaging scheme is examined by plotting the Lyapunov exponents obtained for each order of averaging. If the Lyapunov exponent curves approach the exact curve as averaging order is increased, it is a good evidence that the averaging scheme is convergent to the exact solution.

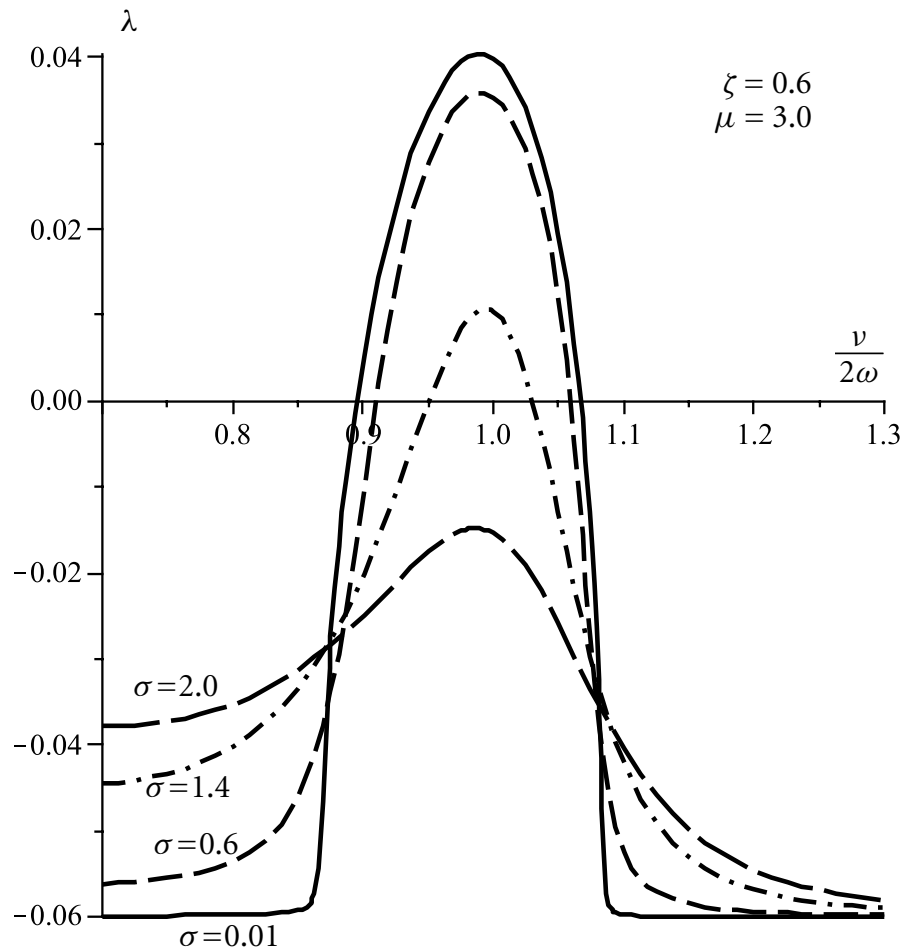


**Figure 3.1** Typical Lyapunov Exponent vs.  $v/2\omega$  Curves

## 3.2 Monte Carlo Simulation of Lyapunov Exponents

### 3.2.1 Numerical Algorithm

In this section, a procedure for evaluating Lyapunov exponents of the trivial solution of the equation of motion of a column under bounded noise axial loading is presented. The procedure may be applied to the exact or averaged equations of motion; however the exact equations will be used to demonstrate the method as follows:

### Step 1 - Linearize equations of motion about trivial solution

If the nonlinear terms in  $a$  in the exact equation of motion (2.2.8) are ignored, one obtains

$$\begin{aligned}
 da &= \varepsilon a \left\{ -\frac{\zeta\omega}{\nu} \left[ 1 - \cos(2\kappa\tau + 2\phi) \right] + \kappa\Delta_0 \sin(2\kappa\tau + 2\phi) \right. \\
 &\quad \left. - \frac{\mu\omega^2}{2\kappa\nu^2} \left[ \sin(2\kappa\tau + 2\phi - \tau - \bar{\Psi}) + \sin(2\kappa\tau + 2\phi + \tau + \bar{\Psi}) \right] \right\} d\tau, \\
 d\phi &= \varepsilon \left\{ -\frac{\zeta\omega}{\nu} \sin(2\kappa\tau + 2\phi) + \kappa\Delta_0 \left[ 1 + \cos(2\kappa\tau + 2\phi) \right] \right. \\
 &\quad \left. - \frac{\mu\omega^2}{2\kappa\nu^2} \left[ \cos\tau + \frac{1}{2} \cos(2\kappa\tau + 2\phi - \tau - \bar{\Psi}) \right. \right. \\
 &\quad \left. \left. + \frac{1}{2} \cos(2\kappa\tau + 2\phi + \tau + \bar{\Psi}) \right] \right\} d\tau.
 \end{aligned} \tag{3.2.1}$$

This system may also be augmented by derivative of the noise,  $\bar{\Psi}$ ,

$$d\bar{\Psi} = \left( \frac{\varepsilon}{\nu} \right)^{1/2} \sigma dW. \tag{3.2.2}$$

Unlike the equations of variation in Section 2.3, the phase angle,  $\phi$ , should not be linearized for the trivial solution. This is because the amplitude alone dictates the stability, and the phase angle is not necessarily small for a stable system.

### Step 2 - Write forward Euler time step equation

The augmented system shown in equations (3.2.1) and (3.2.2) may be approximated by finite difference equations

$$\begin{aligned}
 \Delta a &= \varepsilon a \left\{ -\frac{\zeta\omega}{\nu} \left[ 1 - \cos(2\kappa\tau + 2\phi) \right] + \kappa\Delta_0 \sin(2\kappa\tau + 2\phi) \right. \\
 &\quad \left. - \frac{\mu\omega^2}{2\kappa\nu^2} \left[ \sin(2\kappa\tau + 2\phi - \tau - \bar{\Psi}) + \sin(2\kappa\tau + 2\phi + \tau + \bar{\Psi}) \right] \right\} \Delta\tau, \\
 \Delta\phi &= \varepsilon \left\{ -\frac{\zeta\omega}{\nu} \sin(2\kappa\tau + 2\phi) + \kappa\Delta_0 \left[ 1 + \cos(2\kappa\tau + 2\phi) \right] \right. \\
 &\quad \left. - \frac{\mu\omega^2}{2\kappa\nu^2} \left[ \cos\tau + \frac{1}{2} \cos(2\kappa\tau + 2\phi - \tau - \bar{\Psi}) \right. \right. \\
 &\quad \left. \left. + \frac{1}{2} \cos(2\kappa\tau + 2\phi + \tau + \bar{\Psi}) \right] \right\} \Delta\tau, \\
 \Delta\bar{\Psi} &= \left( \frac{\varepsilon}{\nu} \right)^{1/2} \sigma \Delta W,
 \end{aligned} \tag{3.2.3}$$

or in shorter form

$$\Delta \begin{Bmatrix} a \\ \phi \\ \bar{\Psi} \end{Bmatrix} (\tau) = \mathbf{f}(a, \phi, \bar{\Psi}, \tau) \Delta \tau + \mathbf{g}(a, \phi, \bar{\Psi}, \tau) \Delta W, \quad (3.2.4)$$

where

$$\mathbf{f}(a, \phi, \bar{\Psi}, \tau) = \begin{Bmatrix} \Delta a / \Delta \tau \\ \Delta \phi / \Delta \tau \\ 0 \end{Bmatrix}, \quad \mathbf{g}(a, \phi, \bar{\Psi}, \tau) = \begin{Bmatrix} 0 \\ 0 \\ (\varepsilon/\nu)^{1/2} \sigma \end{Bmatrix}.$$

The time step equation therefore becomes

$$\begin{aligned} \begin{Bmatrix} a \\ \phi \\ \bar{\Psi} \end{Bmatrix} (\tau + \Delta \tau) &= \begin{Bmatrix} a \\ \phi \\ \bar{\Psi} \end{Bmatrix} (\tau) + \Delta \begin{Bmatrix} a \\ \phi \\ \bar{\Psi} \end{Bmatrix} (\tau) \\ &= \begin{Bmatrix} a \\ \phi \\ \bar{\Psi} \end{Bmatrix} (\tau) + \mathbf{f}(a, \phi, \bar{\Psi}, \tau) \Delta \tau + \mathbf{g}(a, \phi, \bar{\Psi}, \tau) \Delta W \end{aligned} \quad (3.2.5)$$

### Step 3 - Choose initial conditions

In the case of a deterministic system, it is possible that a wrong choice of initial conditions can lead to incorrect results. For example, the system  $\ddot{y} - y = 0$ , which has the solution  $y = Ae^t + Be^{-t}$ , has an unstable trivial solution due to the  $e^t$  term. However if one chose the initial conditions,  $y(0) = 1$  and  $\dot{y}(0) = -1$ , only the stable eigenfunction survives and the solution becomes,  $y = e^{-t}$ . This result may lead one to erroneously conclude that the trivial solution is stable. Therefore, one needs to avoid choosing initial conditions that are entirely inside a stable eigenspace. This situation is, however, not possible for SODE's ([14], p. 280). Therefore, the initial conditions

$$\begin{Bmatrix} a \\ \phi \\ \bar{\Psi} \end{Bmatrix} (0) = \begin{Bmatrix} a_0 \\ \phi_0 \\ \bar{\Psi}_0 \end{Bmatrix}. \quad (3.2.6)$$

may be chosen freely. Of course the choice  $a_0 = 0$  would always lead to a stable solution, therefore a non-zero number should be chosen.

From the definition of  $\bar{\Psi}$  one can also get

$$\bar{\Psi}_0 = \bar{\Psi}(0) = \left(\frac{\varepsilon}{\nu}\right)^{1/2} \sigma W(0) + \theta. \quad (3.2.7)$$

The fact that  $W(0)=0$  leads to  $\bar{\Psi}_0=\theta$ . Therefore  $\bar{\Psi}_0$  is a uniform randomly distributed variable in  $(0, 2\pi)$ .

#### Step 4 - Perform time stepping

Using a computer program, one may iterate equation (3.2.6) up to any time,  $\tau = T$ , desired. For every time step the random number  $\Delta W$  is given by

$$\Delta W(\tau) = r\sqrt{\Delta\tau}. \quad (3.2.8)$$

where  $r$  is a standard normally distributed number.

#### Step 5 - Calculate Lyapunov exponent

Using equation (1.4.3) one may approximate the Lyapunov exponent:

$$\lambda = \lambda_t = \nu\lambda_\tau = \lim_{\tau \rightarrow \infty} \frac{\nu}{\tau} \ln a(\tau) \approx \frac{\nu}{T} \ln a(T), \text{ if } T \text{ is large,} \quad (3.2.9)$$

where  $T$  is the simulation time. The choice of  $T$  is somewhat arbitrary. It is useful to perform a sensitivity analysis for different values of  $T$  to test convergence. Depending on the convergence rate, and assuming that the convergence is indeed to the exact Lyapunov exponent, one may have to run simulations of different time spans,  $T$ . Figure 3.2 shows typical Lyapunov exponent vs.  $\nu/2\omega$  curves calculated from equation (2.2.8) using different values of  $T$ . It is clear that the convergence is generally quick. This is expected due to the exponential nature of parametric systems.

The time step  $\Delta\tau$ , chosen for the simulation can also affect the results. Generally the smaller the time step is, the better the results are. There are of course practical limits to this as smaller time steps may introduce excessive rounding error due to the extra steps required to reach the termination time  $T$ . Small time steps may also make simulations needlessly computationally expensive, as good results are often attainable with large step. Figure 3.3 shows typical Lyapunov exponent vs.  $\nu/2\omega$  curves simulated from equation (2.2.8) using various time steps. These results show that the curves converge for relatively large time steps.

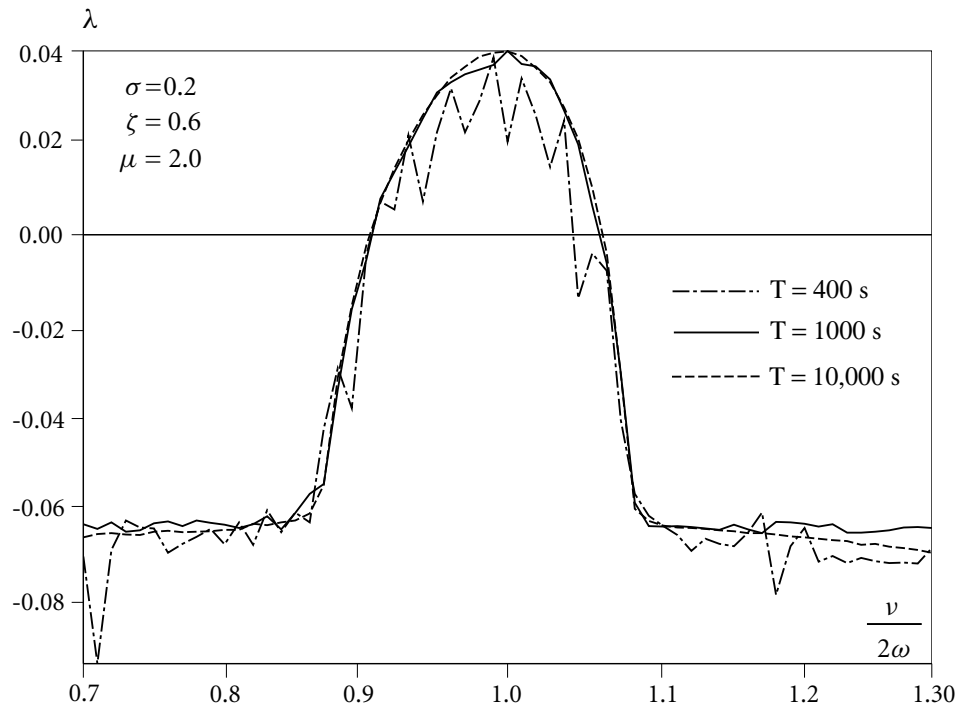


**Figure 3.2** Convergence of Lyapunov Exponent with Increasing T

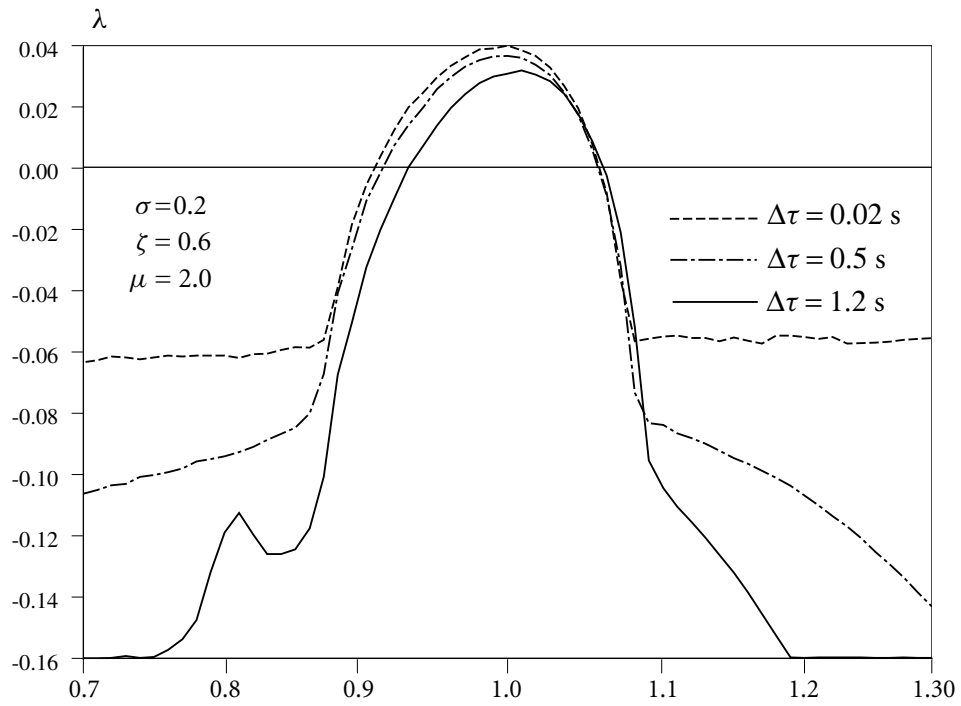


**Figure 3.3** Convergence of Lyapunov Exponent with Decreasing Time Step

### Step 6 - Generate stability curves

The end goal of the simulation is to generate stability curves. This is done by simulating the Lyapunov exponent over a set of  $\nu$  values. The results are then plotted in  $(\lambda, \nu/2\omega)$  coordinates. Stability curves can be generated for a range of damping, load intensity, and noise intensity to show the sensitivity of the system stability to these parameters.

### 3.2.2 Comparison of Analytical and Numerical Solutions

Figure 3.4 shows typical stability curves calculated by the analytical equation (3.1.12) along with the results of simulation of the exact, first order averaged, second order averaged, and the third order averaged systems.

This shows that the analytically derived Lyapunov exponents given by equation (3.1.12) closely match the results from simulation of the exact and higher order averaged equations. It is also clear that as the order of averaging increases the results approach those of the exact system. This is an evidence that the averaging scheme is convergent to the exact system. Note that the analytical and first order averaged curves lie on top of one another. This is of course expected because the analytical result is derived from the first order averaged equations.

## 3.3 Affect of System Parameters on the Lyapunov Exponent of the Trivial Solution

The sensitivity of the stability of a column under axial load to the system parameters is very important. This information may potentially be used to improve a design. In this section stability curves are used to study the effect that damping, load intensity, and noise have on the stability of the trivial solution of this system. Note that the level of nonlinearity does not have an effect on the trivial solution. This is obvious because the nonlinear effects are small near the trivial solution.

Equation (3.1.12) has been shown to provide accurate results, so this equation is used for the analysis. This is especially convenient, since analytical results can easily be used

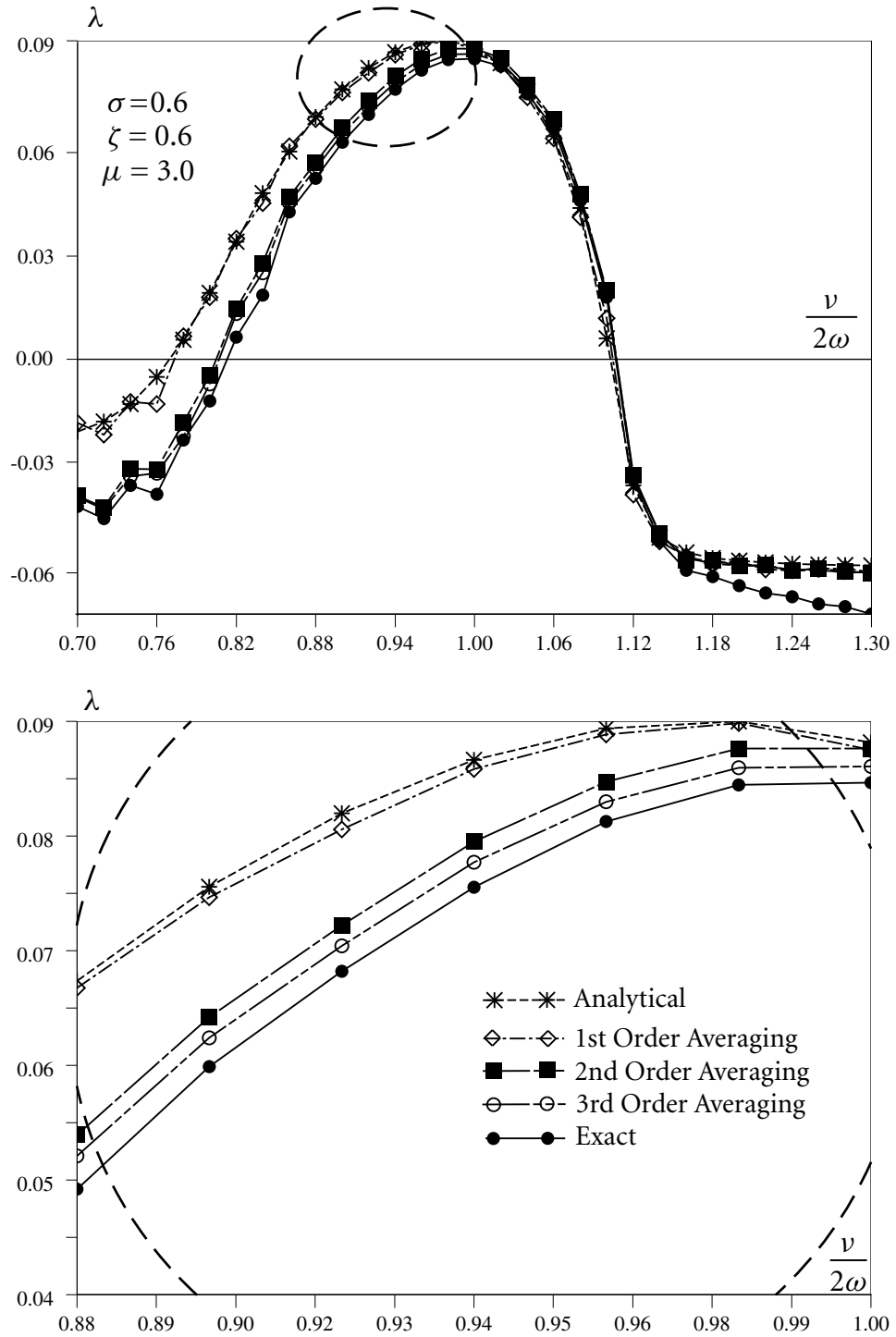


**Figure 3.4** Comparison of Analytical and Averaging Results with Exact - Lyapunov Exponents

to generate 3D stability surfaces, where the third dimension can be the system parameter under investigation.

### **Affect of Damping on the Lyapunov Exponent of the Trivial Solution**

Figure 3.5 shows a typical stability surface in  $(\nu/2\omega, \lambda, \zeta)$  space. It is clear that damping improves stability, as the region of instability (where  $\lambda$  is positive) shrinks as  $\zeta$  is increased. It is easier to see this by taking cross-sections in the  $(\nu/2\omega, \lambda)$  plane as shown in Figure 3.6.

### **Affect of Load Intensity on the Lyapunov Exponent of the Trivial Solution**

Figure 3.7 shows a typical stability surface for varying level of load,  $\mu$ . As one would expect, increasing the load leads to a larger region of instability. This is also clear from the cross-sections in Figure 3.8.

### **Affect of Noise Intensity on the Lyapunov Exponent of the Trivial Solution**

Figure 3.9 presents a typical stability surface in  $(\nu/2\omega, \lambda, \sigma)$  space, while Figure 3.10 shows cross-sections for several  $\sigma$  values. It is interesting that noise seems to generally improve stability by lowering the peak Lyapunov exponent. Noise therefore has a tendency of interfering with the resonance. This is consistent with expectation because noise makes it difficult for the forcing frequency to be tuned to the natural frequency of a system. Noise, however, also seems to slightly de-stabilize the trivial solution in region where it is already stable. This effect is however not studied in detail, and the stabilization of the originally unstable regions is much more dramatic.

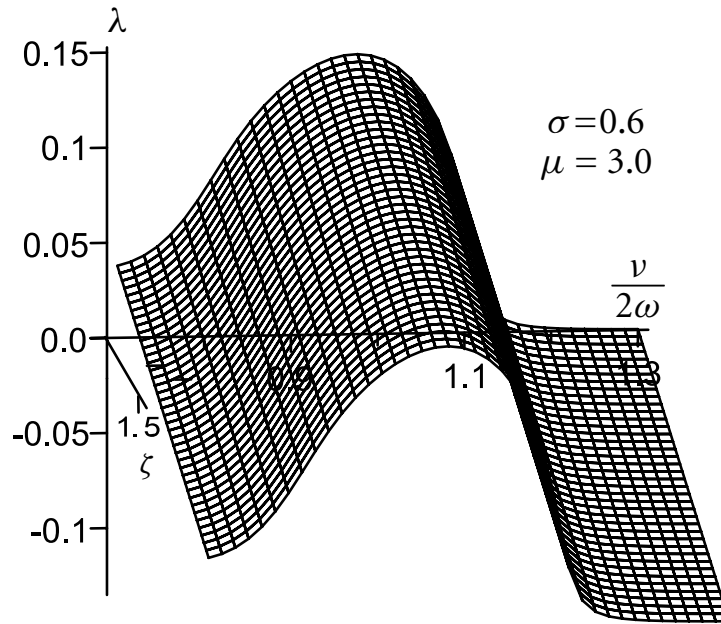


**Figure 3.5** Stability Surface vs. Damping

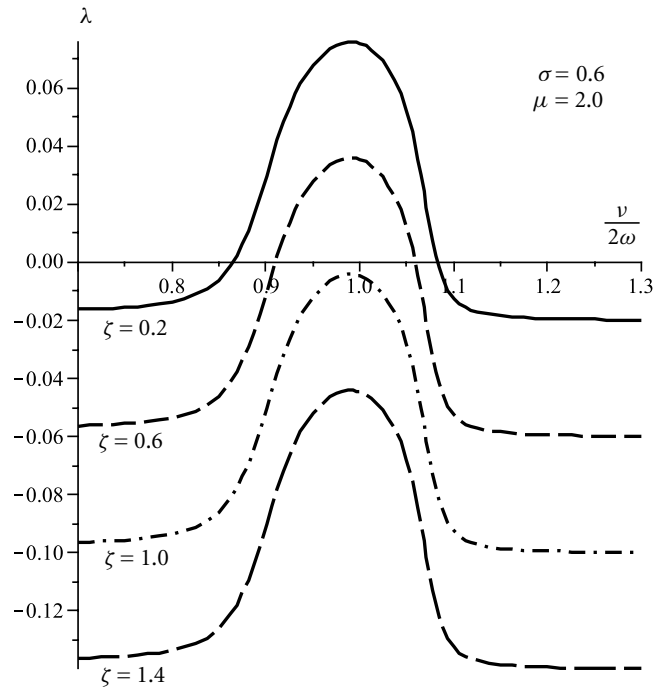


**Figure 3.6** Cross-Sections of Stability Surface vs. Damping

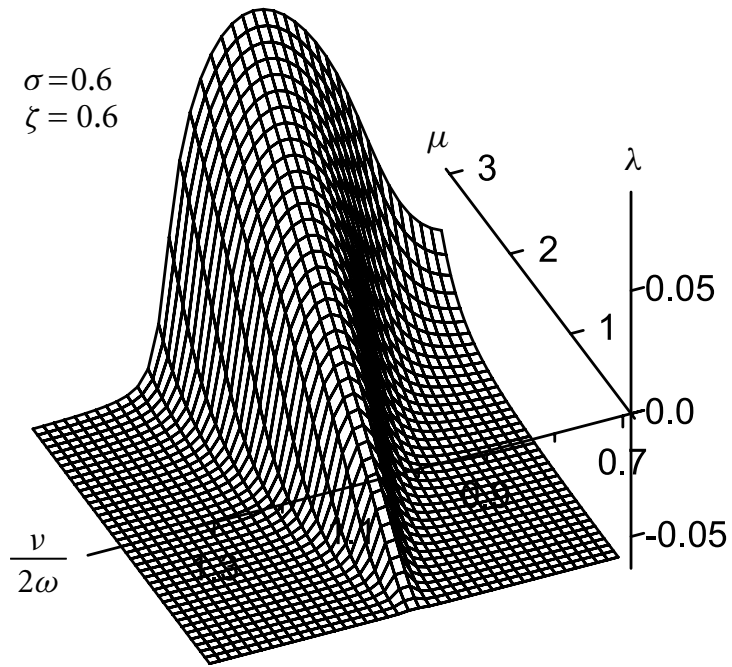


**Figure 3.7** Stability Surface vs. Load Intensity

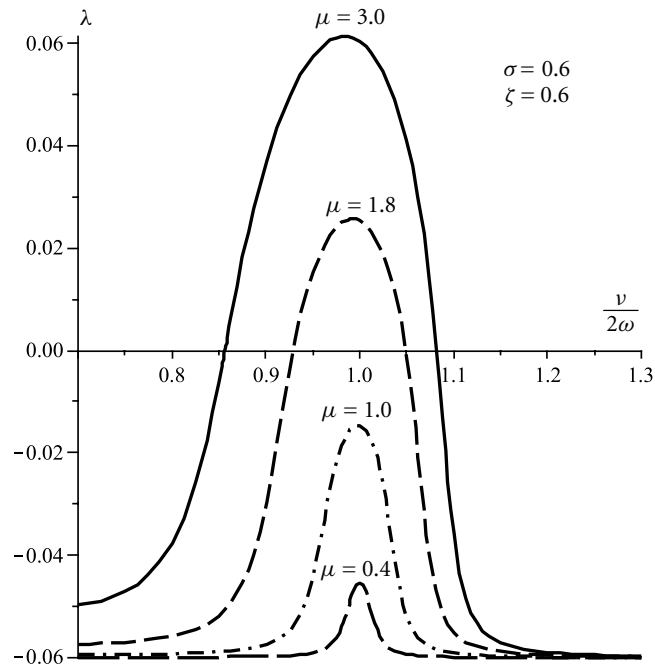


**Figure 3.8** Cross-Sections of Stability Surface vs. Load Intensity

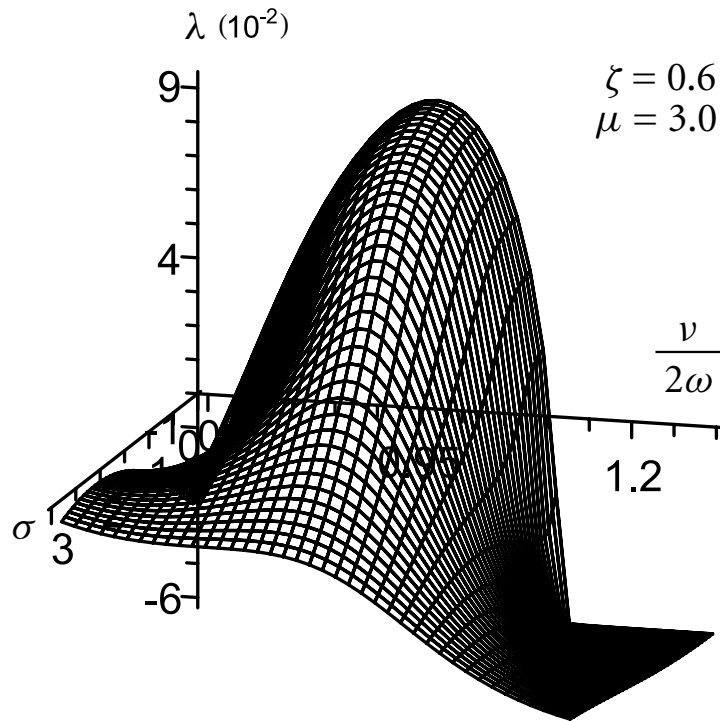


**Figure 3.9** Stability Surface vs. Noise Intensity

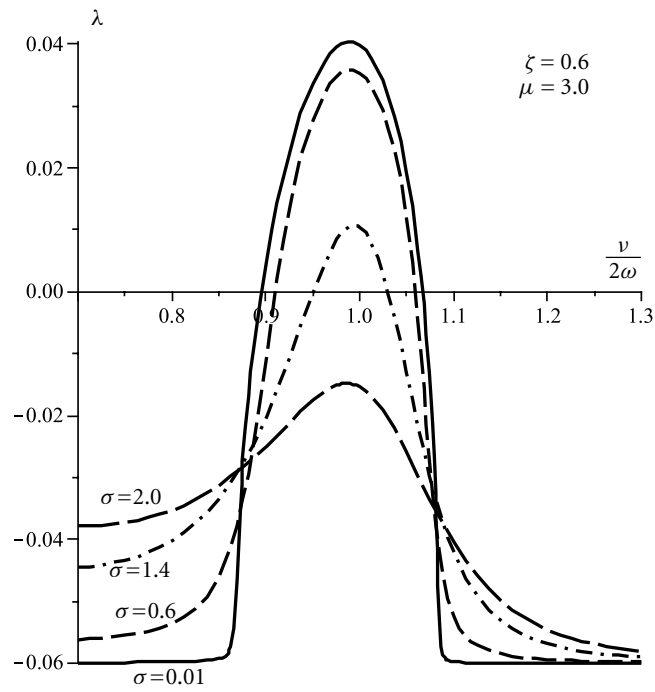


**Figure 3.10** Cross-Sections of Stability Surface vs. Noise Intensity

## 3.4 Remarks and Conclusions

Chapter 3 focused on determination of the stability of the trivial solution of a column subjected to bounded noise axial load by studying the Lyapunov exponent of the system. The first order averaged equations of motion derived in Chapter 2 were used to derive an analytical expression for the Lyapunov exponent. The validity of the analytical expression was then verified by comparison with Monte Carlo simulations of the Lyapunov exponent.

Finally the effect that damping, load intensity, and noise intensity have on stability of the system was examined by studying stability surfaces. It was discovered that damping, as one would expect, has a stabilizing effect, while load magnitude has a destabilizing effect. Noise was actually proven to mostly improve the stability of the system.

# C H A P T E R

# 4

## The Non-Trivial Stationary Solution

### 4.1 Analytical Results – Non-Trivial Stationary Solution

#### 4.1.1 General

Recall the first-order averaged system in equation (2.2.12). If there exist stationary solutions,  $\bar{a}_s$  and  $\bar{\phi}_s$ , then they must themselves satisfy the equation of motion, i.e.

$$\begin{aligned}\bar{a}'_s &= -\varepsilon \left[ \frac{\zeta \omega}{\nu} + \frac{\mu \omega^2}{\nu^2} \sin(2\bar{\phi}_s - \bar{\Psi}) \right] \bar{a}_s, \\ \bar{\phi}'_s &= \frac{1}{2} \varepsilon \left[ \Delta_0 + \frac{3\gamma \omega^2}{2\nu^2} \bar{a}_s^2 - \frac{2\mu \omega^2}{\nu^2} \cos(2\bar{\phi}_s - \bar{\Psi}) \right],\end{aligned}\tag{4.1.1}$$

where

$$\bar{\Psi} = \left( \frac{\varepsilon}{\nu} \right)^{1/2} \sigma \tilde{W}(\tau) + \theta.$$

By dividing the amplitude equation of motion by  $\bar{a}_s$  on both sides, one gets

$$\begin{aligned}\ln \bar{a}'_s &= -\varepsilon \left[ \frac{\zeta \omega}{\nu} + \frac{\mu \omega^2}{\nu^2} \sin(2\bar{\phi}_s - \bar{\Psi}) \right], \\ \bar{\phi}'_s &= \frac{1}{2} \varepsilon \left[ \Delta_0 + \frac{3\gamma \omega^2}{2\nu^2} \bar{a}_s^2 - \frac{2\mu \omega^2}{\nu^2} \cos(2\bar{\phi}_s - \bar{\Psi}) \right].\end{aligned}\tag{4.1.2}$$

Taking the expected values of both sides yields

$$\begin{aligned}\mathbb{E}[\ln \bar{a}'_s] &= -\varepsilon \left\{ \frac{\zeta \omega}{\nu} + \frac{\mu \omega^2}{\nu^2} \mathbb{E}[\sin(2\bar{\phi}_s - \bar{\Psi})] \right\}, \\ \mathbb{E}[\bar{\phi}'_s] &= \frac{1}{2} \varepsilon \left\{ \Delta_0 + \frac{3\gamma \omega^2}{2\nu^2} \mathbb{E}[\bar{a}_s^2] - \frac{2\mu \omega^2}{\nu^2} \mathbb{E}[\cos(2\bar{\phi}_s - \bar{\Psi})] \right\}.\end{aligned}\tag{4.1.3}$$

The expectation operator is an integral operator; therefore the order of expectation and differentiation on the left side may be reversed, yielding

$$\begin{aligned} E[\ln \bar{a}_s]' &= -\varepsilon \left\{ \frac{\zeta \omega}{\nu} + \frac{\mu \omega^2}{\nu^2} E[\sin(2\bar{\phi}_s - \bar{\Psi})] \right\}, \\ E[\bar{\phi}_s]' &= \frac{1}{2} \varepsilon \left\{ \Delta_0 + \frac{3\gamma \omega^2}{2\nu^2} E[\bar{a}_s^2] - \frac{2\mu \omega^2}{\nu^2} E[\cos(2\bar{\phi}_s - \bar{\Psi})] \right\}. \end{aligned} \quad (4.1.4)$$

Note that, as discussed in Section 1.2, the probability distribution of a stationary process is independent of time. This means that  $E[f(\bar{a}_s)]$  and  $E[g(\bar{\phi}_s)]$ , where  $f$  and  $g$  are arbitrary functions, are invariant with respect to time. Therefore the right hand sides in equation (4.1.4) vanish. This leads to

$$E[\sin(2\bar{\phi}_s - \bar{\Psi})] = -\frac{\zeta \nu}{\mu \omega}, \quad (4.1.5)$$

and

$$\Delta_0 = -\frac{3\gamma \omega^2}{2\nu^2} E[\bar{a}_s^2] + \frac{2\mu \omega^2}{\nu^2} E[\cos(2\bar{\phi}_s - \bar{\Psi})]. \quad (4.1.6)$$

Equation (4.1.6) may be written in amplitude-frequency form by using the relationship  $\varepsilon \Delta_0 = 1 - \nu/\omega_0 = 1 - \nu/2\omega$ :

$$\frac{\nu}{2\omega} - 1 = \varepsilon \frac{\omega^2}{\nu^2} \left\{ \frac{3}{2} \gamma E[\bar{a}_s^2] - 2\mu E[\cos(2\bar{\phi}_s - \bar{\Psi})] \right\}. \quad (4.1.7)$$

One is motivated to use equation (4.1.5) to evaluate the expectation of the cosine function in equation (4.1.7). Unfortunately this is very difficult in the general case because the probability distributions of  $\bar{a}_s$  and  $\bar{\phi}_s$  are not known. However, in the two extreme cases of very small noise intensity ( $\sigma = 0$ , i.e. deterministic) and very large noise intensity ( $\sigma \rightarrow \infty$ ), it is possible to determine the expectation of the cosine function.

### 4.1.2 Special Case – Deterministic System

If  $\sigma = 0$  the forcing function  $\bar{\Psi}$  is deterministic, which gives

$$\begin{aligned} E[\cos(2\bar{\phi}_s - \bar{\Psi})] &= \cos(2\bar{\phi}_s - \bar{\Psi}) = \pm [1 - \sin^2(2\bar{\phi}_s - \bar{\Psi})]^{1/2}, \\ E[\sin(2\bar{\phi}_s - \bar{\Psi})] &= \sin(2\bar{\phi}_s - \bar{\Psi}) = -\frac{\zeta \nu}{\mu \omega}, \\ E[\bar{a}_s^2] &= \bar{a}_s^2. \end{aligned} \quad (4.1.8)$$

Therefore the amplitude-frequency relationship is

$$\frac{\nu}{2\omega} - 1 = \varepsilon \frac{\omega^2}{\nu^2} \left\{ \frac{3}{2} \gamma \bar{a}_s^2 \mp 2\mu \left[ 1 - \left( \frac{\zeta \nu}{\mu \omega} \right)^2 \right]^{1/2} \right\}. \quad (4.1.9)$$

In the book "Dynamic Stability of Structures" ([14], p. 114) it is shown that, for this deterministic system, the amplitude-frequency relationship is given by,

$$\frac{\nu}{2\omega} - 1 = \varepsilon \left\{ \frac{3\gamma}{8} \bar{a}_s^2 \mp \left[ \frac{\mu^2}{4} - \left( \frac{2\zeta \omega}{\nu} \right)^2 \right]^{1/2} \right\}. \quad (4.1.10)$$

Figure 4.1 shows a comparison of the results given by equations (4.1.9) and (4.1.10). The reason for the difference is that the derivation in [14] uses the approximation  $\nu \approx 2\omega$ , while equation (4.1.9) is obtained without any approximation. It is expected therefore that equation (4.1.9) will provide more accurate results over a wider range of frequency ratio  $\nu/2\omega$ . This is shown to be true in Section 4.2.1.

The stability of the nontrivial solutions in the deterministic case is discussed in [14]. The approximation  $\nu \approx 2\omega$  is however not used in the stability analysis; therefore the stability results obtained are also valid for the curves described by equation (4.1.9). It is shown in this book that the top curves of Figure 4.1 are stable while, the bottom curves are unstable.

### 4.1.3 Special Case – High Noise Intensity

A combined analytical-numerical approach may be used to determine the amplitude-frequency relationship for the case of high noise intensity. Monte Carlo simulation is used to determine  $E[\cos(2\bar{\phi}_s - \bar{\Psi})]$ . This value is then substituted into the amplitude-frequency relation in equation (4.1.9). The method is as follows:

#### Step 1 - Generate a stationary solution

Using the forward Euler Monte Carlo scheme discussed in Section 1.3 simulate a sample from the equations of motion. If a stationary solution exists and is asymptotically stable, then the response will eventually approach this solution. Figure 4.2 shows a typical realization of  $a$  from the original equation of motion (2.2.8). This realization appears to reach a stationary solution at approximately time  $T_1$ . There is no analytical method to determine

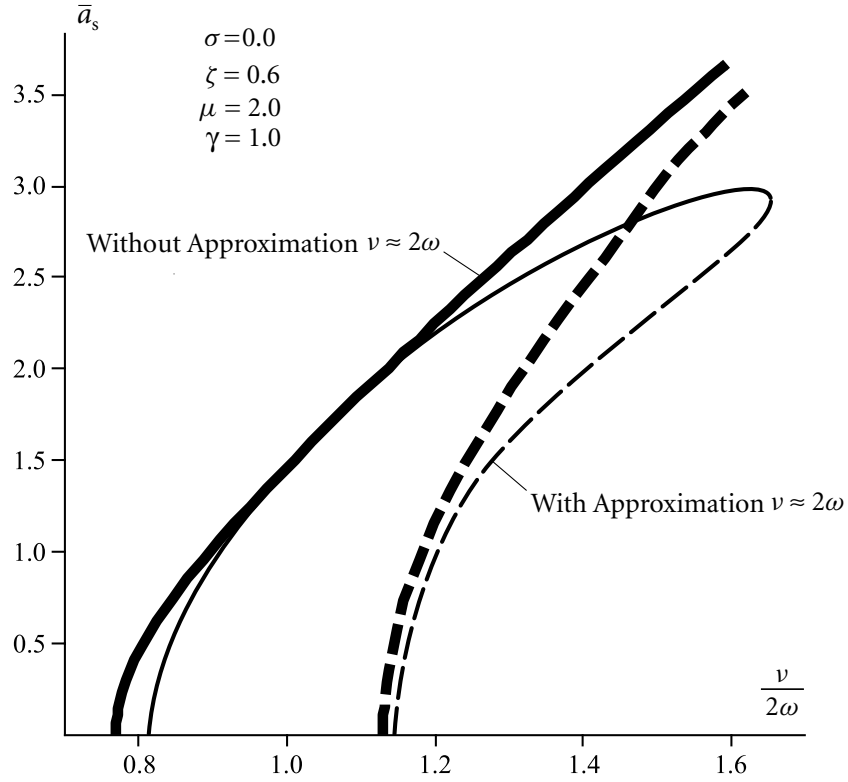


**Figure 4.1** Comparison of Amplitude-Frequency Relationships Obtained With and Without the Approximation  $\nu \approx 2\omega$

$T_1$ ; however, since the simulation is not computationally expensive, one may simply choose a large value.

### Step 2 - Perform time averaging

After time  $T_1$  the amplitude in the original equation of motion (2.2.8) has reached a stationary solution. If the system is further assumed to be ergodic, then time averaging of  $\cos(2\bar{\phi}_s - \bar{\Psi})$  will yield the expected value desired. The time  $T_2$  in Figure 4.2 should be chosen to be much larger than  $T_1$  to ensure the average calculated is accurate.

### Step 3 - Repeat simulation for increasing levels of noise

Figure 4.3 contain a plots of  $E[\cos(2\bar{\phi}_s - \bar{\Psi})]$  and  $E[\sin(2\bar{\phi}_s - \bar{\Psi})]$  from simulation, the Lyapunov exponent of the trivial solution, and the analytical result of equation (4.1.5) vs. noise intensity,  $\sigma$ . The simulations are done with  $\nu = 2\omega$  to ensure the existence of a

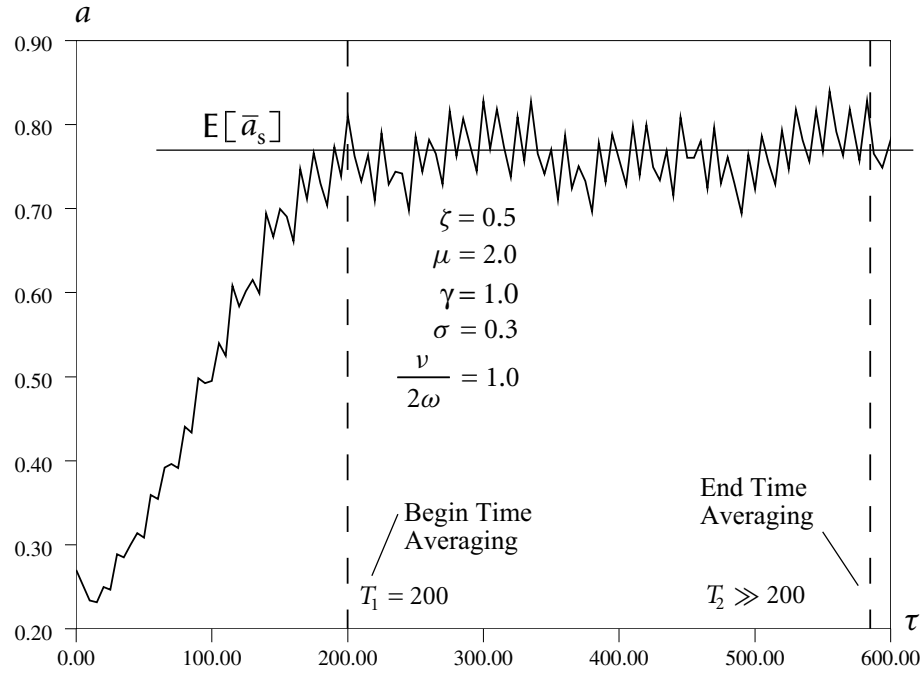


**Figure 4.2** Stationary Solution - Time Averaging

non-trivial stationary solution. This figure shows that  $E[\cos(2\bar{\phi}_s - \bar{\Psi})]$  nears zero for relatively small noise intensity  $\sigma$ .

The divergence of  $E[\sin(2\bar{\phi}_s - \bar{\Psi})]$  from the analytical value given by equation (4.1.5) shown in Figure 4.3 occurs at exactly the  $\sigma$  level where the Lyapunov exponent become negative. Therefore the divergence can be explained by the fact that the trivial solution becomes stable and begins to affect the trajectory of the system.

Also of note is that there is a discrepancy between the analytical and simulated values of  $E[\sin(2\bar{\phi}_s - \bar{\Psi})]$ . This is because the simulation is done using the original equations of motion (2.2.8), while the analytical results are from the averaged equations of motion (2.2.12). Figure 4.4 shows these same two values when simulation is done using the averaged equations of motion. As expected, there is near perfect correlation in this case.

It can be shown that this decay of  $E[\cos(2\bar{\phi}_s - \bar{\Psi})]$  to zero with increasing noise is typical of the system in equation (2.2.8). The decay rate is inversely related to damping  $\zeta$ . Figure 4.5 shows this relationship, where  $\sigma_{1\%}$  is the noise intensity level required for  $E[\cos(2\bar{\phi}_s - \bar{\Psi})]$  to reach 1% of its value in the deterministic ( $\sigma = 0$ ) case.

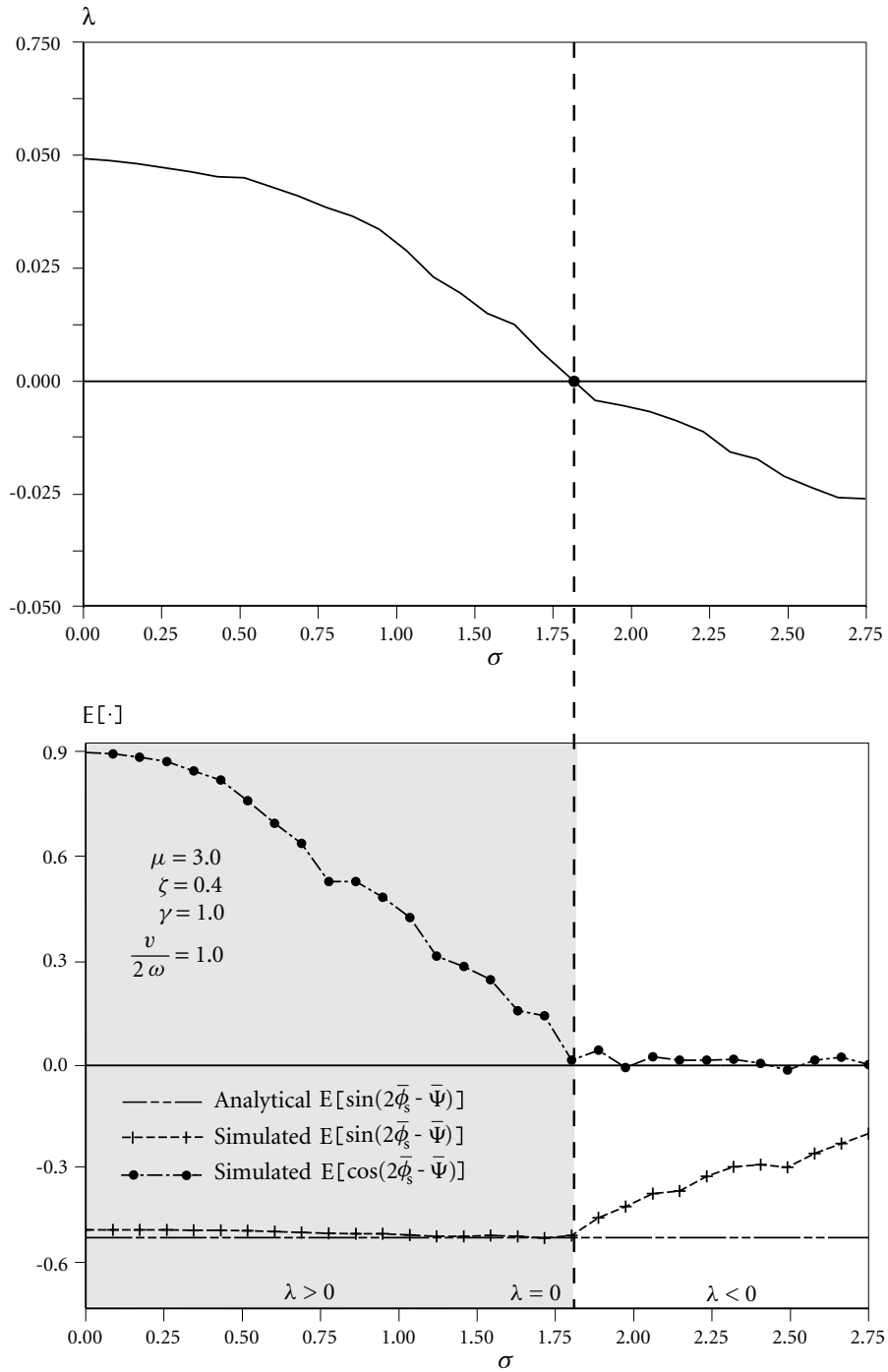


**Figure 4.3**  $E[\cos(2\bar{\phi}_s - \bar{\Psi})]$  vs.  $\sigma$

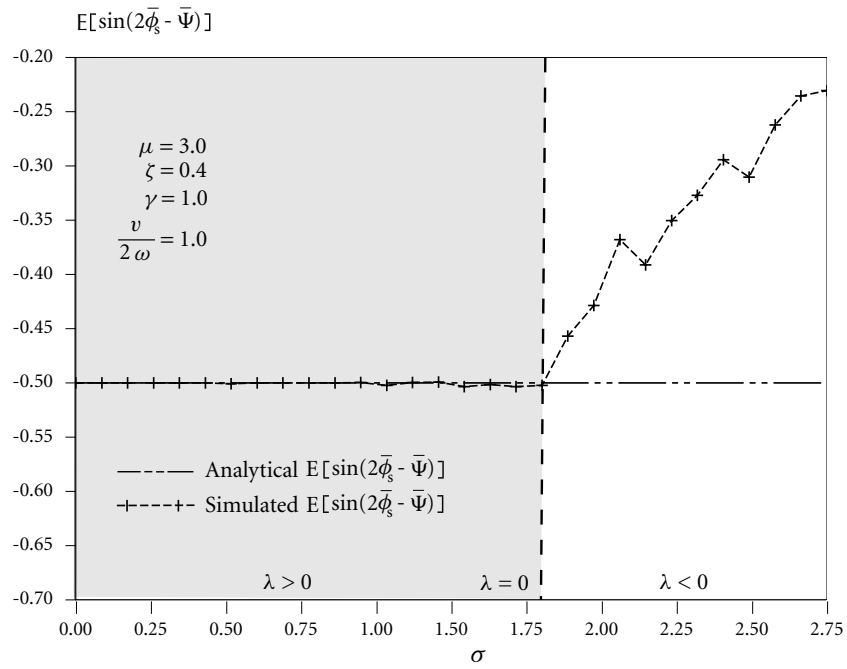


**Figure 4.4**  $E[\sin(2\bar{\phi}_s - \bar{\Psi})]$  with Averaged Equations

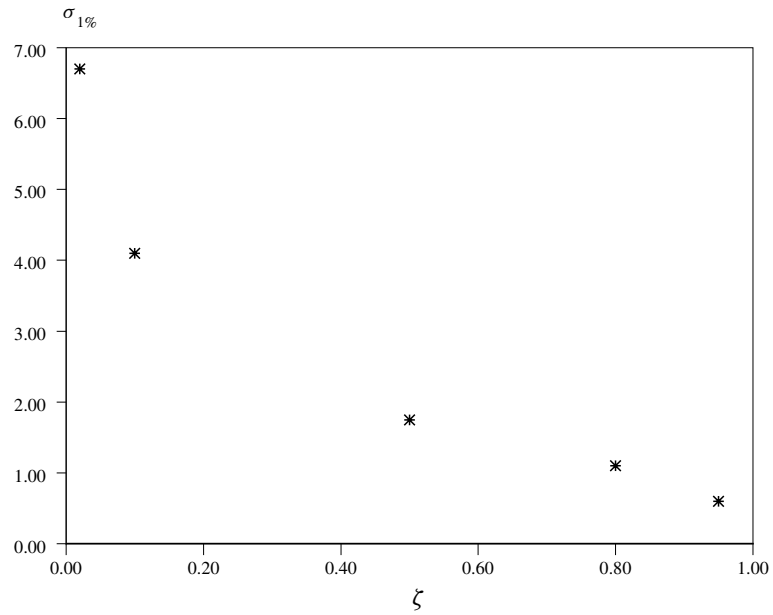


**Figure 4.5** Relationship Between  $E[\cos(2\bar{\phi}_s - \bar{\Psi})]$  and  $\zeta$

#### Step 4 - Apply result to analytical equation

Given that the expectation of the cosine term in equation (4.1.7) tends to zero with increasing  $\sigma$ , the amplitude-frequency relationship approaches

$$\frac{\nu}{2\omega} - 1 = \varepsilon \frac{3\gamma\omega^2}{2\nu^2} E[\bar{a}_s^2]. \quad (4.1.11)$$

Therefore instead of an upper and lower curve, one is left with just one central curve in the extreme case as  $\sigma \rightarrow \infty$ . Figure 4.6 shows this shifting that occurs when  $\sigma$  is increased. Note that the amplitude axis is now given as  $E[\bar{a}_s^2]$ . This is because it is difficult, and not necessary to obtain the average given the second moment. Also note that in the stochastic case the amplitude-frequency relationship is not strictly amplitude vs. frequency, but rather a relationship between the second moment of amplitude and frequency.

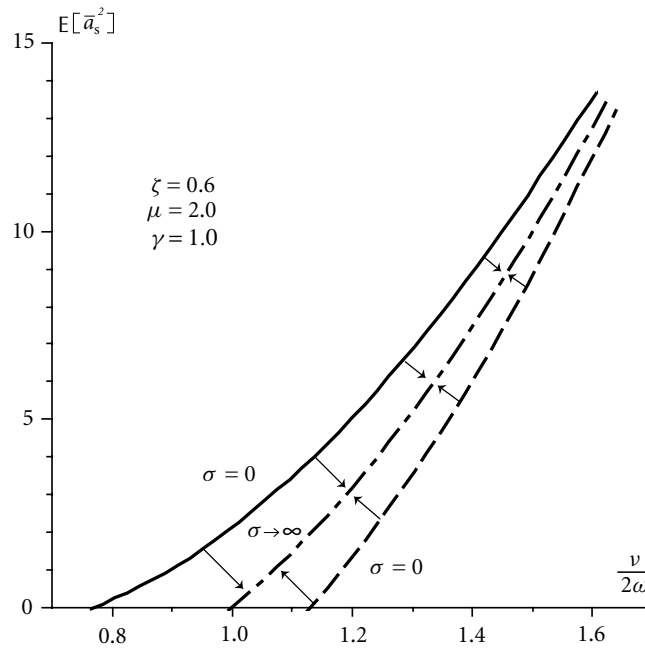


**Figure 4.6** The Amplitude-Frequency Relationship for Limiting Cases of Noise

The region between the stems of the top and bottom nontrivial solutions is also the region of trivial solution instability. Therefore Figure 4.6 coincides with the trivial solution Lyapunov exponent results from Chapter 3, where it was shown that the region of trivial solution instability shrinks with increasing  $\sigma$ .

## 4.2 Monte Carlo Simulation of Non-Trivial Stationary Solution

### 4.2.1 General

The Monte Carlo method is essentially an experimental method. One begins a simulation and observes the outcome. Unfortunately this means that peculiarities such as unstable non-trivial solutions (bottom curves in Figures 4.1 and 4.6) cannot be examined via Monte Carlo simulation. This is because a system will diverge exponentially from an unstable solution if given even the slightest perturbation and is therefore not observable (theoretically even floating point rounding in a computer simulation is potentially enough to de-stabilize the system). Therefore all further discussion of non-trivial solutions is directed towards the stable non-trivial solution.

Note that while it is possible to use the Fokker-Planck equation to determine the probability distribution of  $\phi$  in Chapter 3, this is not possible for the nonlinear system as the equations of motion are coupled. Therefore, for the general case of finite  $\sigma$  one has to use Monte Carlo simulations to determine the amplitude-frequency relationship.

Recall steps 1 and 2 from Section 4.1.3. These same steps may be used to determine the amplitude-frequency relationship directly from simulation, if, instead of time averaging  $\cos(2\bar{\phi}_s - \bar{\Psi})$ , one simply averages  $\bar{a}$  as shown in Figure 4.2. Note that when using simulation one is able to choose to average  $E[\bar{a}_s]$  as opposed to second moment  $E[\bar{a}_s^2]$ .

### 4.2.2 Special Case – Deterministic System

In order to validate the amplitude-frequency relationship for deterministic systems in equation (4.1.9), it is necessary to compare with the results from simulation of the exact equation of motion. Figure 4.7 presents the amplitude-frequency obtained from simulation using of exact equations of motion, and the curves predicted by equations (4.1.9) and (4.1.10).

Both equations provide a good approximation for  $\nu \approx 2\omega$ ; however it is evident that equation (4.1.9) provides a better estimation over a broader range.

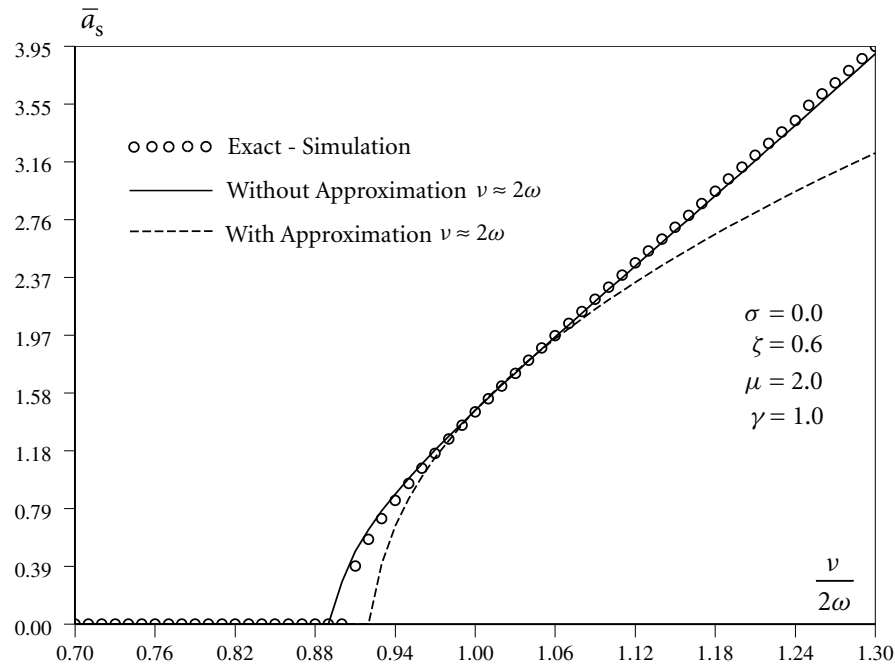


**Figure 4.7** Comparison of Approximate Analytical and Simulated Exact Amplitude-Frequency Curves

### 4.2.3 Special Case – High Noise Intensity

The shifting tendency of the amplitude-frequency relationship can also be verified by simulation. Figure 4.8 shows typical amplitude-frequency curves obtained from the exact equation of motion for increasing  $\sigma$ . It appears that the stem of the curve approaches  $\nu/2\omega = 1$  as  $\sigma$  increases, which provides some verification to equation (4.1.11).

## 4.3 Affect of System Parameters on Non-Trivial Stationary Solution

In this section the effect that damping, load intensity, and the level of nonlinearity have on the non-trivial stationary solution is studied via amplitude-frequency curves. The effect of noise intensity was discussed in Section 4.2.2. The amplitude-frequency curves in this section are all obtained from simulation of the exact equations of motion.

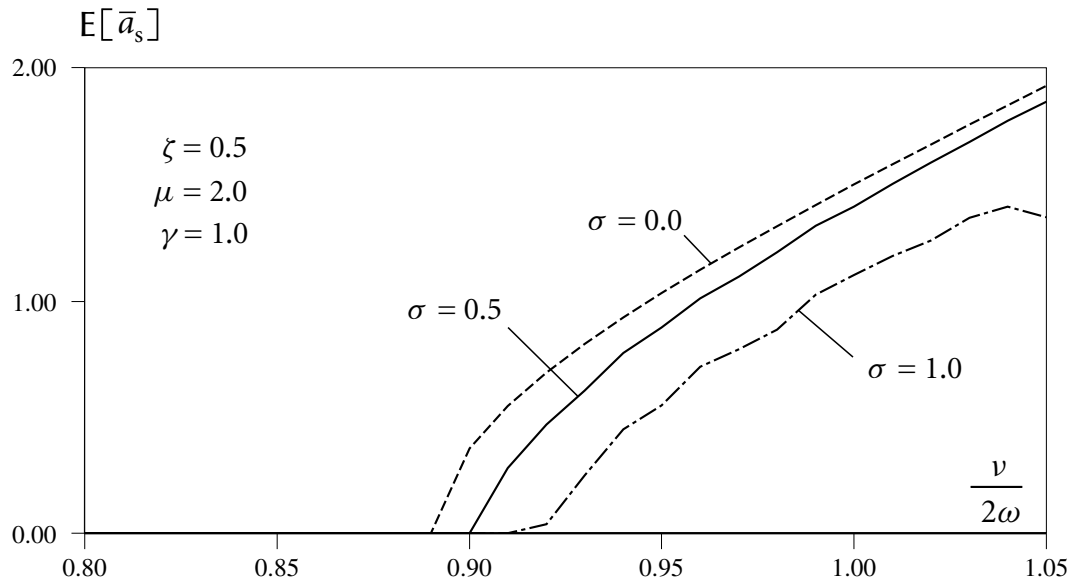


**Figure 4.8** The Effect of Noise on the Amplitude-Frequency Relationship

**Affect of Damping on Non-Trivial Stationary Solution**

Figure 4.9 shows a typical plot of the amplitude-frequency relationship for various levels of  $\zeta$ .

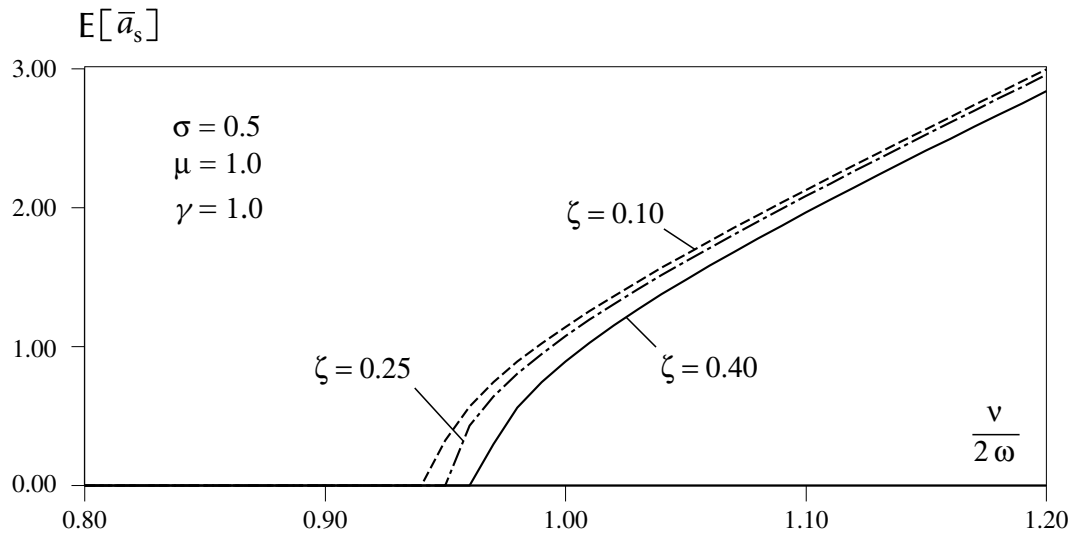


**Figure 4.9** Amplitude-Frequency Relationship vs. Damping

It is clear that increasing damping shifts the amplitude-frequency curve down and to the right. This is equivalent to shrinking the region of trivial solution instability, and is consistent with the results of Chapter 3. The existence of unstable non-trivial solutions cannot be verified by simulation.

### **Affect of Load Intensity on Non-Trivial Stationary Solution**

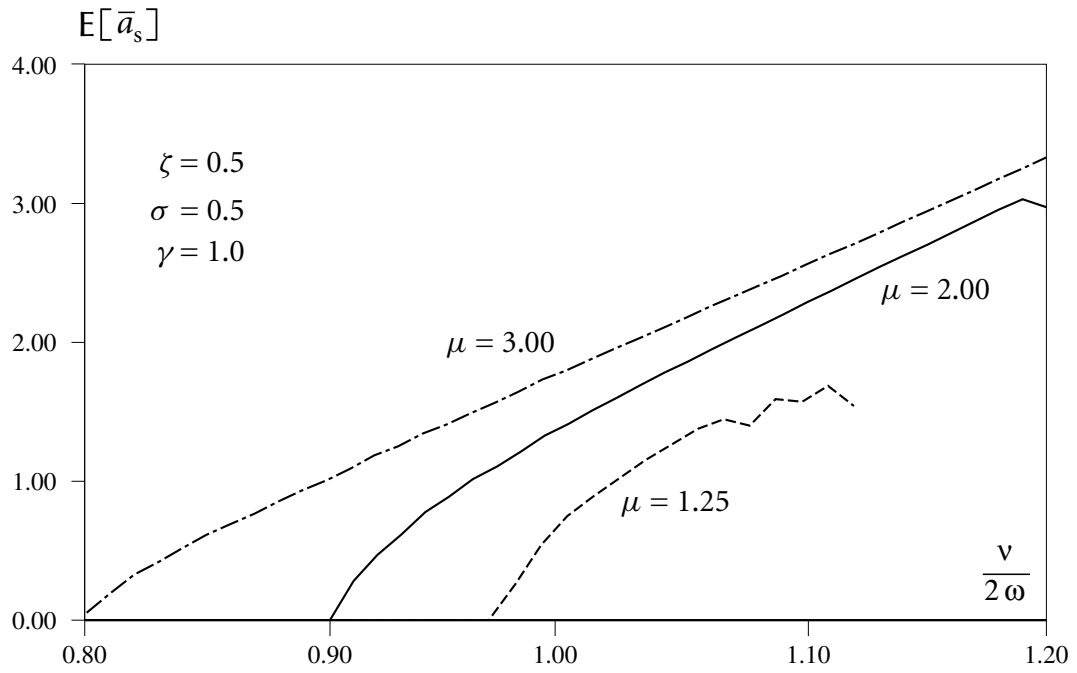
Figure 4.10 shows typical amplitude-frequency curves for various levels of  $\mu$ . As one might expect, increasing the load intensity shifts the amplitude-frequency curve up and to the left, which also indicates that the region of trivial solution instability is being increased. This is also consistent with the results of Chapter 3.

Note that the amplitude-frequency curves are all created by averaging the results over several simulations. This generally smooths the curves, however it indirectly creates the waviness on the right side of the curves in Figure 4.10. This is because for small load intensity the trivial solution quickly (with respect to increasing  $\nu$  not time) regains stability for  $\nu > 2\omega$ . This second stable solution makes it difficult to consistently obtain realizations of the system that converge to the non-trivial solution. The trivial solution therefore interferes with the averaging technique used to smoothen the curves. However, without averaging over several simulations the curves become even worse, as they jump back and forth between zero and the non-trivial solution.

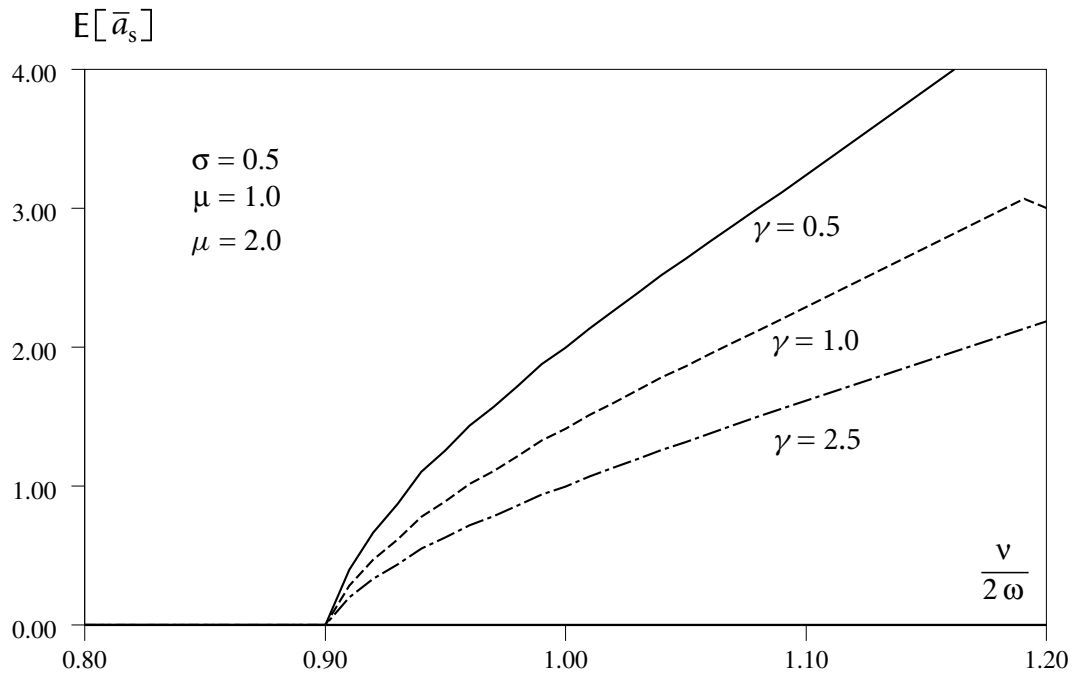
### **Affect of Nonlinearity on Non-Trivial Stationary Solution**

Figure 4.11 shows a typical amplitude-frequency curves for various levels of  $\gamma$ . These curves show that the amplitude-frequency relationship grows large for decreasing  $\gamma$ . This result is expected, because it is known that the response of linear systems grows without bound in the region of trivial solution instability.

Nonlinearity, however, does not shift the bifurcation point where the trivial solution becomes unstable. This is also expected because the nonlinear and linear systems have the same trivial solution stability behaviour.



**Figure 4.10** Amplitude-Frequency Relationship vs. Load Intensity



**Figure 4.11** Amplitude-Frequency Relationship vs. Nonlinearity

## 4.4 Remarks and Conclusions

In Chapter 4 the non-trivial amplitude-frequency relationship for a column under bounded noise axial load was determined via both a combined Monte Carlo simulation-analytical method as well as from Monte Carlo simulations directly. The deterministic system was also studied as a special case where the noise intensity tends to zero.

The method for generating non-trivial stationary solutions that was developed in this chapter is used in Chapter 5 to study the stability of these same stationary solutions.

The effect that damping, load intensity, nonlinearity, and noise intensity have on the amplitude-frequency relationship was also studied. It was shown that noise intensity, nonlinearity, and damping have stabilizing effects, while load intensity has a de-stabilizing effect. These results are all consistent with the results of Chapter 3.

# C H A **5** P T E R

## Stability of The Non-Trivial Stationary Solution

### 5.1 Monte Carlo Simulation of Lyapunov Exponents

The stability of the non-trivial stationary solutions can be determined by studying the Lyapunov exponents of the linearized equations of variation. The equations of variation, even for the first order averaged system, are too complex to solve analytically. Therefore the method of Monte Carlo simulation is applied to study these equations of variation.

Because the method of simulation is applied, one is inclined to use the original equations of motion. The only benefit of using an approximate equation of motion when simulating is savings in computing time. This is however not a significant problem in the system under study; therefore the original equations of motion will be used.

Consider the linearized equations of variation given by equation (2.3.14). This may be treated as an entirely new system and the stationary solution,  $(a_s, \phi_s)$ , may be thought of as inputs to the system along with  $\tilde{\Psi}$ . The difficulty comes in choosing the stationary solutions to use as inputs. One cannot arbitrarily choose a stationary solution, as it must satisfy the original equations of motion. The approach used therefore is to simulate two systems simultaneously. The first system being original exact equations of motion, and the second system the equations of variation about the stationary solution. The output of the first system is therefore the input of the second system. The details of the method are as follows:

**Step 1 - Generate a stationary solution**

Using the method developed in Section 4.1.3, generate a stationary solution,  $(a_s, \phi_s)$ , from the original equations of motion.

**Step 2 - Initiate simulation of linearized equations of variation**

After simulation time  $T_1$  (see Section 4.1.3 for description) has passed, choose initial conditions for the equations of variation. These initial conditions can be chosen freely or even randomly. Then use the forward Euler scheme as discussed in Section 1.3 to simulate the equations of variation. Continue to simulate the original equations of motion because the outputs of the original system,  $(a_s, \phi_s)$ , are an input to the equations of variation.

**Step 3 - Generate stability curves**

While both  $u$ , and  $v$  need to be stable for the method to yield results, only the stability of  $u$  is important in this system as it is the equation of amplitude variation. Therefore Lyapunov exponents need to be calculated from the  $u$  equation as follows

$$\lambda = \lambda_t = v\lambda_\tau = \lim_{\tau \rightarrow \infty} \frac{v}{\tau} \ln |u(\tau)| \approx \frac{v}{T} \ln |u(T)|, \text{ if } T \text{ is large.} \quad (5.1.1)$$

Note that the absolute value of  $u$  must be taken because the variation about the stationary amplitude,  $a_s$ , could be either negative or positive. For the original equations of motion, the amplitude is always a positive value so it is not necessary to take the absolute value.

The stability curves can be obtained according to steps 5 and 6 of Section 3.2; simply substituting  $u$  for  $a$  and  $v$  for  $\phi$ . In this case, the simulation time  $T$  should be chosen such that  $T \gg T_1$ .

Note that the equations of variation are derived by assuming the existence of stable stationary solutions. This method therefore seems to be somewhat of a catch-22, as whenever it works it will always yield stable solutions. It is still useful however for studying the degree of stability, i.e. exponential rate of decay, and also to study the effect that changing parameters have on stability.

Also note that, while the Lyapunov exponents obtained actually describe the stability of the equations of variation, they are usually just termed the Lyapunov exponent of the stationary solution.

## 5.2 Affect of System Parameters on the Lyapunov Exponent of the Non-Trivial Solution

In this section the effect of system parameters on the Lyapunov exponent of the non-trivial stationary solution is discussed.

In simulating the Lyapunov exponents of the non-trivial stationary solutions one encounters some interesting results. Figure 5.1 shows a typical stability curve for both the trivial and non-trivial solutions of the original equations of motion (2.2.8). Also overlaid in this figure is the amplitude-frequency diagram of the system, with stability indicated by line type. As expected the Lyapunov exponent of the trivial solution becomes positive (i.e. trivial solution becomes unstable) at the same point (referred to as the left peak) that the Lyapunov exponent of non-trivial solution becomes negative (i.e. non-trivial solution becomes stable). What is not expected is the small peak on the right side. This peak should probably not be there, and is likely caused by the same phenomenon discussed in Section 4.3, where the stable trivial solution interferes with the simulation of the non-trivial solution. This peak is useful, however, as it helps to identify the bifurcation point where the trivial solution regains stability. The region between the two peaks in non-trivial solution Lyapunov exponent curve is therefore the trivial solution instability region. Note also that the non-trivial stationary solution does not exist left of the first peak, so its Lyapunov exponent curve begins at this point.

The effect of damping is very difficult to study and is not included in the discussion. The difficulty occurs because for small damping the system converges to the non-trivial stationary solution very slowly.

### Affect of Noise Intensity on the Lyapunov Exponent of the Non-Trivial Stationary Solution

Figure 5.2 shows a typical plot of the Lyapunov exponent of the non-trivial stationary solution for various levels of noise intensity. The peaks once again describe the width of the zone of trivial solution instability.

This figure shows a very interesting effect of noise. The region of trivial solution instability is decreased with increasing noise as expected; however the stability of the non-trivial

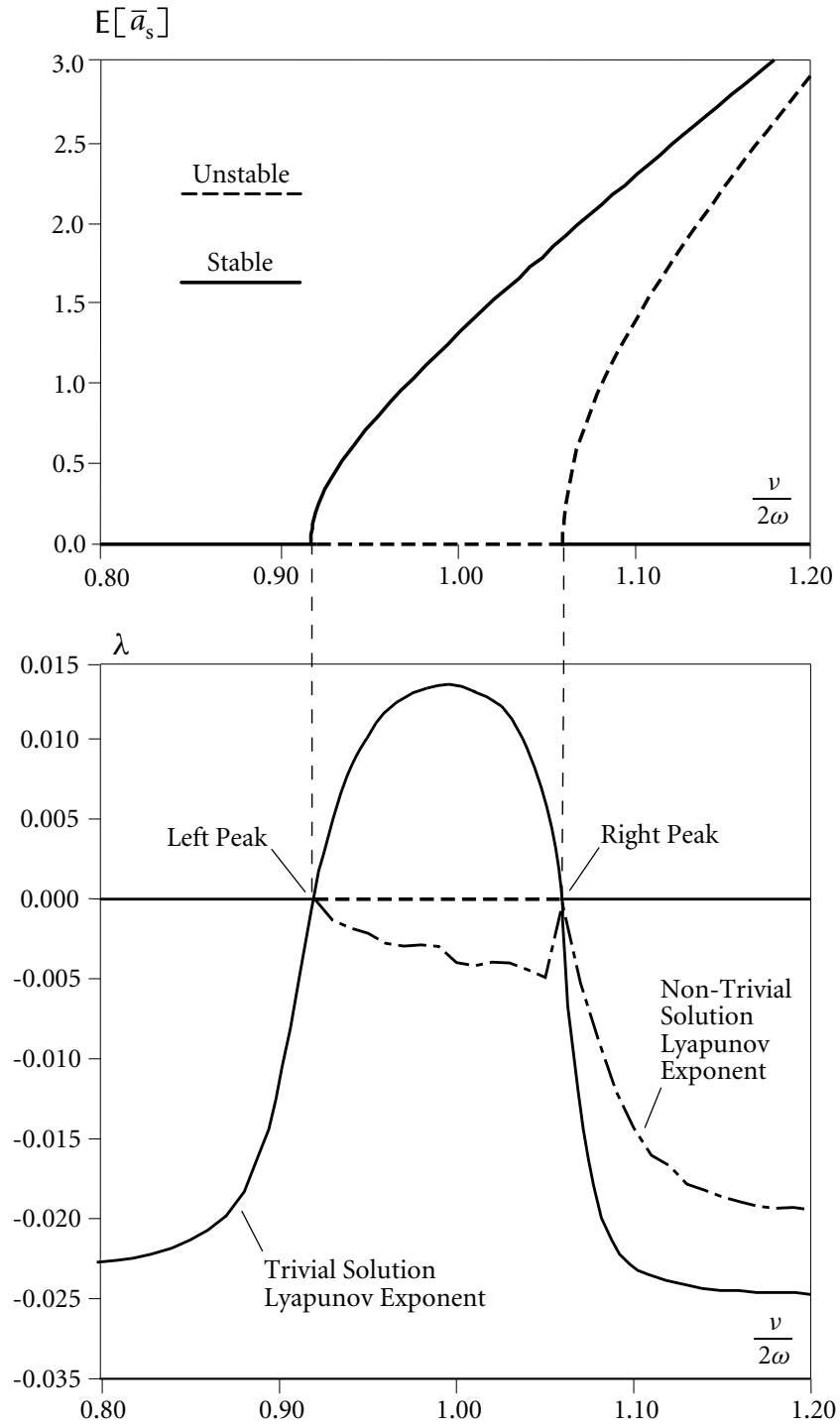


**Figure 5.1** Lyapunov Exponent of Non-Trivial Stationary Solution

solution is actually reduced. This is similar to the effect of noise on the stability of the trivial solution. Therefore it seems that noise causes the Lyapunov exponents of both the trivial and non-trivial solutions to tend to zero.

Note that for very small noise intensities the Lyapunov exponent of the non-trivial solution approaches a constant value. This is an interesting and unexpected result.

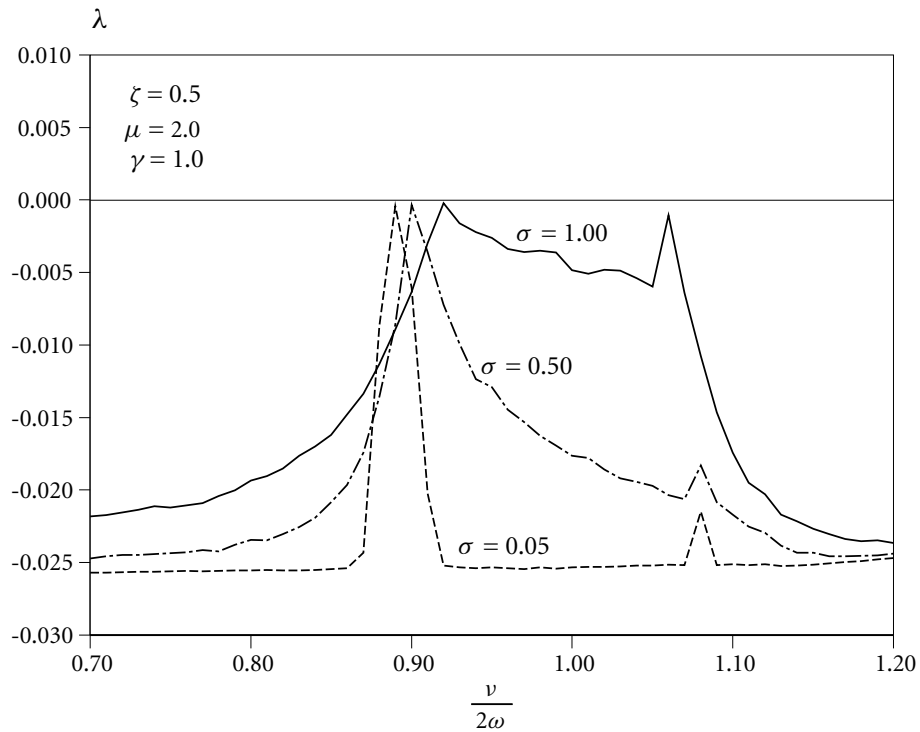


**Figure 5.2** Non-Trivial Stationary Solution Stability Curve vs. Noise Intensity

### Affect of Load Intensity on the Lyapunov Exponent of the Non-Trivial Stationary Solution

Figure 5.3 shows a typical plot of the Lyapunov exponent of the non-trivial stationary solution for various values of load intensity,  $\mu$ .

It appears that the Lyapunov exponent of the non-trivial stationary solution, where it is stable, seems relatively unaffected by load intensity. Near  $\nu \approx 2\omega$  all three curves lie on top of one another. The load intensity however has a pronounced effect on the width of

the trivial solution instability zone (distance between peaks). The peaks converge on each other, showing that damping improves trivial solution stability.

### **Affect of Nonlinearity on the Lyapunov Exponent of the Non-Trivial Stationary Solution**

Figure 5.4 shows a typical plot of the Lyapunov exponent of the non-trivial stationary solution for different levels of nonlinearity,  $\gamma$ . Note that nonlinearity does not shift the peaks at all, which indicates that the region of trivial solution instability is unchanged by nonlinearity. This is consistent with the results in Chapters 3 and 4. Figure 5.4 also shows that increasing nonlinearity improves stability, because the Lyapunov exponent decreases.

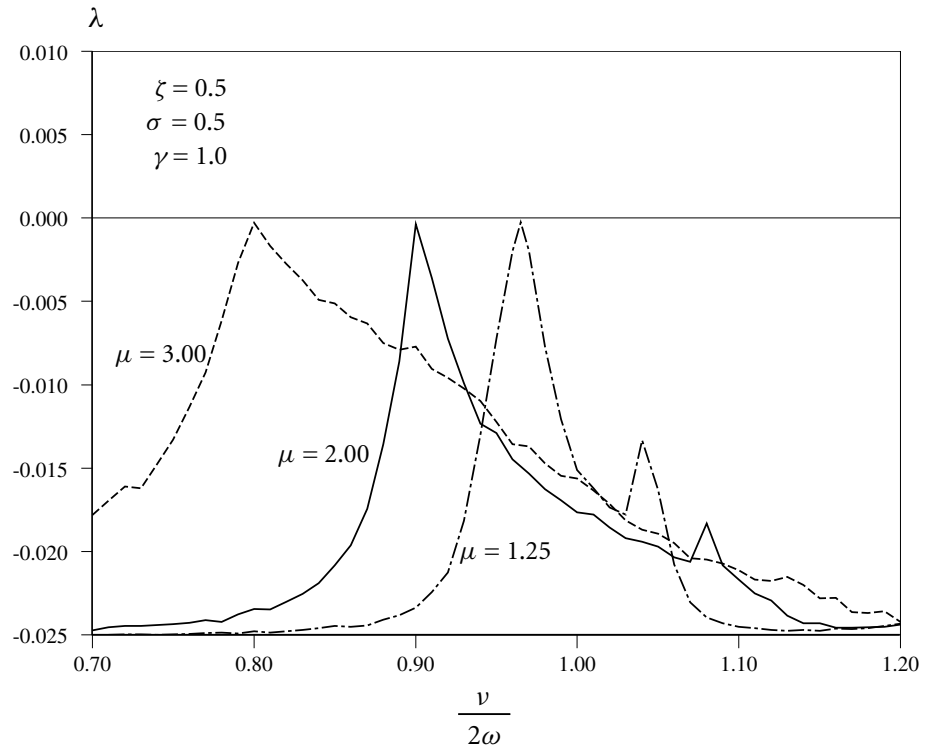


**Figure 5.3** Non-Trivial Stationary Solution Stability Curve vs. Load Intensity

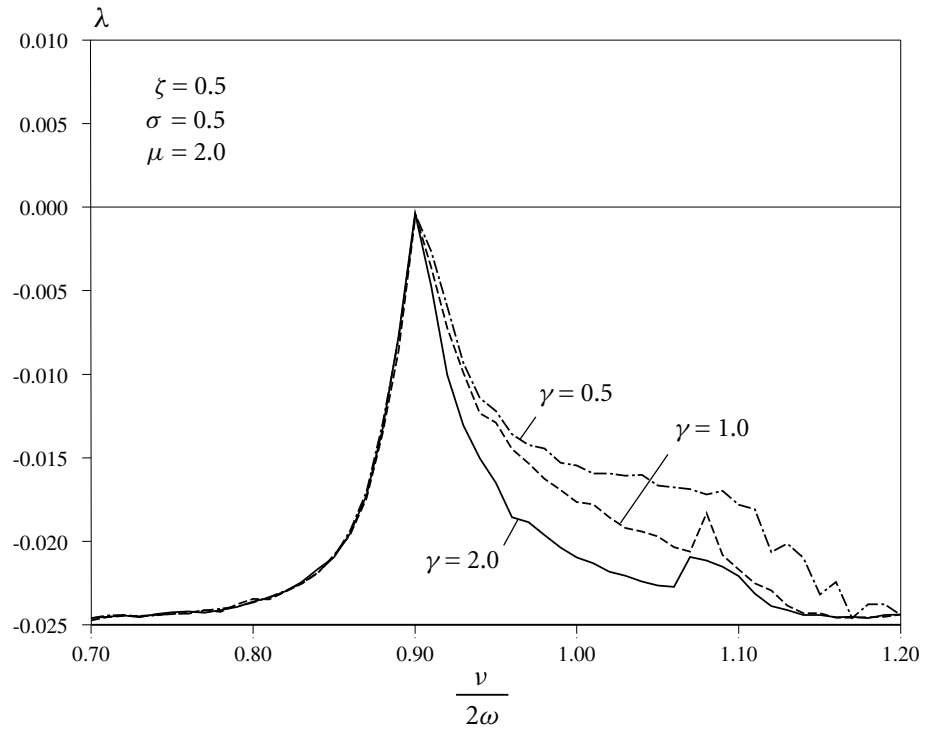


**Figure 5.4** Non-Trivial Stationary Solution Stability Curve vs. Nonlinearity

## 5.3 Remarks and Conclusions

In this chapter the stability of the non-trivial stationary amplitude of vibration of a structural column under bounded noise axial loaded was investigated. The stability was determined by studying the Lyapunov exponents of the equations of variation about the stationary solutions via Monte Carlo simulation.

The stationary solutions of the equations of motion of this system are actually an input to the equations of variation. Therefore Monte Carlo simulations is used in a dual role: generating both an input stationary solution to the equations of variation, and determining the Lyapunov exponents of these equations.

The effect that load intensity, nonlinearity, and noise intensity have on stability is also studied. It is shown that, as one might expect, load increases Lyapunov exponents of the system, while noise and nonlinearity decrease the Lyapunov exponents.

# C H A 6 P T E R

## Conclusions

### 6.1 Summary

Columns are the most critical component of many structures. The failure of one column can often lead to progressive collapse of the entire structure. Column stability is therefore a very important aspect of structural design. In this thesis the stability of a structural column under dynamic axial load is investigated.

Real world structural loadings are random processes. Therefore a bounded noise process is used in this thesis to model the axial loading of the column. A bounded noise process is chosen because its statistical properties can be closely matched to those of real processes such as wind loading or wave/tidal forces. Despite the loading being random in nature, many concrete results are obtained by use of Lyapunov exponents.

The equation of motion of the system is derived and simplified by using the method of averaging. The averaged equations are then used to derive an analytical expression for the Lyapunov exponent of the trivial solution. The Lyapunov exponent is the average growth rate of the system therefore it directly gives the stability of the system. It is also shown that the introduction of noise into periodic loading improves the stability of the trivial solution.

The general equation of motion of a column under axial load is nonlinear; therefore there exist non-trivial stationary solutions of the equation of motion. Physically this means that the system may exhibit stable non-zero amplitudes of vibration. The relationship between

the amplitude of this stationary solution and the forcing frequency, or the amplitude-frequency relationship, is derived analytically in the case of a noise-free periodic load. In the general case of a "noisy" loading, Monte Carlo simulation is used to study the amplitude-frequency relationship.

The stability of the non-trivial solutions is also studied via Lyapunov exponents. This is done indirectly by studying the stability of equations of variation about the stationary solutions. It is shown that the non-trivial solution is de-stabilized by the introduction of noise into a periodic loading.

## 6.2 Extension of Research

In this thesis Monte Carlo simulation proved to be well suited to the study of bounded noise excitation. The simulations yielded consistent results with little computational expense. Therefore the numerical methods used in this thesis might be easily extended to the study multiple degrees-of-freedom systems under bounded noise excitation.

Bounded noise processes may also be used to approximate wide-band processes if the noise intensity is taken to be large. Therefore the results obtained in this thesis may also be extended to systems under wide-band excitation.

Finally, this thesis shows that noise has a primarily stabilizing effect on the un-deformed (un-buckled) state of columns under axial excitation. Therefore noise could potentially be introduced into systems as a control technique. A major benefit of using noise as a control technique is that, while it would be active control, it would not require any sensing of the states of a structural system.

## 6.3 Future Work

In this thesis, Monte Carlo simulation is used in a primary role to determine both the stationary solutions of columns under bounded noise axial load and the stability of these solutions. Ideally, one would be able to derive analytical expressions of stability and use simulation only in a verification role. Unfortunately analytical results are difficult to obtain for this system because of the complexity of the equations of motion. The main stumbling

block is the nonlinearity that is present in this system, which makes solution of the Fokker-Planck equation very difficult, more difficult than the original equation of motion of the system. However, further investigation of analytical solutions is warranted, because the stability of a dynamical system can never be fully described by a set of simulations.

The stability results of this thesis would also be complemented by determination of the moment stability of the system via moment Lyapunov exponents.

The effect of damping on the Lyapunov exponents of the non-trivial solution was not studied in this thesis. To gain a complete picture of this system, this should be studied further.

# Bibliography

1. N. BOGOLIUBOV AND A. MITROPOLSKI. *Asymptotic Methods in the Theory of Non-linear Oscillations*. Gordon and Breach, New York, 1961.
2. R. L. BORELLI AND C. S. COLEMAN. *Differential Equations A Modelling Perspective*. John Wiley & Sons, Inc., Toronto, 1998.
3. C. F. CHAN MAN FONG AND D. DE KEE. *Perturbation Methods, Instability, Catastrophe, and Chaos*. World Scientific Publishing Co. Pte. Ltd., Singapore, 1999.
4. P. HAGEDORN. *Nonlinear Oscillations*. Akademische Verlagsgesellschaft, Wiesbaden, 1978. Translated By Wolfram Stadler - 1981.
5. Q. HUANG. *Stochastic Stability of Viscoelastic Systems*. PhD thesis, University of Waterloo, Waterloo, Ontario, Canada, 2008.
6. O. C. IBE. *Fundamentals of Applied Probability and Random Processes*. Elsevier Academic Press, Burlington, MA, 2005.
7. P. E. KLOEDEN AND E. PLATEN. *Numerical Solution of Stochastic Differential Equations*. Springer-Verlag, Berlin, 1992.
8. Y. K. LIN AND G. Q. CAI. *Probabilistic Structural Dynamics: Advanced Theory and Applications*. McGraw-Hill, New York, 1995.
9. Y. K. LIN. *Probabilistic Theory of Structural Dynamics*. Robert E. Krieger Publishing Co., Inc., New York, 1967.
10. N. C. NIGAM. *Introduction to Random Vibrations*. The MIT Press, Cambridge, MA, 1983.
11. Y. I. OSELEDEC. A multiplicative ergodic theorem. Lyapunov characteristic number for dynamical systems. *Transactions of the Moscow Mathematical Society*, **19**, 197–231, 1968. English translation.
12. A. A. SHABANA. *Theory of Vibration*. Springer - Verlag, New York, 1991.

13. D. TONGREN. *Approaches to the Qualitative Theory of Ordinary Differential Equations Dynamical Systems and Nonlinear Oscillators*. World Scientific Publishing Co. Pte. Ltd., Singapore, 2007.
14. W.-C. XIE. *Dynamic Stability of Structures*. Cambridge University Press, New York, 2006.